Increase of SPV Penetration in LV Grids by Smart Charging of EVs

- the Italian Scenario -

Master's Thesis

Riccardo Carollo

Aalborg University
Department of Energy Tecnhology
Pontoppidanstræde 101
DK-9220 Aalborg

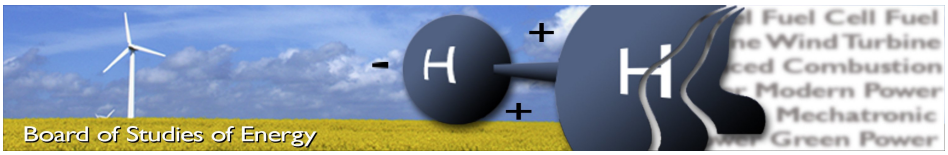

Title:	Increase of SPV Penetration in LV Grids by Smart Charging of EVs: the Italian Scenario
Semester:	3^{rd},4^{th}
Project period:	02.09.14 to 27.05.14
ECTS:	50
Supervisors:	Jayakrishnan Radhakrishna Pillai Sanjay K. Chaudhary
Industrial Supervisor:	Pietro Raboni (ABB)
Project group:	WPS3-951

Riccardo Carollo

SYNOPSIS:

Large SPV integration in LV grids is limited by a series of grid bottlenecks, such as voltage magnitude variations at the end of radial feeders, overloading the network components and voltage phase unbalance.
This work analyzes how the introduction of EVs in the LV network can potentially solve these grid bottlenecks and increase the feeder PV hosting capacity, in an example set of the Italian case study. Different EV charging scenarios are proposed, based on the present electricity tariffs for Italian residential customers (Time-of-Day, Net Metering functionality) and future possible developments such as the adoption of voltage droop control functionality for the EV charger, the introduction of real time pricing in the distribution network and the use of EV's Vehicle-to-Grid functionality.

Copies:	3
Pages, total:	86
Appendix:	1
Supplements:	CD

By signing this document, I confirm that the report does not include plagiarism.

Contents

Preface

This report has been written during 9^{th} and 10^{th} semester, from the 2^{nd} of September 2014 until the 27^{th} of May 2015, at the Department of Energy Technology at Aalborg University. The purpose of this work is to evaluate to what extent EVs' charging strategies can increase the share of PV distributed generation in distribution grids, with a model of a residential Italian LV network used as case study. In this work the software MATLAB^{TM} and DIgSILENT PowerFactory have been used. This report has been written using LaTeX.

The contents of this work do not necessarily represent the views of ABB DMPC PG Solar.

Reader's guide The used information in the report has been found in literature, reports, information from the supervisors and from lectures. Through the report there will be references to these sources, which can be found in the Bibliography. The method for referring to these sources is the IEEE citation method, where it refers with [number]. Reference in languages different from English are so indicated in the bibliography, e.g. (in Italian). All references used can be found in the CD attached to the present report. Tables, figures and equations are labeled with the number of the chapter. The CD attached to the report contains the simulation models and codes, and the references that were available as PDF.

Acknowledgments I would like to thank my supervisors Jayakrishnan Radhakrishna Pillai, Sanjay K. Chaudhary and Pietro Raboni for their valuable guidance and help provided, and Antonio Rossi from ABB for the solar measurements data and the support provided.

Finally, I would like to thank my family for their support and encouragement.

Aalborg University, May 27, 2015

Riccardo Carollo
<rcarol13@student.aau.dk>

Abstract

In the past few years, SPV installations in Italy have increased dramatically, providing more than 7.5% of the national electricity consumption in 2014. Most of the installed SPV capacity is allocated in the distribution network, and the majority of the installations is represented by single-phase rooftop SPVs connected to residential LV grids. Those large SPV shares lead to network integration issues such as voltage rise, overloading of the network components and voltage phase unbalance. Electric Vehicles (EVs) are a technology in rapid expansion whose connection is expected to take place in the LV network as well. EVs might represent a possible solution to the SPV integration issues, since they can be used as fast distributed battery storages, and consume locally part of the excess PV generation.

The purpose of this work is to propose different EV charging strategies, based on the present electricity tariffs and future developments of the electricity market as well as the EV technology, and to analyze their impact on the grid bottlenecks that limit an increase in the penetration of the PV hosting capacity in LV networks.

For the scope of this work, a model of a residential LV network is recreated using the software DIgSILENT PowerFactory, by adapting to the Italian case study a CIGRÉ benchmark. The PV hosting capacity and the grid bottlenecks at the present state of the grid are investigated, in order to determine what are the limiting factors for an increase in the PV installations. The present electricity tariffs for Italian residential customers are analyzed, together with possible future technical (voltage droop control, Vehicle-to-Grid functionality) and economical (Distribution Locational Marginal Pricing) developments. According to this analysis, 4 scenarios are identified, and the EV load profiles are generated with MATLAB for each of them and introduced in the simulation model.

The analysis of the simulation results revealed that the present Time of Day (TOD) tariffs are inefficient in the integration of EVs and SPV in residential grids. There has been found a positive correlation between the number of EVs in the network and the increase in the PV hosting capacity for the other scenarios analyzed, which, according to the scenario and the EV share in the network, increases between 18 and 64% compared to the present value. However, a series of EV integration issues are still registered, regarding the voltage magnitude variations and voltage phase unbalance. The proposed future developments mitigate some of the integration issues, without solving them completely.

The results of the analysis conducted in this work shows that there exist a series of limitations in the mutual benefit between PV and EV technologies in LV distribution grids. EVs can increment the PV hosting capacity in the existing LV networks without the need for grid reinforcements, however, the impact of considerable shares of EVs requires additional research. The results of this work can be adapted to other European LV networks.

Nomenclature

List of Acronyms

BEV	Battery Electric Vehicle
CIGRÈ	International Council on Large Electric Systems (in French: *Conseil International des Grands Réseaux Électriques*)
DLMP	Distribution Locational Marginal Price
DOD	Depth of Discharge
DPL	DIgSILENT Programming Language
DSO	Distribution System Operator
EU	European Union
EV	Electric Vehicle
FCEV	Fuel Cell Electric Vehicle
HEV	Hybrid Electric Vehicle
HV	High Voltage
ICE	Internal Combustion Engine
IEEE	Institute of Electrical and Electronics Engineers
IPCC	Intergovernmental Panel on Climate Change
LMP	Locational Marginal Price
LV	Low Voltage
MCC	Marginal Cost of Congestion
MEC	Marginal Energy Cost
MLC	Marginal Loss Cost
MV	Medium Voltage
OHL	Overhead Line
OLTC	On Load Tap Changer
PCC	Point of Common Coupling
PEV	Plug-in Electric Vehicle
PF	Power Factor
PHEV	Plug-in Electric Vehicle
PV	Photovoltaic
RES	Renewable Energy Sources
RMS	Root Mean Square

SOC	State of Charge
SPV	Solar Photovoltaic
TOD	Time of Day (Electricity Tariff)
TOU	Time of Use
TSO	Transmission System Operator
V2G	Vehicle-to-Grid
VDC	Voltage Droop Control
%VUF	Percentage Voltage Unbalance Factor

List of Symbols

c_{DLMP}	Distribution Locational Marginal Price rate	c€/kWh
c_{PV}	Electricity base price for the PV injected energy	c€/kWh
c_{TOD}	Electricity base price rate	c€/kWh
C_{rated}	Battery rated capacity	kWh
CS	Energy payback for the PV owner (*Contributo Scambio*)	€
c_{V2G}	Cost associated with Vehicle-to-Grid operation	c€/kWh
$c_{wearout}$	Cost of the battery wear-out associated with V2G operation	c€/kWh
E_{dom}	Domestic yearly energy consumption	kWh
E_n	Cycled energy in the battery cycle life	MWh
E_{PV}	PV yearly energy production	kWh
E_{self}	PV energy self-consumption	kWh
E_{wit}	Energy withdrawn	kWh
E_{inj}	Energy injected	kWh
f_{co}	Coincidence factor	-
P_{dom}	Domestic load demand	kW
P_{max}	Maximum EV power demand	kW
P_{meas}	Rated power of the PV power unit used for measurements	kW
P_{PV}	PV active power output	kW
s	Scaling factor of the PV power output	-
SOC_{arr}	Battery SOC at the arrival at the charging point	kW %
V	Voltage magnitude	V
V_n	Negative sequence voltage component	V
V_p	Positive sequence voltage component	V
λ	Loss sensitivity coefficient	p.u.
η_{cha}	EV charger charging efficiency	p.u.
η_{dis}	EV charger discharging efficiency	p.u.
η_{dri}	EV driving efficiency	kWh/km
η_{net}	V2G cycle net efficiency	p.u.
$I_{l,\phi}$	Line current in line l and phase ϕ	A
$R_{l,\phi 1\phi 2}$	Real part of the line impedance $Z_{l,\phi 1\phi 2}$ for line l	Ω
$\theta_{I,l,\phi}$	Angle of phase current ϕ in line l;	rad
$\theta_{I,n,\phi}$	Angle of phase current ϕ at the node n	rad

1 Introduction

The Electric Vehicle (EV) technology is now in its early stages, but its proliferation is expected to exponentially increase in the next few years. The Solar Photovoltaic (SPV) technology is instead already a significant power source in many countries, including Italy where in 2013 it provided more than 7% of the national electricity demand.

The spread of EVs and PVs is expected to increase, and to create power quality issues in the power network, especially on the Low Voltage (LV) side. However, since PV generation is predictable to some extent and the EV is a flexible load, a combination of the two technologies can mutually help the increase in number of both EV fleet and PV installed units to be plugged-in to the grid.

This report investigates how, and to what extent, different EV charging strategies can increase the PV hosting capacity in the case of an Italian residential LV network. The hosting capacity is defined as the maximum PV installed capacity that can be allocated into the LV network without the violation of any of the grid constraints assumed. Those constraints are based on power quality indicators such as voltage magnitude, voltage phase unbalance and maximum loading of the network components.

This first chapter contains the introduction and the background for this work, which lead to the definition of the Problem Statement. A list of objectives and the limitation of this work are then discussed, then the methodology employed in the project is introduced. In the end, an introduction to the content of each chapter in the report is to be found in the outline section.

1.1 Background

Global warming, the increase in the average temperature of Earth's climate system, is one of the main issues of our time. This phenomena has evidence in instrumental temperature records, melting of major stores of land ice such as the glaciers in the Northern Hemisphere and in the consequent rise of the sea levels [1]. Almost all the scientific community nowadays agrees that global warming is caused by increasing concentrations of greenhouse gases produced mainly by human activities.
The Intergovernmental Panel on Climate Change (IPCC) stated in 2013 that the largest driver of global warming is carbon dioxide (CO_2), which is emitted mainly by fossil fuel combustion and cement production [1].

The transportation sector is nowadays responsible to almost one fifth of global CO_2 emissions: for this reason it is a good candidate to apply the decarbonization of the human activities [2], [3]. The replacement of Internal Combustion Engine (ICE) vehicles with Electrical Vehicles (EVs) is a step in that direction as of private transportation [4].

EVs are now a technology in rapid expansion: in 2012, the global stock was of 180.000 units (0.02% of total passenger cars) and by the year 2020 it is expected to have 20 millions of electrical/hybrid vehicles on the road worldwide (2% of total passenger cars in 2020) [3]. Fig. 1.1 shows a prediction of the evolution of EV market in the decade 2010-2020. This increasing trend is confirmed by the more recent data on sales, with more than 200.000 EVs sold in 2013 and more than 280.000 sold in 2014 worldwide [5], [6].

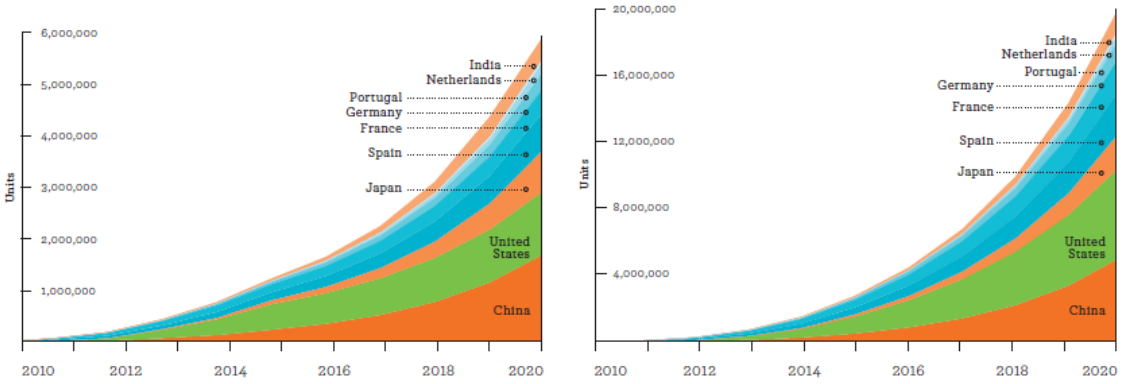

Figure 1.1: Sales (on the left) and stock (on the right) targets for EV until 2020 [3].

Apart from CO_2 emissions savings, EVs present other advantages when compared to ICE vehicles, including no noise emissions, better reliability due to the reduced number of mechanical components, independence from oil availability and price fluctuations, reduced costs of operation and better overall efficiency [2].

However, the electricity generation sector must be reconsidered as well, for the electrification of private transportation to be effective in CO_2 reduction. Charging private vehicles using electricity generated from conventional fossil fuel power plants might solve some of the problems on a local level, e.g. air pollution in big cities, but on a global perspective, the impact is negligible [2].

For this reason the share of Renewable Energy Sources (RES) in electricity generation should increase. Renewable energy is defined as energy that comes from resources which are naturally replenished on a human timescale: some examples are sunlight, wind, tidal and waves. The exploitation of RES for electricity production is virtually CO_2-free, and it is not affected by shortages. One technology able to convert sunlight into electricity is Solar Photovoltaics (SPV).

SPV has experienced a considerable growth in the last decade, and in 2013 it reached 138.9 GW of global cumulative installed capacity, with 38.4 GW installed only that year [7]. Italy represent an interesting case study for its high penetration of SPV. At the end of 2013 the cumulative installed capacity was 17.928 GW, 13% and 22% of the world and EU-27 total respectively [7], as shown in Fig. 1.2.

This considerable share resulted in a yearly production in the year 2013 of 21,229 GWh, equivalent to more than 7% of the 2013 national energy consumption [8].
PV generation units have typically small rated capacities when compared to conventional power plants, and are scattered on the territory [9]. As a result, the vast majority of the PV installed capacity is connected to the distribution grid. In the Italian case study, at the end

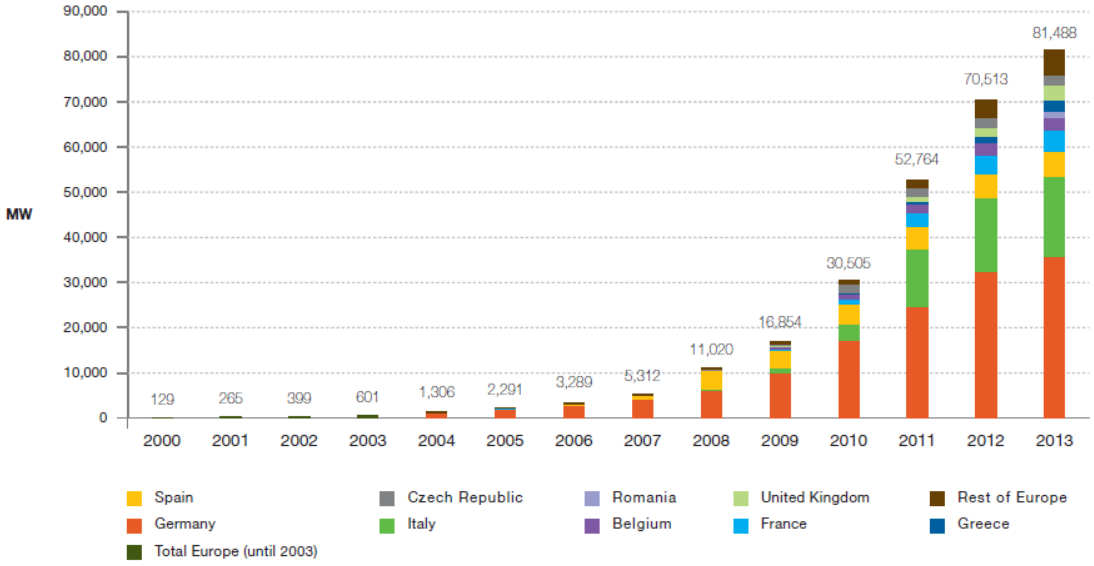

Figure 1.2: Evolution of European PV cumulative installed capacity [7]. At the end of 2013, Italy is for the third year in a row the second country for PV installed in the EU-27.

of 2012 96% of the total number of PV units were installed in the LV grid, accounting for the 31% of the PV installed power [10].

Referring to [11], [12], high PV shares introduce power quality issues to the LV grids. Distribution networks were planned for a one-way power flow operation only [13]. For this reason the reverse power flow, which can occur when the PV generation exceeds the local load demand, can result into overvoltages over the admissible range along LV feeders, and overloading of network equipments such as cables and distribution transformers. Since most of PV units have a rated power in the range of few kW, and they are mostly connected to a single phase of the grid only, another integration issue is represented by voltage phase unbalance.

The EV load is expected to introduce issues in the LV network as well. Since the electrification of the transportation sector is still at an initial stage, the number of charging points will be limited in the near future. For this reason the EV owners will charge their vehicle mainly at home, plugging their EV to a residential socket [2]. EVs represent an additional load, for which the LV grid was not designed and sized: a single vehicle recharging its batteries has a power demand in the range of few kW, comparable to the average household consumption [2]. The peak load introduced by unplanned EV charging can lead to overloading of the network components such as cables and transformers, overheating and undervoltages in the distribution grid.

Since PV is intermittent, but on some way predictable power source [14], and EVs are flexible loads, different researches suggest that one technology might be complementary to the other. Referring to [12], [15] and [16], the implementation of distributed storage systems in LV feeders has been presented as a solution to overcome overvoltages and overloading of the distribution transformer, when the active power generation is higher than the load demand. Those distributed storage systems can be represented by EVs, when plugged into the electrical

grid. EVs in the near future will be able to modify their charging profile according to real-time signals, helping to reduce the integration issues, in a process called smart charging [2].

1.2 Problem Statement

The integration of PV generating units in LV networks is limited by the presence of grid bottlenecks, such as voltage magnitude variations, overloading of the network equipments and voltage phase unbalance.

Guaranteeing high power quality standards while using an increasing share of intermittent, partially unpredictable renewable energy sources is a challenge for Distribution System Operators (DSOs) in the future. Better coordination between RES production and load consumption is necessary, in order to reduce the need for investments in reinforcing or upgrading the power grid infrastructure.

EVs are a recently developing technology whose connection will take place mainly on the LV network, due to the size of the EV batteries and the present lack of a fast charging infrastructure. Several studies suggests how EVs can be used as distributed battery storages. The EV charging process could reduce the reverse power flow in the LV feeders, main cause of the limits to a further increase in the PV hosting capacity, by absorbing power close to the PV generating units. The local consumption of the PV generated energy bring also economic advantages for an electric customers who owns both a PV unit and an EV, in the form of savings in the electricity bill by an increased share of self-consumed energy.

According to these conclusions, some objectives for this project have been found and are presented in the next section.

1.3 Objectives

The main objective of this work is to propose different EV charging strategies, and to analyze their impact on the grid bottlenecks for large integration of PV units in LV residential networks. The Italian scenario is chosen as a case study.

To achieve this objective the following tasks have been completed:

- Investigate the present hosting capacity for PV generating units in a test case Italian LV distribution grid, and determine any grid bottlenecks;
- Propose an optimization process to minimize the cost for the residential customer who owns an EV and a PV unit for each of the proposed scenarios;
- Apply EV charging scenarios based on the EV driving and availability patterns and the present electricity tariffs for Italian residential customers;
- Apply technical (voltage droop control, Vehicle-to-Grid functionality) and economical scenarios (Time-of-use Tariff, Net Metering, Locational Marginal Pricing) to integrate more SPVs and EVs in the distribution grid;
- Propose a new approach for the evaluation of the cost related to the battery wear-out associated with Vehicle-to-Grid functionality;
- Introduce different EV shares in the residential LV model, and evaluate the impact on the network PV hosting capacity and grid bottlenecks for each of the scenarios proposed;

1.4 Methodology

As the test case network for investigating the influence of high penetration of SPVs and EVs on distribution grids, a benchmark grid model based on the CIGRÈ European Low Voltage network is recreated using the software DIgSILENT PowerFactory. A series of modifications on the original model are proposed, including the lengthening of the radial feeder, the inclusion of single-phase connections and the modeling of individual loads and generating units. These modifications aim to adapt the model to the Italian scenario, where single-phase connections are predominant in residential LV networks. The proposed modifications are tested with a series of simulation analysis based on voltage sensitivity.

The domestic load and the PV generating profiles used in this work are based on measurements data from an ABB solar irradiance sensor and a study on the European domestic load profiles. Unbalanced load flow simulations are conducted, and data about loading of all network components, voltage magnitude and voltage phase unbalance at any node of the grid is collected and used as indicators of the grid power quality, in order to determine eventual grid bottlenecks. The maximum PV hosting capacity in the network is calculated using an iterative algorithm developed using a DIgSILENT Programming Language (DPL) script.

After the evaluation of the PV hosting capacity at the present state of the grid, the impact of different EV charging scenarios is analyzed. The EV load profiles are generated as the output of an optimization process, where the EV load demand is the control variable, the cost for the EV owner is the cost function and the constraints considered are those derived from the battery State of Charge (SOC), the availability for home-charging and the charger technology. The EV availability for home-charging and the EV energy demand are generated with a MATLAB script from a normal distribution function, based on data from an EU survey about Italian car drivers' habits.

New functionalities based on forecasting future development of the electricity market and EV technology are analyzed. *Voltage droop control* for the EV charger is implemented through an iterative co-simulation process, where the maximum allowed EV power demand is calculated with MATLAB, and the feedback on the voltage level at the bus where the EV is connected is performed with PowerFactory. The implementation of an application of real time pricing, *Distribution Locational Marginal Pricing (DLMP)*, is proposed. The price signals of DLMP are based on unbalanced loss sensitivity analysis. A new approach to calculate the cost associated with battery wear-out during Vehicle-to-Grid (V2G) operation, based on the energy that can be cycled in the battery cycle life, is proposed and implemented in MATLAB.

1.5 Limitations

Some assumptions and limitations are considered in this work, and they are listed as follows:

- The residential LV grid modeled in this work has a radial structure; other configurations, such as ring or mesh grid, or modifications of the grid topology are not taken into consideration. Only one feeder of the LV grid has been modeled in detail, while the other feeders connected to the secondary side of the MV/LV transformer are modeled as aggregate loads;

- It is assumed that the modeled MV/LV transformer is not equipped with On-Load Tap Changer (OLTC) functionality. The analysis is limited to the LV side of the network

only; any impact of EVs and PVs on the MV and HV sides of the network is not analyzed in this work;

- It is assumed that every household in the modeled LV grid has a rooftop PV unit connected to a single-phase inverter, and a single-phase EV charger. For simplicity reasons all residential units, individual PV units and EV chargers are modeled with the same rated power. Cloud transients and differences in the installations of the PV units, such as tilt and orientation angles, are not considered; for this reason all the PV units modeled follow the same generation profile;
- In the implementation of voltage droop control for the EV charger, the same droop control is applied to all the EV chargers in the network, regardless of their location in the grid or the EV battery SOC;
- The chemistry of the EV batteries and the effects of temperature and discharge rate on their lifetime are not considered;
- The participation of EVs and PVs in other markets apart from day-ahead is not analyzed in this work;
- Control strategies for active and reactive power control from EVs and PVs are not investigated in this report;
- Power quality issues such as harmonics, flicker, frequency fluctuations etc. are not considered in this work;

1.6 Outline of the Report

- **Chapter 1: Introduction**
  This first chapter contains the background on which this work is based, the objectives, the limitations there have been considered and the methodology followed in this work.
- **Chapter 2: State of Art**
  In this second chapter the theoretical background on which this work is based is presented. First, an overview on distribution networks is introduced, with focus on LV residential grids in the Italian scenario. Then follows an analysis of LV loads in residential grids, and the description of their modeling process. PV technology is then presented, with focus on grid integration issues and the Italian case study. The power quality indicators used to determine the PV hosting capacity in the LV feeder, and their limits assumed as constraints are then discussed. In the end of the chapter the Electric Vehicle (EV) technology is presented. The EV integration issues in LV networks, the proposed solutions such as voltage droop control and Vehicle-to-Grid functionality (V2G), and the EV operation in terms of driving patterns and charging points are discussed.
- **Chapter 3: Adaptation of the CIGRÈ Benchmark Model**
  In this chapter the modeling of the residential LV network is presented. At first, the CIGRÈ European LV benchmark is analyzed. A modified version of the benchmark model is then proposed and implemented, in order to better represent the Italian case

study. The adapted model is presented and tested, through a series of analysis based on voltage sensitivity. In the end, the PV hosting capacity at the present state of the grid is evaluated on the proposed simulation model.

- **Chapter 4: Integration of EVs and PV units in the network**
  In this chapter the EV is introduced into the network model, and its impact on the grid bottlenecks and the PV hosting capacity is evaluated and discussed. First, Time Of Day tariff (TOD), the available tariff for Italian residential customers, is analyzed and the EV load modeled accordingly is introduced into the network. The bottlenecks and the new PV hosting capacity are evaluated for this scenario. Net Metering functionality is then analyzed, and the same simulations are performed. In the end the results are compared and a list of conclusions on the present electricity tariffs for Italian customers in terms of PV and EV integration in the network is presented.

- **Chapter 5: EVs in Future Distribution Grids**
  In this chapter future developments of the distribution grid are presented. An approach based on loss sensitivity is proposed to determine real-time marginal pricing, with the purpose to stimulate the self-consumption of the PV generated energy by applying varying prices according to the location and the grid conditions. The implementation of V2G functionality is analyzed, and the new approach to model the cost associated with the battery wear-out is presented and implemented. The same evaluations as for the previous scenarios are conducted, and in the end the results are compared.

- **Chapter 6: Conclusions and Future Works**
  In this final chapter the results of the simulations are discussed, and the advantages and drawbacks of the integration of EVs and PVs in LV distribution grids are analyzed on both the EV owner and the DSO perspective. In the end, future works are presented.

2 State of Art

In this chapter the theoretical background of this work is presented. In the first section, the structure and operation of distribution grids is analyzed, with focus on the grid bottlenecks for an increase in the PV penetration. Then follows a description of the elements connected to LV distribution grids, from residential loads to generating units such as SPV. The issues regarding the integration of high shares of PV units in those grids are summarized after a literature review. In the end, the EV as a load in the system is presented, and its potential as distributed battery storage in the system, as well as its limits, are described.

2.1 Distribution Grids

In this first section of this chapter, typical structures of distribution grids are presented. First, an overview of distribution grids is presented, followed by a more detailed description of radial distribution network in the Italian case study, on which this work focuses. The issues related to the bi-directional power flow that can occur in these grids with the increase in the PV installations are presented, with focus on the Italian case study.

2.1.1 Composition of a Power Network

A power network is composed of a transmission system and a distribution system. While the transmission system is responsible for the bulk transfer of electrical energy from the generating power plants to the major load centers, the distribution system has the task to supply, with high power quality and reliability, all the local customers with an appropriate voltage level [17]. A schematic representation of a power grid is displayed in Fig. 2.1.

Distribution systems can be subdivided into Medium Voltage (MV) networks, also called primary distribution systems, and LV networks, or secondary distribution systems. MV networks have nominal voltages in the tens of kV, while LV networks usually have nominal voltage of 400 V [19].

The vast majority of electrical customers are connected at LV level, and supplied via feeders connected to MV/LV distribution substations [17]. Most of the RES installed capacity is nowadays connected to the distribution network as well. While large wind turbines and solar power plants are generally connected to the MV level, units with smaller rated capacity, including most of the installed PV capacity, are connected to the LV level [10].

2.1.2 Structure of a Distribution Network

The most common configuration for distribution networks is the radial topology. Radial distribution networks are composed of feeders which are supplied by one end only, typically

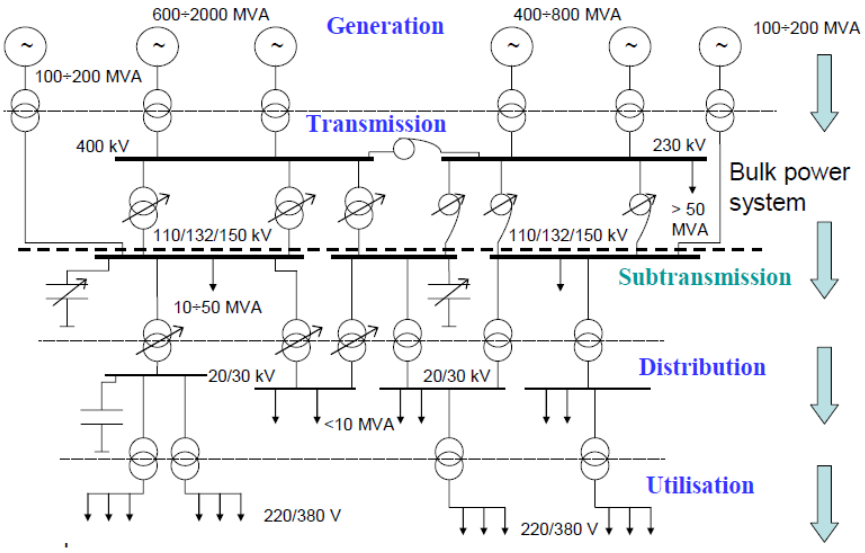

Figure 2.1: Typical scheme of the electrical power grid with the range of voltage levels commonly used in continental Europe [18].

connected to the busbar at the secondary side of a distribution transformer.

The radial topology has the main advantage of economy in the installation when compared to other topologies, such as ring or mesh grids [20]. The drawbacks are related to the power quality level. The high impedance of the conductors used in LV networks result into voltage variations in conditions of high load demand or high distributed generation power production. These variations are more evident for the customers connected close to the end of the feeder, where the impedance from the distribution transformer reaches its maximum, and can exceed the design limits [20].

Traditionally LV distribution networks were designed for one-way power flow, from the medium voltage substation to low voltage customer loads [21].

The voltage drop ΔV in a line such as the one represented in Fig. 2.2 can be approximated as:

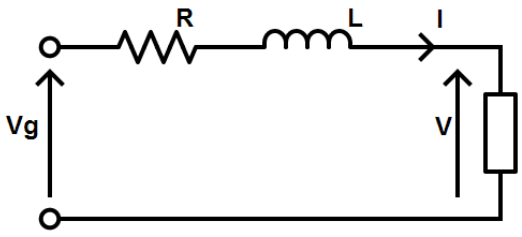

Figure 2.2: Single line diagram of a three phase AC line.

$$\Delta V \simeq \frac{RP + XQ}{V} \tag{2.1}$$

where P and Q are the active and reactive power exchanged at the Point of Common Coupling (PCC), R is the line resistance, X is the line reactance and V is the line voltage.

It is relevant to notice that the R/X ratio for the conductors used in LV networks, both OHLs and cables, is usually high, often over unity [22]. This means that the active power has greater influence than the reactive power on the voltage magnitude, when compared to the transmission network. High shares of distributed generation units, such as SPV, can lead to reverse power flow in the feeder, from the customers to the distribution transformer. In such a case the term $P = P_{gen} - P_{load}$ becomes negative, resulting in a voltage rise ΔV which can go above the allowed limits at the end of the feeder.

2.1.3 Italian Distribution Network

The Italian distribution network is operated using a 20 kV MV network connected through transformers to a 400 V LV network. Apart from rare exceptions, where an above average service continuity is required and the ring grid is used, e.g. in hospitals, all the Italian distributed network is operated with a radial structure [20].

It is common practice to use more than one type of conductor along the same feeder, with larger cross-section in the beginning of the feeder and smaller cross-section close to the end, due to the lower current flowing in the line [17], [20].

Another relevant characteristic of the Italian LV network is the predominant use of single-phase load connections, especially in residential grids [20]. The use of single-phase connections applies also for the considerable share of installed distributed generation: the use of single-phase PV inverters is allowed for sizes up to 6 kW, and the vast majority of the current installations, mainly composed of rooftop PVs, is below this limit [10].

More detailed data about the network elements will be presented in the next chapter, together with the description of the simulation model.

2.2 Low Voltage Loads

In this second section of the chapter the most common loads in residential LV grids, domestic load and public illumination, are presented. The electric load due to the EV home-charging process is presented separately in Section 2.4.

2.2.1 Household Loads

The household load profile is the sum of all load profiles of the residential electrical loads, such as appliances, air conditioning, illumination, and others [23]. Household loads represent the majority of LV loads, and due to the low individual energy demand they are usually connected to a single-phase of the grid only [9], [20]. Even if the LV feeders are planned in order to maintain a fair distribution of single-phase loads among the three phases, a certain level of load unbalance is always present in the grid, known as *background unbalance* [24].

The domestic load profile proposed in [25] was used for modeling the load demand of the residential units of this work. The original profile has been obtained by measurements from a sample of buildings in Wales, and it represents one of the best approximation of standard European residential load profiles [25]. In order to obtain a smoother profile, and because the PV measurements used are on a hourly base, the original load profile has been adapted to hourly resolution from the original 5 minutes one. A comparison between the 5 minutes

resolution data and the 1 hour average data, for one example of one day of the year, is presented in Fig. 2.3.

The so obtained domestic load profile has a peak load of 3.76 kW and a yearly consumption of 2979.71 kWh. These values suit the Italian case study: in 2012 the average yearly Italian household consumption was 2298.85 kWh, ranging from a minimum of 1772.83 kWh in Imperia (Liguria) to a maximum of 2999.84 kWh in Carbonia (Sardinia) [26].

It has been assumed in this work a constant Power Factor (PF) of 0.95 for the domestic load demand, and a rated power of the connection to the grid of 4.50 kW; all the assumption regarding the residential load are summarized in Table 2.1.

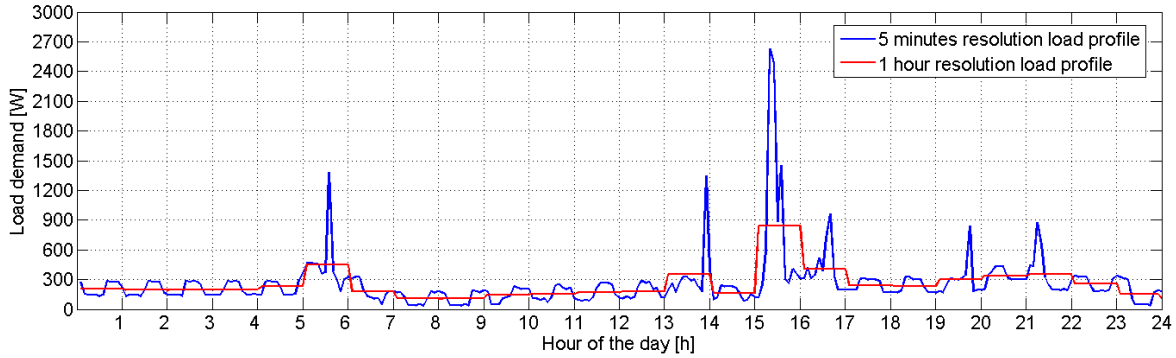

Figure 2.3: Comparison between the 5 minutes resolution measurement data and the 1 hour average resolution data, used in this work as a domestic load profile, during an example of one day of the year.

Table 2.1: Assumptions made in the modeling of the single-phase residential load.

Parameter	Value	Unit
Rated power	4.50	kW
Peak consumption	3.76	kW
Yearly consumption	2979.71	kWh
Power Factor (PF)	0.95	-

The various loads in the grid usually do not absorb their rated power simultaneously, so the maximum system power demand is always lower than the sum of the single load rated powers. A parameter used to describe this phenomena is the *coincidence factor* f_{co}, defined as the ratio between the system maximum power demand P_M and the sum of the single loads maximum demand $P_{M,i}$ [20], as expressed by Eq. 2.2.

$$f_{co} = \frac{P_M}{\sum_{i=1}^{n} P_{M,i}} \tag{2.2}$$

To simulate the coincidence of residential loads in the grid, three different profiles are created by shifting the original profile one week forward and backward, so the consumption profile for a Monday is replaced by the consumption profile of another Monday, etc.

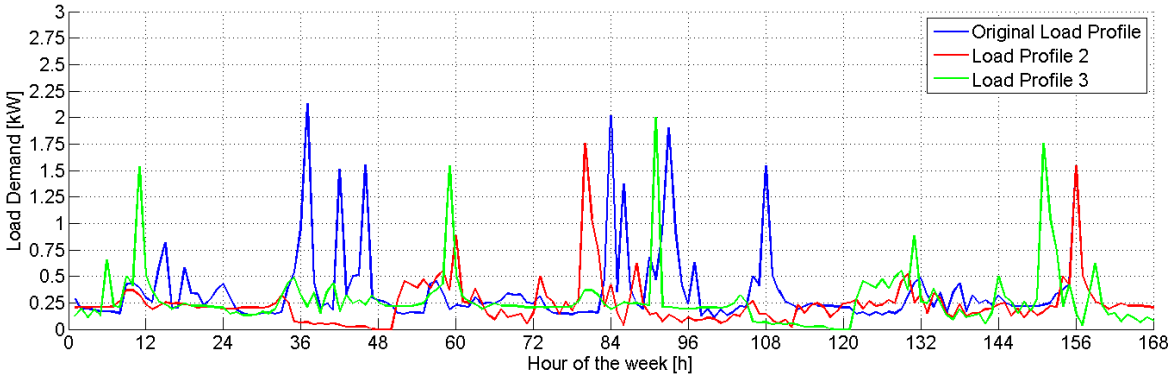

Figure 2.4: Comparison between the three residential load profiles generated from the original measurement data over one week of simulation.

A comparison of the three different profiles on a weekly base can be seen from the plot of Fig. 2.4. The resulting system residential load has a coincidence factor $f_{co} = 0.56$, a value suitable for residential loads [20].

2.2.2 Public Illumination

Another common load in residential districts is represented by public illumination. An approximation used in this work, is to model the public illumination network as an aggregate load, with two different power demand levels: ON (1 p.u.) and OFF (0 p.u.). The aggregate load represents the sum of all the individual light pole loads. In the model an aggregate loads representing the cable cabinet is created, accounting for approximately 8% of the present state of the grid load demand. Since the single-phase light poles are distributed equally among the three phases, the aggregate load will be modeled as a three-phase balanced load.

The load profile in this work will be derived from the PV power output irradiance measurements, with OFF state when the PV generation is not null and ON state anywhere else. Public illumination loads are commonly connected to dedicated feeders. For this reason the aggregate load representing public illumination will be connected to the LV side of the distribution transformer.

2.3 Solar Photovoltaics

In this section the PV technology and how its integration in LV networks affects the grid power quality are presented. A brief overview of the PV share and its future forecast is presented in Section 2.3.1. The issues related to a high share of PV generation in distributed grids are then presented. In the end, a definition of the maximum hosting capacity in a distribution network, based on a set of power quality indicators, is proposed.

2.3.1 Present Share and Future Forecast

The solar PV global installed capacity has reached 138.9 GW in 2013, and future forecasts show how this number is going to increase in the next years [7]. Regarding Italy, the trend on the cumulative installed PV capacity is constantly increasing while the new installations,

after a boom in 2012, are now in a decreasing trend. This tendency is illustrated in the plot of Fig. 2.5.

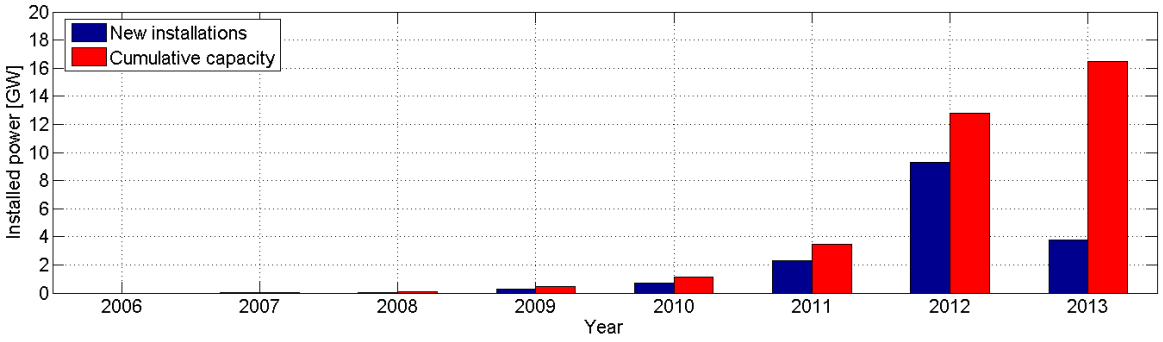

Figure 2.5: Yearly installations and cumulative installed PV capacity in Italy from 2006 to 2013 [10], [27], [28]. While the cumulative capacity is still increasing, the yearly installations are decreasing due to reductions in the governmental subsidies and saturation of the LV grids.

Referring to [29], in some Italian distribution networks the installation of new PV units has been delayed until reinforcements of the distribution network are operated. The saturation of the hosting capacity in most of the distribution network explains the decreasing trend in the installations of new PV capacity, displayed in Fig. 2.5.

2.3.2 Issues in the Integration of PV Units in LV Grids

Some of the main issues that prevents large integration of PV units in LV networks are voltage rise, overloading of network equipments and voltage phase unbalance [12], [15], [22].

Voltage rise is a direct consequence of the reverse power flow on the feeders [12]. This phenomenon occurs when in the same feeder high SPV generation meets low load conditions, and it is more relevant in long feeders with high impedance, as described in Eq. 2.1. Voltage rise is a particularly relevant issue in LV network: because of the resistive characteristic of LV conductors, active power (such as PV active power output) has a greater impact than reactive power over the grid voltage [22], [30].

Voltage rise is harmful for the grid infrastructure and the customers connected to it. The application of a voltage over the design limit can lead to degradation due to long-term heating and eventually to a failure of the electronic component [31]. If the upper voltage limit at the PCC is exceeded, voltage rise will also result into a regulation or curtailment of the power output of PV systems, resulting in loss of renewable energy [32].

Another issue is represented by overloading of network equipments such as MV/LV transformers and LV cables [15], [33]. Currents over the design limits will result into overheating of the network component, and consequent loss of life.

One more problematic issue is represented by voltage phase unbalance. Although significant efforts are made by the utilities in equal distribution of loads and distributed generation, a perfect balance of load and generation among network phases it is not always possible [13]. Voltage phase unbalance may occur even when all loads and generating units connected have the same rated power, due to differences in the generation and load profiles [24]. An increase in the distributed generation installed power can result into an amplification of the background unbalance over the defined limits.

Other known issues of the PV penetration in LV grids, such as grid unintentional islanding, complexity of network protection relays coordination and frequency fluctuations [9], [12], [34], are not investigated in this work.

2.3.3 Hosting Capacity for Photovoltaics in Low Voltage Grids

The *hosting capacity* for photovoltaic generation in a power system is *'the degree of PV share that the power system can accept without endangering the reliability or quality of power'* [35].

The impact of PV generation in a distribution network can be quantified by using a set of indicators about power quality. Those analyzed in this report include voltage magnitude, phase unbalance and overloading of network components. Once defined the limits for those parameters, the hosting capacity is defined as the *maximum share of PV* for which *none of those constraints is violated.*

In the following paragraphs the indicators used to define the hosting capacity are presented, and their limit values used as constraints are specified.

Voltage Magnitude

As introduced in section 2.1.2, due to the high R/X ratio of the LV conductors, the influence of active power on the voltage level is considerable in LV grids, and high shares of PVs can lead to voltage rise. Under normal operating conditions a ±10% range around the nominal voltage value for 95% of the week, measured as the 10 minutes mean RMS, is the limit imposed by the EN 50160 requirements [36]. It has to be highlighted that this constraint applies to the whole distribution network, including both the LV and the MV levels. Since in this project the impact on the MV level is not considered, for conservative reasons a voltage limit of ±5% on the LV level, at any time, is selected.
To summarize, it will be used as a requirement that the voltage magnitude V (measured as phase-to-neutral for single-phase, phase-to-phase for three-phase) in any of the i LV nodes of the grid, always fulfill the equation:

$$V_{min} \leq V_i \leq V_{max} \tag{2.3}$$

The $[V_{min}\ V_{max}]$ range for three-phases and single-phase connections is summarized in Table 2.2.

Table 2.2: Voltage magnitude rated values and admissible range for single-phase and three-phase connections.

	Single-phase	Three-phase
V_{rated} [V]	230.00	400.00
V_{min} [V]	218.50	380.00
V_{max} [V]	241.50	420.00

Phase Unbalance

Voltage unbalance represents the difference in magnitude between the phases of a three-phases system. Voltage unbalance is harmful for the grid for different reasons, including overheating of AC electrical machines and increased losses in the distribution transformer [21].

Voltage unbalance can be defined by using the Percentage Voltage Unbalance Factor (%VUF) [37]. %VUF is calculated as the ratio of the negative sequence voltage component V_n to the positive voltage sequence component V_p, as in Eq. 2.4.

$$\%VUF = \frac{V_n}{V_p} \cdot 100 \tag{2.4}$$

The positive and negative sequence voltage components can be obtained from the line voltages, by using Eq. 2.5 and 2.6, where $a = 1\angle 120°$ and $a^2 = 1\angle 240°$.

$$V_p = \frac{V_{ab} + aV_{bc} + a^2V_{ca}}{3} \tag{2.5}$$

$$V_n = \frac{V_{ab} + a^2V_{bc} + aV_{ca}}{3} \tag{2.6}$$

The EN50160 limit for voltage unbalance is 2.00% [36]. This value will be used as a constraint in order to define the maximum PV hosting capacity. The voltage phase unbalance constraints can be expressed then by Eq. 2.7.

$$\%VUF_i = \frac{V_{n,i}}{V_{p,i}} \leq \%VUF_{max} = 2.00\% \tag{2.7}$$

Overloading of Network Components

Overloading of network components affects the thermal regime in both the distribution transformer and the system conductors.

For the distribution transformer it is selected that the current should not exceed the maximum rated current at any time. This conservative constraint can be formulated as:

$$I_{trafo} \leq I_{trafo,max} \tag{2.8}$$

Regarding the network conductors, the limit is set according to their ampacity value. The *ampacity* of a conductor is the RMS value of the line current which the conductor can continuously carry while remaining within its temperature rating. A common practice for LV and MV installations is to refer directly to the datasheets provided by the cable manufacturer for the ampacity limits [20]. The data used in this project are taken from a manufacturer datasheet [38] and are listed in Table 3.5. Given the ampacity $I_{max,j}$ for the j cable in the network, the constraint will be that at any time is respected the equation:

$$I_j \leq I_{max_j} \tag{2.9}$$

To summarize, the PV hosting capacity is evaluated as the distribution network PV installed power that never leads to a violation of the constraints expressed by Eq. 2.4, 2.7, 2.8 and 2.9. In this work, the hosting capacity value is evaluated as the rated power that each individual PV unit in the network can reach, rather than the number of PV units of a specific rated power that can be plugged into the network. The PV hosting capacity and the constraints are evaluated on a yearly base, in order to consider the seasonal behavior of PV production and residential load demand.

2.3.4 PV Generation Profile

The PV generation profile used in this work has been obtained from measurement data provided by ABB. The PV installation where the measurements were conducted is located in the city outskirts of Florence, Italy. The measurement profile has one year length and hourly resolution. An example of the PV generation profile during one week is presented in Fig. 2.6.

The main characteristics of the PV generation profile are summarized in Table 2.3. Since the rated power of the PV units modeled in this work is variable, the PV generation profile is scaled accordingly, by using a process described in Section 3.3.

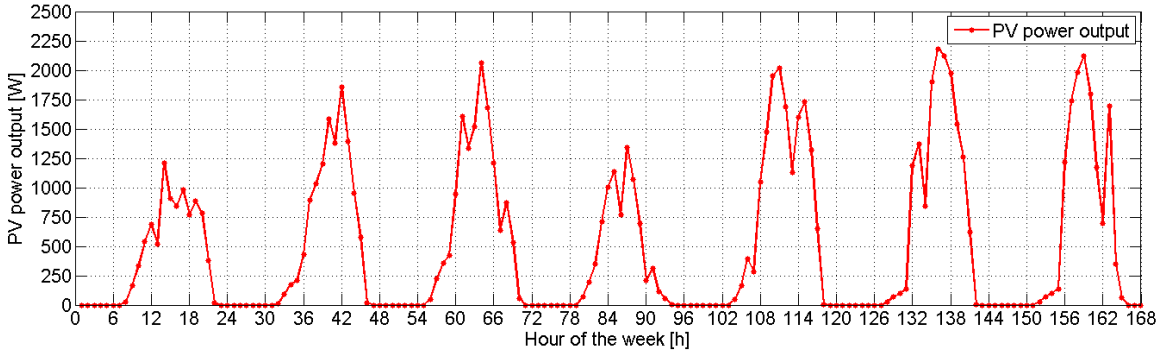

Figure 2.6: Example of the PV generation profile during one week of simulation.

Table 2.3: Main parameters of the PV installation where the measurements are conducted.

Parameter	Value	Unit
Rated power	2.80	kW
Peak production	2.78	kW
Yearly production	3395.73	kWh
Installation type	Rooftop PV	-
Azimuth angle	90° (east)	-
Tilt angle	15°	-

2.4 Electric Vehicles

In this last section of the chapter the EV technology is analyzed and a model of the EV load is proposed. First, the assumptions on which the model of the EV is created are presented, both regarding the battery modeling and the EV driving and availability patterns. The theoretical background and the modeling of Vehicle-to-Grid (V2G) and Voltage Droop Control are then illustrated. In the end, the issues due to an increased EV share in the power network, the solutions found in the literature, and the possible benefits of using EVs as distributed storages in networks with high PV share are presented.

2.4.1 EV technology

An EV is a vehicle that uses one or more electric motors for its propulsion. This general definition of EV includes road vehicles, rail vehicles, electric boats, electric aircrafts, and any other possible application of electricity for traction [2], [39]. In this project the focus will be on electric city cars. The term *EV* will be used in this project to refer to this particular application of electric motors.

There exist several types of commercially available EVs, which can be grouped into Plug-in Electric Vehicle (PEV), Fuel Cell Electric Vehicle (FCEV) and Hybrid Electric Vehicle (HEV) [2]. The objective of this work is to investigate the contribution of EVs in increasing the PV hosting capacity in a power network. For this reason the focus from now on will be on PEVs only, since FCEV and HEV do not directly charge their batteries from the grid [2].

The PEV battery market is nowadays covered mainly by three technologies: lead-acid, nickel metal hydride (NiMH) and lithium-ion (Li-ion) [40], [41]. Li-ion is the most promising technology for its high specific energy (Wh/kg) and power (W/kg) [2], and it is expected to be the most widespread battery technology in new EV applications [42]. For this reason Li-ion will be the only battery technology on which this work will focus its attention.

A commercially available Li-ion based EV city car, the 2014 Nissan Leaf, has been chosen as a model in this project. The capacity of the Li-ion battery pack is 24 kWh, which for the average driving efficiency 0.18 kWh/km η_{dri} allows a maximum range R_{max} of 133 km. Technical information about the vehicle can be found in Table 2.4.

Table 2.4: Nissan Leaf main technical specifications [43].

Parameter	Symbol	Value	Unit
Battery capacity	C_{rated}	24	kWh
Average driving efficiency	η_{dri}	0.18	kWh/km
Maximum range	R_{max}	133	km

Many factors affect the battery lifetime, one of the most important being the *State of Charge* (SOC) [40]. SOC is defined as the % value of the charge left in the battery compared to the battery rated capacity. The *cycle life* is defined as the number of complete charge–discharge cycles that the battery can perform, before its nominal capacity falls below a specified limit. This limit is set, in this work, as 80% of the battery initial rated capacity [40].

SOC values should be reduced from the theoretical 0-100% range for not deteriorating the battery lifetime and guaranteeing safe operation. Referring to [44], the lowest SOC admissible for Li-ion batteries to preserve their performances is 20%. The upper charge should also be limited, in order to avoid overcharging and safety related issues [45]. A upper value of 90% is set in this work.

To summarize, the EV Li-ion battery model used in this project will operate in the 20-90% SOC range. This restriction results in a maximum range of 93 km. The hypothesis on the battery are summarized in Table 2.5.

2.4.2 Battery Charger

It is likely that in the near future EV owners will charge their vehicle mainly at home, due to the drivers' habits and the present lack of charging infrastructures [2], [46], [47]. For these reasons, in this project only the EV home-charging is considered.

The EV charger modeled in this work is based on the specifications of the single-phase 3 kW charger provided with the Nissan Leaf [43]. Table 2.6 presents a summary of the charger model used in the simulations.

Due to the 85% charging efficiency η_{cha}, the full power charging $P_{max,DC}$ at the battery side will result in a 3.53 kW load $P_{max,AC}$ on the grid side. The Power Factor (PF) of the EV charger is reported to be in the range from 0.98 lagging to the unity factor [48], [49]. In this work the PF is assumed to be 1.

Table 2.5: Assumptions on the battery model.

Parameter	Value	Unit
Maximum SOC	90%	-
Minimum SOC	20%	-
Maximum range	93.1	km

Table 2.6: EV charger model used in the simulations [43].

Indicator	Symbol	Value	Unit
Power input $[AC]$	$P_{max,AC}$	3.53	kW
Power output $[DC]$	$P_{max,DC}$	3.00	kW
Input voltage	V_{rated}	230	V
Maximum current	I_{max}	16	A
Charging efficiency	η_{cha}	0.85	-
Discharging efficiency	η_{dis}	0.85	-
Power Factor	PF	1	-

2.4.3 Vehicle-to-Grid functionality

The basic concept of V2G is that an EV, when parked and plugged into the network, can either absorb energy and store into its batteries or discharge the batteries and provide power back to the grid [2], [40].

The implementation of V2G presents several advantages for the EV user and for the local DSO. On the DSO perspective, an EV with V2G functionality can be used as a distributed, fast acting energy storage. It can provide power in peak load times, reducing the network load and consequently reducing or deferring network upgrades, provide ancillary services and regulating power. The integration of EVs with V2G functionality will allow power systems to be more flexible with the synchronization between generation and load, since the EV can act both as a load and a generator, and thus accommodate higher shares of intermittent RES, such as PV [40].

On the EV and PV owner perspective, the use of V2G functionality can increase the self-consumption by storing the exceeding PV energy during daylight hours and powering the domestic load during peak hours. The EV can also generate revenue by storing the energy purchased when the price is low, and then providing part of the energy back to the network or the residential unit when the price is higher.

The V2G concept presents some limitation and drawbacks. The overall net efficiency of the V2G process depends on the product between the charging and the discharging efficiency of the EV battery, and can be calculated as:

$$\eta_{net} = \eta_{dis} \cdot \eta_{cha} \tag{2.10}$$

For the Li-ion battery of the EV analyzed in this work, the values of η_{dis} and η_{cha} are presented in Table 2.4, both assumed equal to 85%. This results in a net efficiency of 72.25%. This means that for every kWh provided by the EV back to the network requires approximately 1.38 kWh to be charged in order to restore the original SOC.

Another parameter that cannot be neglected in the analysis of V2G is the additional wear-out introduced by a more frequent and aggressive cycling of the battery, and the connected cost for the EV owner. Every additional charge-discharge cycle introduced by V2G operation will result in an additional consumption of the battery life compared to the normal operation.

For Li-ion batteries, such as the one of the Nissan Leaf analyzed in this work, the previously defined cycle life is dependent on the DOD of the charge-discharge cycle and other factors, such as ambient temperature and the discharge rate, which will not be analyzed in this work and left for future works. The relationship between cycle life and DOD is exponential, as it can be seen from Fig. 2.7

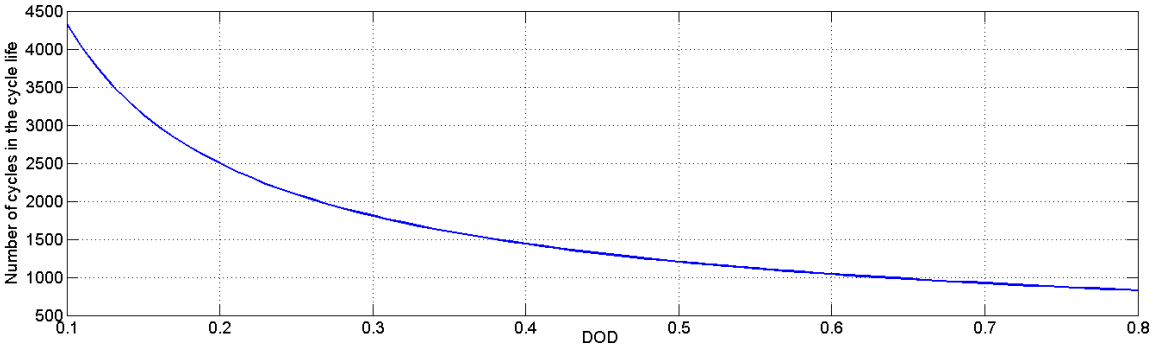

Figure 2.7: Exponential relations between DOD and cycle life for Li-ion batteries [40].

The curve of Fig. 2.7 has been approximated by [40] with Eq. 2.11.

$$ln(L) = -0.795 \cdot ln(D) + 6.5425 \tag{2.11}$$

which can be rewritten as:

$$L = 694 D^{-0.795} \tag{2.12}$$

where L is the battery life as number of cycles and D is the DOD of the charge-discharge cycle. In other words, each cycle of depth D will consume $1/L$ of the total cycle life.

A more detailed evaluation of the cost connected to the battery wear-out in V2G operation will be presented in Section 5.2, where the V2G functionality is added to the EV load modeling. In the next section, driving patterns for EVs in terms of energy demand and availability for home charging are proposed and discussed.

2.4.4 EV Driving Patterns

The driving patterns of EVs consist of data about the EV availability for charging and the SOC at the arrival at the charging spot. With the knowledge of the driven distance and the vehicle average efficiency in terms of kWh/km, it is possible to determine the SOC at the arrival at destination and, with simple calculations, the time and energy needed to restore the SOC to the desired level.

As presented in the introduction of this project, the EVs today on the road are a small fraction of the total number of cars; for this reason real EV driving patterns are difficult to obtain. Referring to [2], [50], the assumption that the EV users will follow the same driving patterns as ICE users is an acceptable approximation; therefore, the analysis of the driving data of conventional cars will be used to create driving patterns for EVs in this project.

Regarding the Italian case study, the 2012 EU mobility survey reports how in Italy a private car stays parked for more than 90% of the time [51]. This can be seen from the left plot of Fig. 2.8, where the average travel time of ICE vehicles during a week is compared between various EU countries. In the survey it has been highlighted how the average driving time for Italian ICE drivers is almost independent from the day of the week and around 1h15'; this means that for approximately 22h45' every day (over 92% of the time) the vehicle is parked somewhere.

As introduced in the previous section, in this project it is assumed that EVs can only be charged at home. This means that the time when the car is available for charging is smaller than the time the car is not used for driving: for example a commuter may park his/her vehicle at the working place where there is no EV charger available.

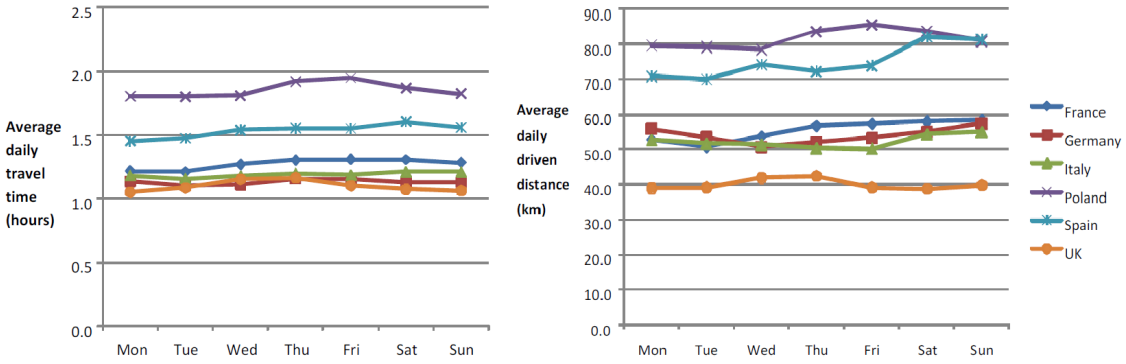

Figure 2.8: Average daily travel time per day of the week (left plot) and average daily driven distance (right plot) for a series of EU countries [51].

In this work some assumptions are made to define the EV availability for home charging; by EV availability is meant the time the EV is plugged into the network, regardless of the battery's SOC. Based on the data about home departure and arrival times and the average

number of trips done in a day found in the EU survey [51], it is assumed that the maximum availability for home charging will occur during the weekdays from 00:00 to 8:00 and from 19:00 to 24:00, and during the weekend. The probability of the EV being able to charge during these hours is set to 90%.

A lower value (50%) is set during the working hours, from 8:00 to 12:00 and from 14:00 to 19:00 during all the weekdays. As the survey reports how *'in Spain, Italy and France there is some share of individuals who return home in between of the working day'* [51], during the lunch break on the weekdays, from 12:00 to 14:00, an intermediate level of EV availability (70%) is assumed.

A visual representation of the EV availability for charging in the weekdays and the weekend is plotted in Fig. 2.9.

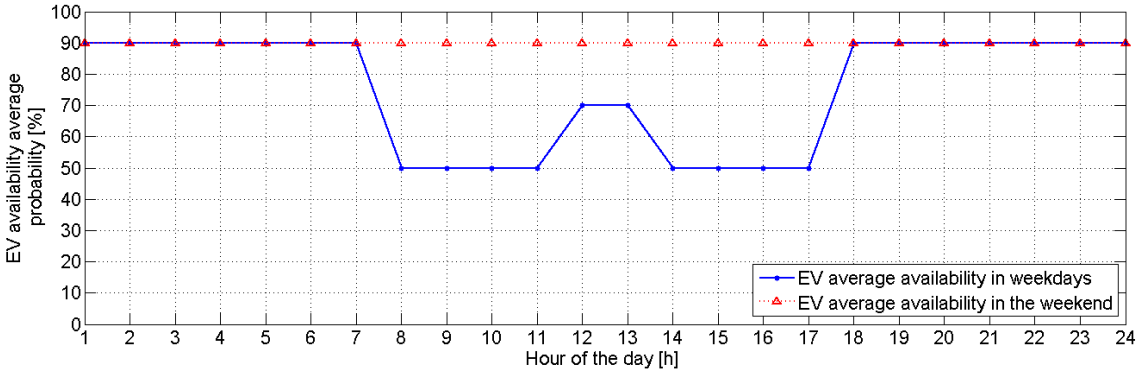

Figure 2.9: Scheme of the probability of the EV to be available for home-charging in the weekdays and the weekend [51].

From data about the driven distance and the average driving efficiency (0.18 kWh/km, see Table 2.4), the EV energy demand can be calculated. According to the EU mobility survey [51], the average daily driving distance in Italy is approximately 50 km, with limited differences between weekdays and weekend, as shown in the right plot of Fig. 2.8.

In this project the EV daily driven distance is selected randomly from a normal distribution, having mean 50 km and standard deviation 5. The standard deviation value has been chosen in order to have all the values in the range 0-93 km. The lower limit is set to give physical meaning to the driving distance, while 93 km is the maximum distance that the chosen EV can cover within the assumed 20-90% SOC range, as presented in Table 2.5.

2.4.5 EV Integration Issues in LV Grids

The EV charging process raises a number of technical issues for the DSO, due to the large amount of energy required, which can reach or even exceed the domestic load demand.

If the Nissan Leaf modeled in this work is driven for 50 km a day (the average driven distance in Italy) for 300 days in a year, the yearly energy demand will be:

$$E_{EV} = D_{day} \cdot 300 \cdot \frac{\eta_{dri}}{\eta_{cha}} = 50 \cdot 300 \cdot \frac{0.18}{0.85} = 3176.74 \text{ kWh/y}$$

where D_{day} is the average daily driven distance, η_{dri} is the average driving efficiency and η_{cha} is the EV charger efficiency. The EV yearly consumption is in this case more than the

domestic load demand considered for this work (2979.71 kWh/y, as presented in Table 2.1).

This additional load can result into increased line losses in the system, overloading of network components and voltage variations below the minimum limit along the feeder. The introduction of the EV home-charging load is particularly relevant in residential LV networks, where the uncoordinated charging of the EVs can overlap with the evening household power consumption, resulting in an increased peak load demand the network was not designed for [30], [48].

Another integration issue is represented by voltage phase unbalance. Since single-phase chargers will be the most common configuration in LV grids, it is possible that an unequal distribution of the EV chargers over the three phases will lead to voltage imbalance in the LV feeder [49]. It has to be remarked that since the residential customers in Italy are usually connected to a single phase of the LV system only, the phase unbalance due to EV charging can increase the already existing network background unbalance (introduced in paragraph 2.2.1).

2.4.6 Voltage Droop Control Functionality for the EV Charger

A possible solution to the issues that the EVs introduces in the power network is represented by Voltage Droop Control (VDC). With VDC functionality, the EV charger active power demand is controlled according to the voltage level at the connection point [52]. If the voltage V is lower than the rated value V_{rated}, the maximum power demand of the EV charger is decreased, until it is reduced to zero for a minimum voltage level V_{min}.

This method can help reducing the voltage variations in a power system, by reducing the EV load demand in case of undervoltage at the bus where the EV is connected, and shifting part of the EV load demand to hours where the voltage is higher.

Several voltage droop control strategies can be implemented. In this work the analysis is limited to one of the simplest, represented by a linear slope. A graphical representation of linear voltage droop control can be found in Fig. 2.10 and can be mathematically expressed as:

$$P_{droop}(V) = \begin{cases} P_{rated} & V \geq V_{rated} \\ K_p \cdot (V - V_{min}) & V_{min} < V < V_{rated} \\ 0 & V \leq V_{min} \end{cases}$$

where K_p is defined as:

$$K_p = \frac{P_{max}}{V_{rated} - V_{min}} \tag{2.13}$$

According to the constraints assumed in Sec. 2.3.3, it is assumed in this work to have $V_{min} = 0.95$ p.u. of the rated voltage.

2.4.7 Use of EVs to Increase PV Penetration in LV Grids

Battery storage is one of the main technologies used as a storage system [53], and the use of EVs as distributed battery storages represent a particular application of this technology.

A deferrable load, or flexible load, is an electric load which needs to be supplied for a part of the day and which can be deferred in time, Examples of flexible loads are air conditioning, heat pumps and some appliances, while other loads such as illumination do not have this property. EVs are flexible loads [2], since the battery charging process can be delayed and/or

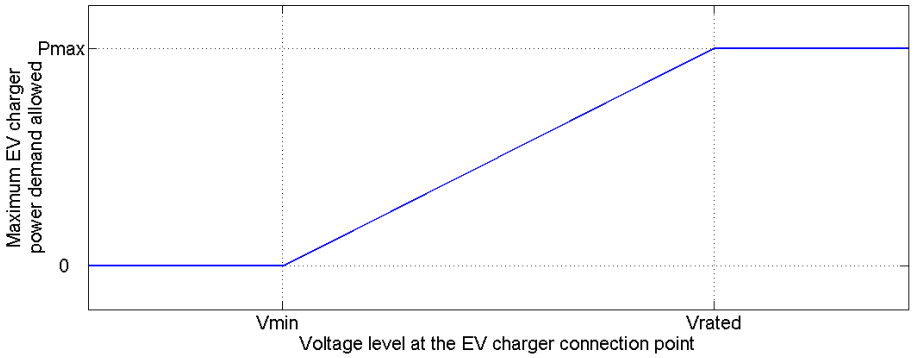

Figure 2.10: Scheme of the maximum charging power allowed with voltage droop control functionality. The EV is allowed to charge at full power for voltages over the rated value, while the charging is forbidden in case to undervoltages over 5%. The intermediate voltages result into intermediate charging power allowed.

modified in order to adapt to the network conditions or to meet more convenient electricity prices. For this reason the synchronization between the PV production and the EV load demand can be possible. Day-time charging reduces the evening load peak and increases the PV local consumption [30]. Referring to [54], it has been suggested how EVs can be used as a storage device for the surplus power generated by PV units, reducing the amount of power brought from the power utility and limiting the reverse power flow due to PV generation.

The use of EVs to solve the voltage rise problem in LV feeders with high penetration of PV is analyzed in [55]. The paper focuses on LV networks with high share of PV generation and EV demand, concluding that a relatively small EV penetration in residential grids is sufficient for providing voltage support during high PV generation periods, if the EV load demand is synchronized with the peaks of the PV production.

Voltage phase unbalance is another issue, introduced in LV grids by single-phase connections of Distributed Generation and load [24]. Voltage phase unbalance in the network can be reduced, if the EVs charge accordingly to the voltage of each phase, self-consuming the PV generated energy independently for each phase.

2.5 Electricity tariffs for Residential Customers

2.5.1 Time of Day tariffs

Time of Day (TOD) tariffs, also known as Time of Usage (TOU) tariffs, are used to avoid excessive load peaks in the grid, by applying a variable price according to the time of the day. A higher price is set during peak load periods, and lower rates during off-peak load period. The electrical customer can decide whether to shift part of the energy demand during off-peak hours, or pay accordingly.

An application of TOD tariffs, named *Tariffa Bioraria*, is at the present day the only electricity tariff available for Italian residential customers, such as those connected to the residential network analyzed in this work [56].

A more detailed description of the Italian TOD tariff, inclusive of the analysis of the final price formation, is available in Section 4.2.

2.5.2 Net Metering Service

Net metering is a service available for an electric consumer who also owns a generating unit, such as SPV. By using net metering service the energy produced, and not instantaneously self-consumed, can be delivered to the local distribution network, and it can be used to offset the electric energy provided by the DSO to the customer during the applicable billing period. In the event that the consumer's generation exceeds the consumption over the billing period, the customers is paid for the energy sold to the network, at a price per kWh lower than the cost of the purchased electricity.

In the Italian case study Net Metering is put on top of the above mentioned TOD tariff. Since the cost of the electricity purchased from the DSO is always greater than the reward for the excess energy fed into the grid, this service is most profitable when the energy is self-consumed. For this reason Net Metering represents the most profitable option for customers that own deferrable loads, such as EVs, since deferrable loads can variate their load demand to increase the self-consumption of the PV generated energy.

Net Metering service in the Italian scenario is analyzed in Section 4.3.

2.5.3 Real Time Pricing

Real time pricing (RTP) represents a future development of TOD tariff: with RTP the price of electricity varies with time according to the grid conditions, such as the loading level of the network components and the voltage magnitude, so as to better represent the variable costs of energy generation, transmission and distribution [57], [58].

Supplying an electric load during conditions of load peak demand is for the DSO more expensive than to supply the same load during off-peak hours, due to congestion in the network and higher line losses. Similarly, during peak load conditions the value of the PV generated energy is higher, since it can help reducing the loading of the distribution network by providing locally part of the needed energy.

An application of Real Time Pricing, Distribution Locational Marginal Pricing (DLMP), is proposed as a future scenario and analyzed in Section 5.1.

2.6 Summary

Large integration of PV generation in LV grids is limited by the presence of grid bottlenecks such as overvoltages, voltage phase unbalance and overloading of the network components. The introduction of EVs in the network can potentially solve these bottlenecks, since the EV charging process can absorb part of the PV generated energy and reduce the reverse power flow in the feeder. On the other hand, the introduction of EVs does present a series of integration issues as well, since the EV charging process, when combined with the residential peak demand, can result into undervoltages in the network and possible overloading of the network components. For EV and PV technologies to mutually benefit each other, the grid bottlenecks for the PV integration have to be identified and EV charging strategies have to be designed accordingly.

3 Adaptation of the CIGRÈ Benchmark Model

Based on the theoretical background presented in the previous chapter, a model of a LV residential grid for the Italian case study is built. Using the CIGRÈ benchmark model for LV networks as a starting point, an adapted model is proposed and tested. The present PV hosting capacity of this adapted model is investigated, and the grid bottlenecks are determined.

3.1 Analysis of the CIGRÈ benchmark model

A benchmark model is chosen, in order to maintain the important technical characteristics of a real grid, while reducing the complexity and the wide range of differences between the existing LV networks.

The LV network model developed within the EU project *Microgrids*, adopted by the Task Force CIGRÈ C6.04.02 as a European benchmark model for LV networks [59], has been considered for this work as a starting point.

3.1.1 Description of the CIGRÈ benchmark model

A schematic representation of the benchmark model is shown in Fig. 3.1.

The model represents a LV network powered from the LV busbar of a MV/LV transformer, serving a residential area through underground cables. One feeder is modeled in detail, while the others are represented with an aggregate load connected to the LV busbar of the transformer (not displayed in the figure).

The residential customers are represented as aggregate loads. Those aggregate loads and distributed generation units are connected along the length of the feeder and its branch. The benchmark model provides a load profile for the residential loads, which is plotted in Fig. 3.2. The feeder parameters are listed in Table 3.1, while the transformer main characteristics are described in Table 3.2.

DIgSILENT PowerFactory has been used to recreate the model of the benchmark LV network. The network elements characteristics are modeled according to the data of [60].

3.1.2 Limits of the Original Benchmark Model

By conducting an analysis based on unbalanced load-flow simulations, it can be seen how the benchmark model represents a strong grid, with no power quality issues or overloading of any

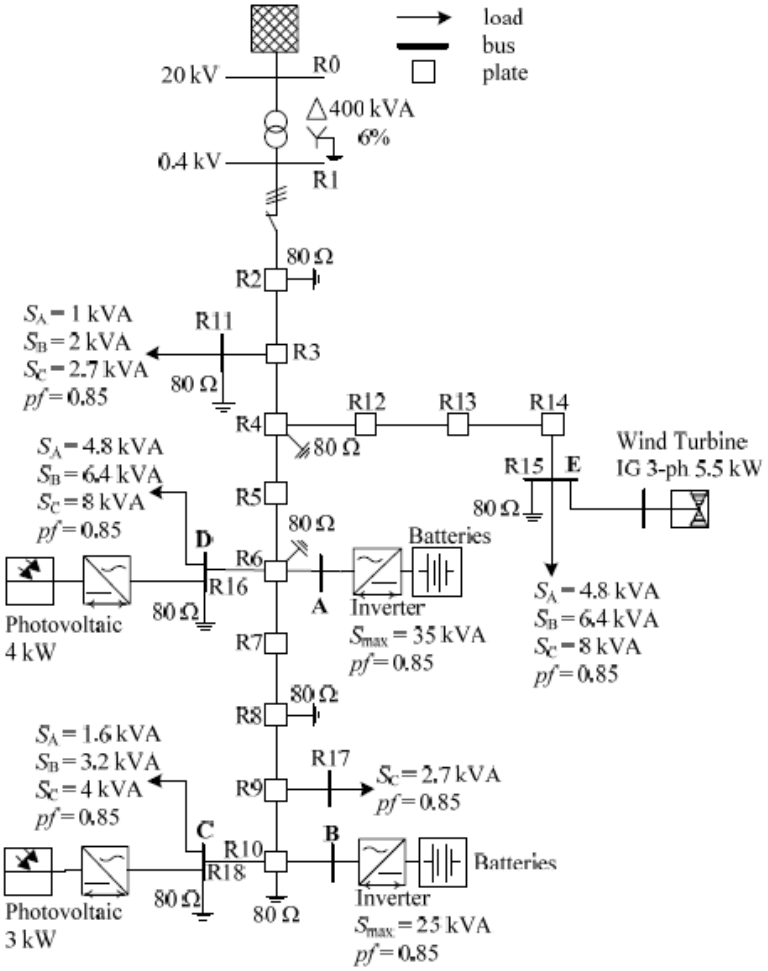

Figure 3.1: CIGRÈ LV distribution network benchmark [60].

Table 3.1: Parameters of the LV benchmark model; Node C is the furthest node (FN) from the distribution transformer.

Parameter	Unit
Grid topology	Radial
Number of feeders modeled in detail	1
Number of household loads	5 (aggregate loads)
Load installed capacity	55.6 kVA
RES installed capacity	12.5 kVA
Impedance from the LV busbar to the FN	$0.084675 + j0.0487\ \Omega$
Voltage sensitivity at the FN (dV/dP)	0.603 p.u./MW
Distance FN - transformer	345 m

Table 3.2: Main parameters of the MV/LV distribution transformer.

Parameter	Value	Unit
Primary voltage	20.0	kV
Secondary voltage	0.4	kV
Rated power	400	kVA
Impedance	5%	-
Connection	Dyn11	-

network component. This represent a limit for the analysis of this project, because the study of smart charging strategies for the EV charging are unnecessary if there is no issue in the integration of PV units in the network.

Even in the unlikely event of $f_{co} = 1$, e.g. 100% load demand compared to the rated power from every residential unit in the grid, the most loaded cable, the segment of the main feeder connected to the distribution transformer, will experience a current of only one third of its ampacity. Regarding the voltage magnitude fluctuations, the scenario with 100% load and no generation does not create issues for the integration of more load in the network. As an example, the voltage profile along the feeder in the 100% load scenario is shown in Fig. 3.3. Data about power quality measurements are available in Table 3.3.

To determine how much PV could be theoretically be installed in the benchmark network, a simplified model of the feeder is proposed, illustrated in Fig. 3.4.

The line is representative of the total length of the feeder. Branches and loads are excluded, and a PV unit is connected at the end of the feeder. This represents the worst case scenario for the PV integration in the grid, since no power is locally consumed, and the impedance between the generation unit and the distribution transformer is the maximum. Both the local

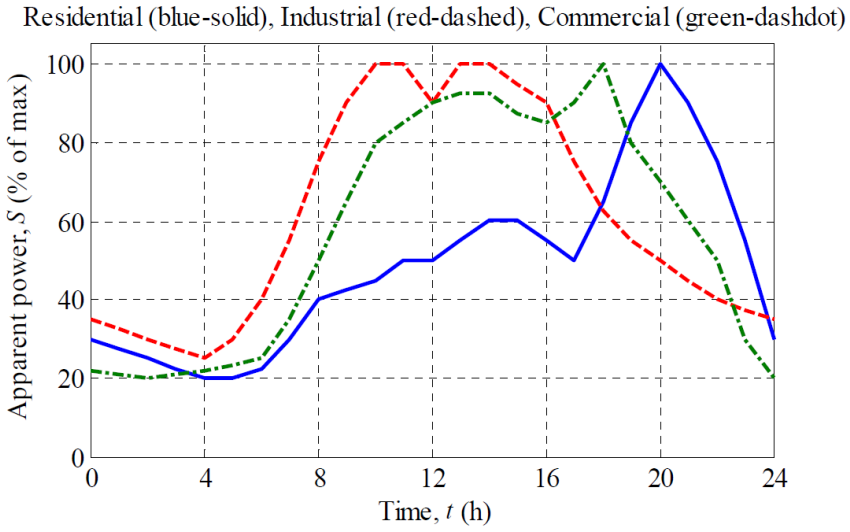

Figure 3.2: Load profiles for household loads (in blue), commercial and industrial loads [60].

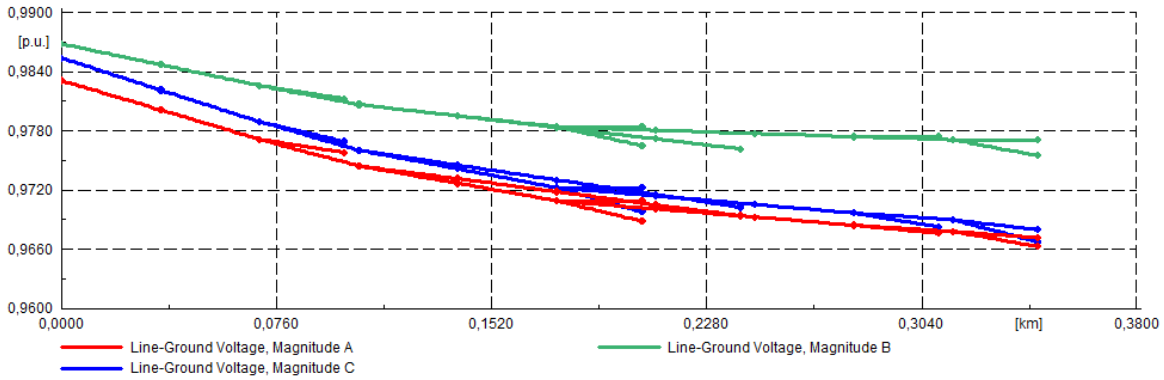

Figure 3.3: Voltage profile along the feeder of the benchmark model with 100% load demand (compared to the rated value) and no generation.

Table 3.3: Data about the present scenario of the benchmark model, worst case scenario (maximum load demand from all the loads), no PV units or EVs connected.

Element	Position	Limit	Value	Unit
Maximum loading of a line	Line 1	100	33.5	% on cable ampacity
Minimum phase voltage	BUS7,A	95.0	96.6	% of the rated value
Maximum phase unbalance	BUS7	2.00	0.65	%VUF

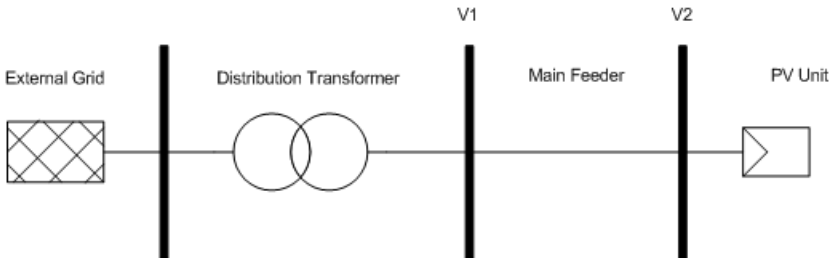

Figure 3.4: Single line diagram of the simplified model of the LV feeder.

load consumption of part of the PV generated energy and the installation of part of the PV installed capacity closer to the distribution transformer will lead to an increase in the PV hosting capacity.

Assuming that the voltage at the secondary side of the transformer is set to 1 p.u., the overvoltage at the busbar at the end of the feeder can be calculated rewriting Eq. 2.1 as:

$$\Delta V = V_2 - V_1 = \frac{R \cdot P + X \cdot Q}{V_1} \tag{3.1}$$

where P and Q are the active and the reactive power outputs of the PV unit, V_1 is the voltage at the busbar 1, R is the line resistance and X is the line reactance. R and X can be calculated by multiplying the distributed parameters r and x of the main feeder conductor by the length of the line l. All the parameters are listed in Table 3.4.

Table 3.4: Parameters used in the simplified benchmark model.

Parameter	Symbol	Value	Unit
Voltage at the transformer secondary side	V_1	1.000	p.u.
Distributed resistance	r	0.163	Ω/km
Distributed reactance	x	0.136	Ω/km
Total length of the feeder	l	0.315	km
Line resistance	R	0.051	Ω
Line reactance	X	0.043	Ω
Cable ampacity	I_{max}	310.0	A

The limits for the installed PV capacity considered are the voltage level at the PV busbar, which should stay in the 0.95-1.05 p.u. range, and the loading of the cable with respect to the cable ampacity.

Eq. 3.1 can be simplified even more considering a unity power factor for the PV units, having these only active power P as output. The line current can now be computed as:

$$I_{line} = \frac{P}{\sqrt{3}V_2} \tag{3.2}$$

The overvoltage at the busbar at the end of the feeder can be written as:

$$\Delta V = \frac{R \cdot P}{V_2} \tag{3.3}$$

Eq. 3.2 and Eq. 3.3 can be used to determine the maximum PV hosting capacity at the end of the feeder. Considering the loading of the line as constraint, Eq. 3.2 can be rewritten as:

$$P_{max,I} = I_{max} \cdot V_2 \cdot \sqrt{3} = 310 \cdot 400 \cdot \sqrt{3} = 214.00 \text{ kW} \tag{3.4}$$

Considering the overvoltage at the end of the feeder as the constraint, the maximum installable PV power can be found as:

$$P_{max,\Delta V} = \frac{V_2 \Delta V}{R} = \frac{400 \cdot 20}{0.051345} = 155.80 \text{ kW} \tag{3.5}$$

From Eq. 3.4 and 3.5, it can be seen how the maximum PV capacity is restricted by the overvoltage at the busbar. In this scenario the loading of the line is limited to 68.8%. The information of the loading of the distribution transformer is in this case not relevant, since the other feeders connected to it are not taken into consideration in this analysis.

155.80 kW of PV installed capacity represents 278% of the grid load demand (55.6 kW, see Table 3.1), and more than 10 times of the installed distributed generation in the benchmark model. It has to be remembered that this scenario represent the worst case condition for the PV integration in the network. The benchmark model is not suitable for a study on PV integration issues, since the PV installed power can be extended way over its present share.

For representing the Italian case study, where individual connections are predominant in LV residential networks as introduced in Section 2.1.3, the simulation of individual loads is limited by the reduced number of connection points in the original benchmark model.

For these reasons the benchmark model has to be modified, by using the procedure explained in the following section.

3.2 Adaptation of the Benchmark Model

In this section the description of the methodology followed to adapt the benchmark model, in order to better represent the Italian case study, is presented. The adapted model is then compared with the original benchmark and tested through an analysis of simulation data.

3.2.1 Modifications on the Original Model

While the main structure of the feeder and the distribution transformer parameters (listed in Table 3.2) are maintained, a series of modifications have been done respecting the criteria presented in [60], and are listed in the following part of this section.

Line Length

The length of the sections that compose the main feeder is increased, from 35 m to 50 m. This modification results in a weaker network, more susceptible to voltage rise, since the line impedance is directly proportional to the length of the feeder.

Two additional segments are added at the end of the feeder, resulting in a total length from the transformer to the furthest node of 510 m, compared to the 345 m of the original model, listed in Table 3.1.

Line Types and Parameters

Single-phase connections are modeled, in order to give a better representation of the Italian case study. A single-phase $6mm^2$ Cu line is modeled to simulate the individual house connection, while the other line types are maintained. Data about the network elements are listed in Table 3.5.

Table 3.5: Data about the network elements in the benchmark model, data from [38], [60].

Line type name	Cross-section (neutral) (mm^2)	R_{ph} (Ω/km)	X_{ph} (Ω/km)	Ampacity (A)	Length (m)
Main_line	120 (120)	0.153	0.136	310	35
Branch_line	70 (50)	0.266	0.151	229	105
Branch2_line	50 (35)	0.387	0.295	188	30
Domestic_line	6 (6)	3.080	0.200	57	30

Loads and Distributed Generation

Individual household loads are modeled rather than the aggregate ones of the original benchmark model. Each individual single-phase domestic connection is modeled as two loads in parallel, representing the normal household profile and the EV charger, and a PV generating unit, as shown in Fig. 3.5. A total of 30 households are individually recreated in the network.

For the domestic load, the profiles described in Section 2.2.1 are used. The PV units follow the generation profile described in Section 2.3.4

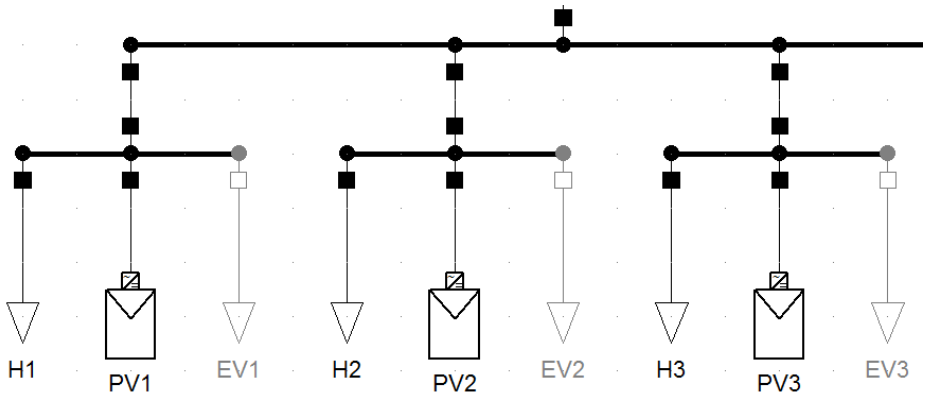

Figure 3.5: Model of three individual households connected to the same busbar. H1-3 loads represent the normal household load, EV1-3 the EV charging points and PV1-3 the PV generating units. Each household bus bar is connected to a different phase of the network to provide current symmetry among the three phases. The EV loads are out of service in this initial stage of the simulations, which in the software used results in the gray coloring.

To model the other feeders connected to the LV side of the distribution transformer, aggregate loads and generating units are used. Two aggregate loads representing the other feeders connected to the MV/LV transformer are modeled using data and load profiles from the benchmark model, while another aggregate load representing public illumination is modeled according to the procedure introduced in 2.2.2.

An aggregate PV generating unit is modeled to represent the distributed generation present in the other feeders. The same generating profile as for the individual PV units, scaled according to the rated power, is used for the aggregate ones.

All the loads and distributed generation units used in the model are listed in Table 3.6, while all the load and generation profiles used are available as spreadsheets in the CD attached to this report.

Table 3.6: Data about the household loads and the PV units in the model.

Network element	Rated power (kVA)	Number of units	Connection	Power factor	Name in the model
Individual units					
Individual PV unit	Variable	30	Single-phase	1	PV1-30
Household load	4.50	30	Single-phase	0.95	H1-30
EV charger load	3.53	30	Single-phase	1	EV1-30
Aggregate units					
Aggregate PV	50.00	2	Three-phase	1	3PV1-2
Public Illumination	12.00	1	Three-phase	1	ILL
Aggregate feeder 1	100.00	1	Three-phase	0.85	AGG_1
Aggregate feeder 2	100.00	1	Three-phase	0.90	AGG_2

A comparison between the adapted model and the original model, based on the parameters of Table 3.1, is presented in Table 3.7.

Table 3.7: Comparison between the parameters of the LV benchmark model and the adapted model; FN = Furthest Node.

Parameter	Unit	
	Benchmark model	Adapted model
Grid topology	Radial	Radial
Number of feeders modeled in detail	1	1
Number of household loads	5 (aggregate loads)	30 (individual houses)
Load installed capacity	55.6 kVA	147 kVA
RES installed capacity	12.5 kVA	Variable
Transformer - FN impedance	$0.084675 + j0.0487\ \Omega$	$0.10368 + j0.08775\ \Omega$
FN voltage sensitivity (dV/dP)	0.603 p.u./MW	0.6735 p.u./MW
Distance FN - transformer	345 m	510 m

The obtained single-line diagram model of the modified benchmark network is shown in Fig. 3.6.

3.2.2 Load Flow Analysis of the Adapted Benchmark Model

The adapted model is tested with an analysis based on unbalanced load flow simulations. BUS8, the furthest node of the feeder, is also the node with the highest voltage sensitivity in the network, and as a consequence it is the bus where the highest variations in the voltage magnitude are registered. For this reason the voltage profile at BUS8 is analyzed.

The load flow simulations conducted show increased variations in the voltage magnitude, when compared to the original benchmark model, but almost always within the +5%/-5% range assumed. This can be visualized from the yearly voltage profile of BUS8, shown in the plot of Fig. 3.7.

The only violation is registered at hour 7907 (11am on the 26^{th} of November). During this hour the load coincidence factor f_{co}, expressed by Eq. 2.2, reaches its maximum value, and the maximum residential load demand results in an undervoltage at the furthest node of the feeder. Since the violation occur only once in one year of simulations, and the undervoltage is above 94% of the rated value, it might be acceptable in the normal operation of a LV distribution grid.

Voltage phase unbalance is limited in this case to background unbalance noise, concept introduced in Section 2.2.1. The %VUF index never violates the 2% constraint, as it can be seen from the plot of Fig. 3.8.

The maximum loading level of all network components is below the maximum values. The line with the maximum loading is a residential cable connection (C15 in the model), with a 34.2% loading compared to the ampacity of the cable. The distribution transformer loading is limited at 58.8% of its rated power. The overall feeder line losses are limited to 558 kWh, less than 0.06% of the yearly load demand. All the simulation results are summarized in Table 3.8.

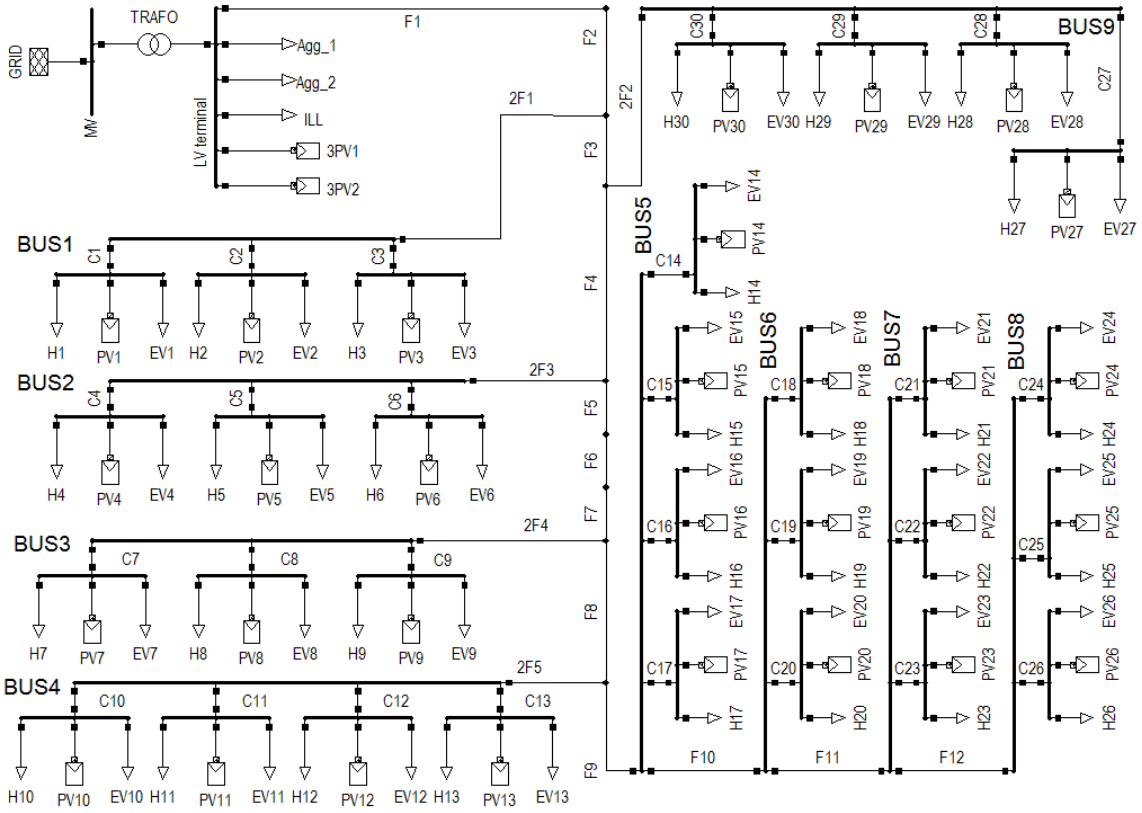

Figure 3.6: DIgSILENT model of the adapted benchmark, used as a model of an Italian residential LV grid in this work.

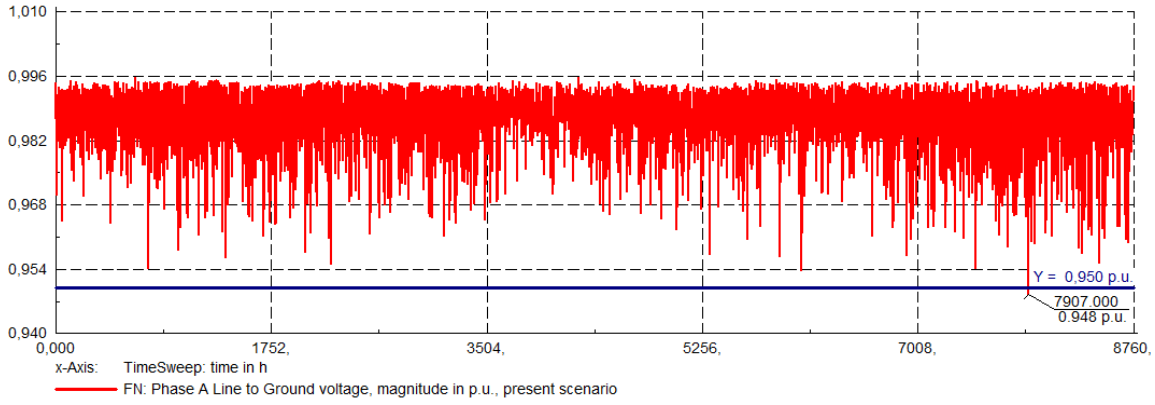

Figure 3.7: Yearly voltage profile of phase A at BUS8 for the present scenario of the grid, with no EVs and PVs installed in the feeder. The -5% voltage constraint is violated only for one hour of the year, hour 7907, due to high simultaneity of residential load demand.

The simulation results are suitable for a LV distribution grid, which is normally sized for future increase of the load demand [17], and leave room for EVs to charge, even if no distributed generation is installed in the network. At the same time, the adapted model is

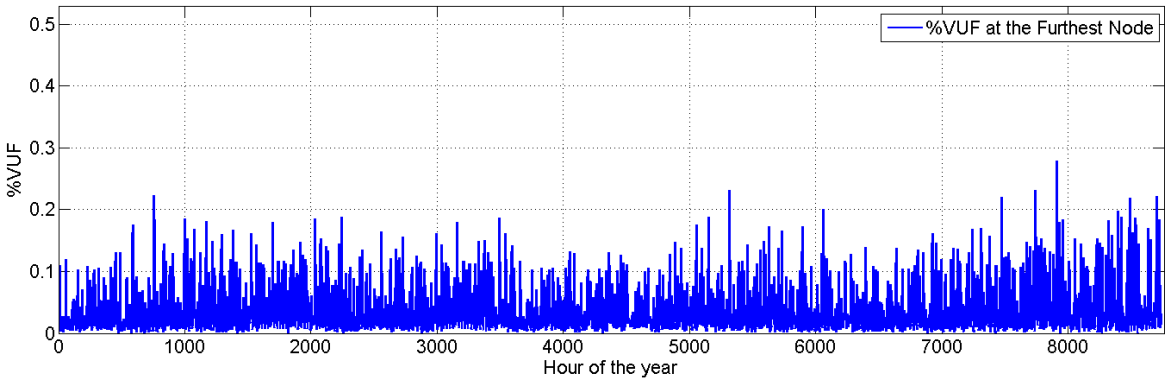

Figure 3.8: Background unbalance in terms of %VUF values for one year of simulation at BUS8, the bus where the highest unbalances are registered.

Table 3.8: Power quality indicators, testing of the model, no PV or EV units in the feeder.

Indicator	Position	Value	Limit
Minimum bus voltage (p.u. on rated value)	BUS8,C	0.948	0.950
Number of occurrences (h/y)		1	
Line losses (% of load demand)	-	0.058	-
Maximum %VUF	BUS4	0.274	2.000
Maximum line loading (% on ampacity)	C15	34.2	100
Maximum transformer loading (% on rated power)	-	58.8	100

proven to be more sensible to voltage fluctuations than the original benchmark model. This might lead to integration issues for high shares of PVs installed in the feeder.

A process to determine the hosting capacity for PV generation in this adapted model will be presented in the next section. The PV hosting capacity will then be evaluated at the scenario for the grid, where no EVs are connected to the network.

3.3 Determination of the Maximum PV Hosting Capacity

An iterative process is proposed for the determination of the maximum PV hosting capacity. The PV generation profile obtained form measurements, described in Section 2.3.4, is multiplied by a scaling factor s. The rated power of each PV unit in the network is calculated as:

$$P_{host} = s \cdot P_{meas} \tag{3.6}$$

where P_{meas} is the rated power of the PV unit where the measurements are conducted (2.80 kW, see Table 2.3). In the beginning the scaling factor s is set to 0. Each iteration increases the scaling factor s by a fixed step. Unbalanced load flow simulations are conducted at each iteration, in order to determine if any of the constraints about the power quality

indicators is violated. The considered constraints regard voltage magnitude, voltage phase unbalance and loading of the network components, as described in Section 2.3.3. If one or more constraints are violated, the maximum PV hosting capacity has been reached.

The algorithm is implemented with a DPL script, and it is illustrated by the flowchart of Fig. 3.9.

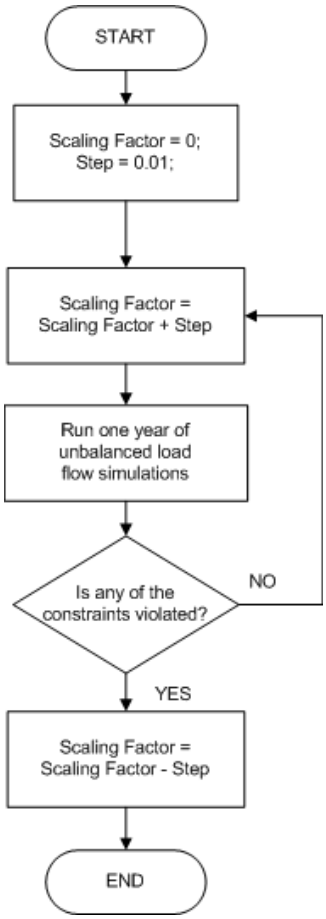

Figure 3.9: Flowchart of the algorithm used in this work to determine the feeder PV hosting capacity.

The maximum PV rated power for each of the PV units in the network is found to be 2.775 kW. This represents the rated power P_i of each of the i rooftop PV units plugged into the grid, which do not violate the assumed constraints at any hour of the year.

The feeder hosting capacity can be calculated as:

$$P_{host} = n_i \cdot P_i = 30 \cdot 2.775 = 83.25 \text{ kW}$$

The PV hosting capacity at the present state of the grid is limited by the voltage magnitude at BUS8, the furthest node of the feeder. Any increase of the PV installed power in the feeder over the P_{host} value previously evaluated will result in a violation of the +5% overvoltage limit assumed as constraint in this work.

As introduced in Section 2.3.2, overvoltages are harmful for the grid infrastructure and the customers connected to it; even if a 5% voltage rise over the rated value does not directly

create particular issues, if combined with a rise in the MV voltage level can lead to violation of the ±10% EN 50160 requirements. Since this project does not take into account modifications in the MV voltage level, any violation of the conservative ±5% voltage range are considered as potentially dangerous and so for conservative reasons there is set the constraint.

The voltage profile of Phase A at BUS8, with the PV rated power scaled to the hosting capacity value, in shown in 3.10. The voltage is always inside the -5% / +5% boundaries; the distributed generation has also a positive effect on the only undervoltage violation registered at the present state of the grid in Fig. 3.7.

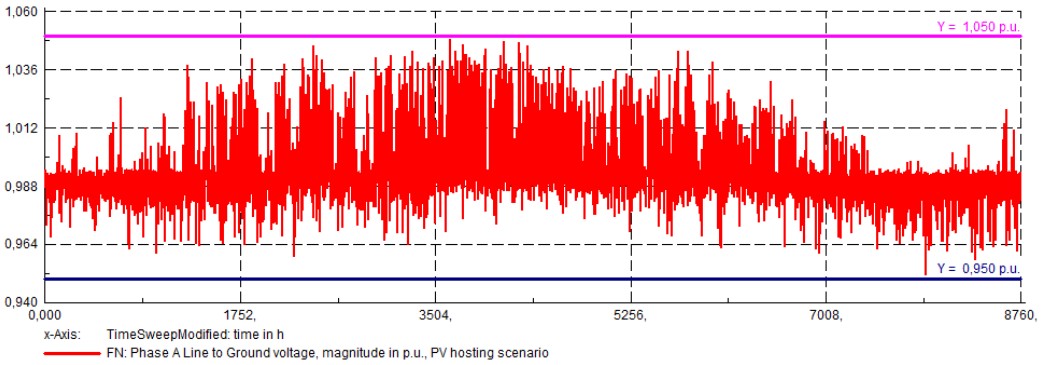

Figure 3.10: Voltage profile of Phase A at BUS8, the furthest node (FN) of the feeder, with the maximum PV hosting capacity reached. Only Phase A is displayed, since all three phases present the same behavior.

Regarding the loading of the network components, no significant overloading situation is registered. Both the most loaded line of the network (Line 1, the first segment of the main feeder) and the distribution transformer never register loading levels over 50% and 60% respectively. The yearly loading profile are shown in the plots of Fig. 3.11 for the line and Fig. 3.12 for the transformer.

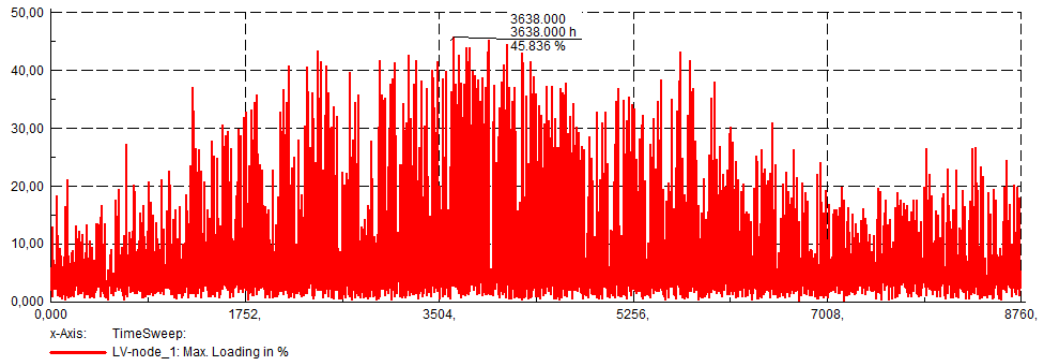

Figure 3.11: Loading of the most loaded line in terms of % of the cable ampacity over one year of simulation, present state of the grid scenario.

Regarding the voltage phase unbalance, Fig. 3.13 shows that in some hours of the year the %VUF index is close to the maximum limit. The voltage disturbances are more frequent in the central hours of the year, where the solar irradiance, and so the PV power output, are on higher on average. All the results about power quality measurements are summarized in Table 3.9.

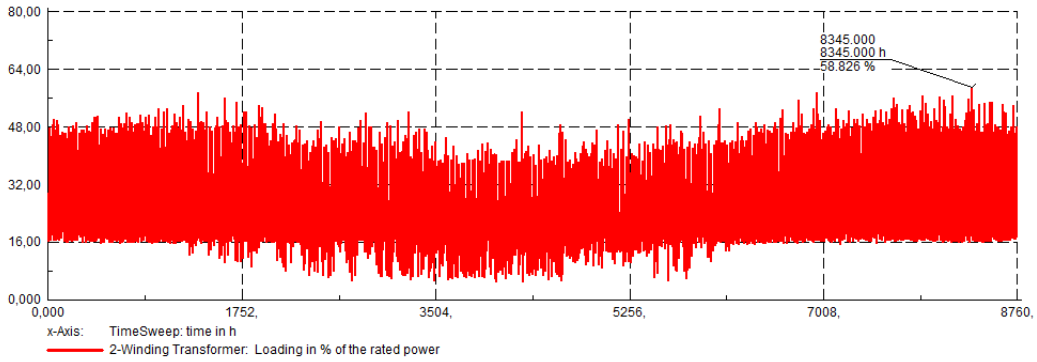

Figure 3.12: Loading of the distribution transformer in terms of % of the rated power over one yer of simulation. The maximum value is limited to 58.8%, leaving room for increased load demand.

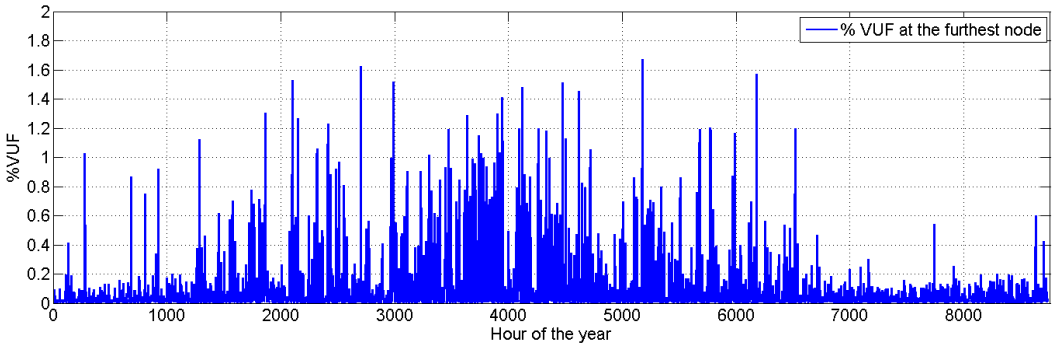

Figure 3.13: Background unbalance in terms of %VUF values for one year of simulation at BUS8, where the highest unbalances are registered, present state of the grid scenario.

Table 3.9: Grid data for the PV maximum hosting capacity during hour 3638, when the one of the limits taken into account is realized.

Indicator	Position	Value	Limit
Maximum phase voltage (p.u. on rated value)	BUS8,A	1.048	1.050
Maximum %VUF	BUS8	1.670	2.000
Maximum line loading (% on ampacity)	Line 1	48.3	100
Maximum transformer loading (% on rated power)	-	58.8	100

From the results obtained in the evaluation of the PV hosting capacity at the present state of the grid, it can be concluded that the voltage related issue are the limiting factor for a further increase of the installed power in the LV radial network considered. For this reason, the use of EVs as distributed storages as a solution to improve the PV hosting capacity seems feasible, since it has been reported as effective in solving voltage rise related issues in [55], [61].

3.4 Summary

The CIGRÉ LV benchmark represents a model of a strong grid, where no issues are registered in the integration of large SPV shares. An adapted model is proposed in this work, where single-phase loads as well as generating units and individual connections are modeled, in order to better represent the Italian case.

The grid bottleneck for the PV integration in the adapted LV residential grid model is found to be the voltage magnitude at the end of the radial feeder. The voltage phase unbalance %VUF index is close to the maximum values for some hours of the year. The loading of all network components, instead, does not represent an integration issue.

The PV hosting capacity at the present state of the grid is 83.25 kW, equivalent to a rated power of 2.77 kW for each of the rooftop PV units modeled.

4 Integration of EVs and PV Units in the Network

In this chapter the Electric Vehicle is introduced in the simulation model of the residential LV network. Two EV charging scenarios are proposed, based on the present electricity tariffs for Italian residential customers. The first considers the present Time of Day (TOD) electricity tariffs for Italian residential customers, while the second scenario includes net metering service, available for customers who own a generating unit, such as SPV, and an EV.

Voltage droop control functionality for the EV charger, described in Section 2.4.6, is implemented for both scenarios. The scenarios are evaluated with and without this functionality, in order to evaluate if and how this affects the EV impact on the grid.

An optimization process is proposed for each scenario, with the EV load demand as control variable and the cost of electricity for the EV owner as cost function. The impact of different EV shares on the grid bottlenecks and the feeder PV hosting capacity is analyzed, and the results are in the end discussed.

4.1 Simulation Procedure

The simulation process proposed to analyze the scenarios can be summarized as follows:

- The EV load profiles are generated as the result of an optimization process, with the use of an algorithm implemented in MATLAB. The control variable is the EV charger load demand, the cost function is the cost of the EV home-charging for the EV owner and the constraints are derived from the EV availability, the driving patterns, the battery SOC and the charger technology. A flowchart of the process used to generate one EV load profile is available in the Appendix in Fig. 1, while the MATLAB scripts used are available in the CD attached;

- The EV load profiles are applied to the simulation model of the LV residential network described in Section 3.2;

- Unbalanced load flow simulations are performed, for one year of simulation, for different EV penetration percentage levels. The EV shares considered in this work are illustrated in Section 4.1.1;

- For each simulation conducted, a list of power quality indicators is extracted from the simulation model and analyzed, in order to determine the impact of the EV loads in the network and the grid bottlenecks;

- By applying the PV hosting capacity algorithm described in Section 3.3, the new PV hosting capacity is determined for both TOD and Net Metering scenarios, for each of the EV shares taken into account.

The parameters considered to evaluate the feeder power quality are: the maximum loading of all the network components, the average and maximum voltage phase unbalance (%VUF), the minimum bus voltage and the feeder line losses. The description of those parameters and their maximum values are available in Section 2.3.3.

All the parameters are evaluated on a yearly base, in order to consider the seasonal behavior of the domestic load demand and the PV power output. In case of one or more violations of one of the constraints selected, the number of occurrences of the violation is presented together with the parameter involved. The simulation's resolution is one hour, so each occurrence represents 1h/y.

4.1.1 EV Shares

Different EV shares are considered, summarized in Table 4.1. The EV chargers, modeled according to the data of Table 2.6, are distributed equally among the three phases along the feeder for every EV share considered, and they are connected to the same phase of the domestic connection and the rooftop PV unit.

Table 4.1: Different shares of EV considered in the simulations; 100% = 1 EV for every residential customer in the feeder.

	EV share (%)				
	(0)	20	50	70	100
Number of EVs in the model	0	6	15	21	30

It is assumed that the EVs are added to the residential feeder starting from the furthest node of the grid, BUS8, and proceeding towards the distribution transformer, following the same conservative approach as in [62].

4.1.2 Voltage Droop Control Implementation

For both the scenarios analyzed in this chapter, the implementation of voltage droop control for the EV charger, introduced in Section 2.4.6, is taken into consideration. Each scenario is evaluated both with and without this functionality, in order to prove its efficacy in reducing the grid bottlenecks for the EV integration in the feeder.

It has been assumed that the lowest voltage at which the EV can still charge, when voltage droop control is applied, is 0.95 p.u. of the rated voltage, being this value defined also as a lower limit for the voltage magnitude in the feeder.

To generate the EV load demand when voltage droop control functionality is applied, an iterative co-simulation process between MATLAB and PowerFactory is used. While the calculation of the EV energy demand, availability for home-charging and maximum allowed charging power demand is performed with MATLAB, the application of the EV load demand, and the measurements of the new bus voltages, are performed using PowerFactory. The co-simulation procedure is necessary, in order to have a feedback on the bus voltage magnitude

where the EV is connected, when the load due to the EV charging process itself is applied. For each simulation hour, the loop for calculating the EV charger maximum power demand is repeated for a fixed number of iterations. This number is set to 10, in order to guarantee the convergence of the process for every hour.

The flowchart of the co-simulation process is available in the Appendix in Fig. 2.

4.2 Time of Day Tariff scenario

4.2.1 TOD Tariff for Italian Residential Customers

As introduced in Section 2.5.1, the electricity tariff available for Italian residential customers, known as *Tariffa Bioraria*, is one example of TOD tariffs.

The final price of electricity for the Italian residential customer, under TOD tariff conditions, is the result of the sum of three components:

- A *fixed component*, independent from the electrical consumption. As described in Table 4.2, this component is the sum of two different constants and a term directly proportional to the customer's connection rated power.

- A component proportional to the *energy consumption*, dependent on the forecasted yearly consumption in kWh. The cost of this component is low for consumption below 1800 kWh/y, in order to promote energy savings, and it increases gradually for the energy consumed over this limit, as it can be seen from Table 4.3.

- A component *dependent on the time of the day* when the electricity is consumed. The Italian TOD tariff differentiates only between peak hours, named F1, to non-peak ones, named F2, by applying two different electricity prices. The off-peak hours are from 19:00 to 8:00 on weekdays and all day on weekends, while the on-peak hours are from 8:00 to 19:00 on weekdays. The time range application is summarized in Table 4.4.

  To encourage the customers to consume during off-peak hours, the electricity price in F2 is more economical than during peak hours. The comparison between F1 and F2 prices is available in Table 4.5.

Table 4.2: Fixed price components in the formation of the final electricity price for the Italian residential customer [63].

Component	Rate	Unit
Grid service fixed rate	20.1120	€/customer/year
Retail fixed rate	25.6332	€/customer/year
Rated power rate	1.3525	€/kW

Using the parameters listed in Table 2.1, on which the residential customer is modeled in this work, the final price of electricity results to be 24.08 c€/kWh during peak hours and 23.45 c€/kWh during off-peak hours. Those values are assumed as base prices in the continuation of this work, and are summarized in Table 4.6.

Table 4.3: Price components proportional to the forecast year consumption in kWh for the Italian residential customer [63].

Consumption range	Rate	Unit
0-1800 kWh/y	0.1088	€/kWh
1801-2640 kWh/y	0.1259	€/kWh
2641-4440 kWh/y	0.1658	€/kWh
> 4441 kWh/y	0.2084	€/kWh

Table 4.4: Time range application of the Italian TOD tariff; F1 = peak hour, F2 = off peak hours.

Time range		Weekdays	Weekend
From	to		
0:00	8:00	F2	F2
8:00	19:00	F1	F2
19:00	24:00	F2	F2

Table 4.5: Prices for peak hours (F1) and non peak ones (F2), for a residential customer as the one modeled in this work.

Component	F1 (€/kWh)	F2 (€/kWh)
Energy Price	0.0673	0.0609
Network Charges	0.0134	0.0134
Excises	0.0227	0.0227

Table 4.6: Final electricity price rates for the residential customer, TOD scenario.

Time application	Symbol	Rate (c€/kWh)
Peak hours	$c_{TOD,F1}$	24.08
Off-peak hours	$c_{TOD,F2}$	23.45

4.2.2 Optimization Process

In this work it is assumed that the main priority for the EV owner is to use his/her vehicle for driving. No modifications of the EV availability for charging according to price signals are proposed in this work. Once defined the EV availability and the EV energy constraints, it is assumed that the EV owner always wants to charge its vehicle at the minimum cost. To generate the EV load demand an optimization process is used, with the EV charger power demand as control variable, and the cost for the EV home-charging for the EV owner as cost function.

This work focuses on the optimization of the cost of the EV home-charging, rather than the minimization of the grid integration issues for EVs and PVs, because private owned network components, such as EVs and PV units, will react only to economic inputs.

The optimization process is implemented with a MATLAB script. The target of the optimization process, or cost function, is the daily electricity cost for the EV home-charging. The cost function can be expressed as an integral of the energy demand of the EV charger $e(t)$, multiplied by the price of electricity $c(t)$, over a period of time dt. The daily cost function can then be expressed as:

$$f(p) = \int_1^{24} e(t) \cdot c(t)\, dt \tag{4.1}$$

Since the TOD prices are constant during each hour i, Eq. 4.1 can be simplified as the sum of the products between the *average* hourly power demand of the EV charger p_i, and the hourly cost of electricity c_i. The optimization process can be now be written as a linear optimization problem. The cost function can now be expressed as:

$$f(p) = c_1 \cdot p_1 + c_2 \cdot p_2 + \cdots + c_{24} \cdot p_{24} = \sum_{i=1}^{24} c_i \cdot p_i \tag{4.2}$$

The charger power demand should be always non negative ($p_i \geq 0$), since no V2G functionality is considered in this scenario, and should not exceed the rated power of the charger ($p_i \leq P_{max}$).

Those constraints are summarized in the equations 4.3.

$$\begin{array}{ll} p_i \geq 0 & i = 1, 2, \ldots, 24 \\ p_i \leq P_{max,i} & i = 1, 2, \ldots, 24 \end{array} \tag{4.3}$$

By formulating the constraints regarding the maximum charging power as in Eq. 4.3, it is possible to take into account the EV availability, by making $P_{max,i}$ to assume the following values:

$$P_{max,i} = \begin{cases} 0 & \text{if the EV is not available} \\ P_{droop,i} & \text{if the EV is available} \end{cases} \tag{4.4}$$

Using Eq. 4.4, the only solution for the charging power p_i, when the vehicle is not available, is $p_i = 0$. If the vehicle is available for home-charging, the maximum power demand can be in the range [0 - P_{droop}], where P_{droop} is the maximum power demand allowed when droop control is activated, and can be calculated by using Eq. 2.13. If no droop control is activated, $P_{droop} = P_{max}$.

Regarding the EV battery SOC, it is assumed as constraint that the SOC is restored to the default value of 90% in the 24h of each day. By knowing the SOC at the arrival SOC_{arr}, based on the driving patterns described in Section 2.4.4, this additional constraint can be formulated as:

$$\sum_{i=1}^{24} p_i = 0.9 - SOC_{arr} \tag{4.5}$$

To summarize the linear optimization problem can be expressed as:

Cost function $f(x) = \sum_{i=1}^{24} c_i \cdot p_i$

Subject to:

$$\left.\begin{array}{ll} p_i & \geq 0 \\ p_i & \leq P_{max,i} \\ \sum\limits_i p_i & = 0.9 - SOC_{arr} \end{array}\right\} i = 1, 2, \ldots, 24$$

4.2.3 Simulations Results

This section presents the results of the introduction of EVs in the model of the residential LV network, in terms of grid bottlenecks and increase of the feeder PV hosting capacity.

At the beginning TOD scenario without voltage droop control is considered, and the results of the introduction of different EV shares are analyzed. Then, voltage droop control functionality is added and the same considerations are performed. In the end, the results are compared.

TOD Tariff without Voltage Droop Control

The optimization process for this case results in an average cost function value $f(p)$ of 875.39 €. The value is obtained as an average between the 30 EVs simulated in the 100% EV share, in order for the measurement not to be influenced by the single driver's habit.

The simulated EVs require on average 3698 kWh/y. The average cost of the electricity for charging the EV is evaluated as the ratio between the average cost function and the average energy demand, resulting 23.67 c€/kWh. This value is much closer to the off-peak cost of electricity F2 (23.45 c€/kWh) than to the peak value, proving the efficacy of the algorithm in minimization of the EV charging cost and the high EV availability during off peak hours.

BUS8 is chosen as an indicator for the minimum feeder voltage, since it is the furthest bus of the feeder (see Fig. 3.6), and the one with the highest voltage sensitivity, where the voltage magnitude perturbations will present their peak values.

Table 4.7 shows the power quality indicators, introduced in Section 2.3.3, evaluated for different EV shares.

Table 4.7: Power quality indicators for different EV shares, TOD scenario, no droop control. Values in red indicates the violation of the limits considered (listed in the first column).

		EV share (%)				
Power quality indicator	Limit	(0)	20	50	70	100
Minimum bus voltage at BUS8 (p.u.)	0.950	0.955	0.952	0.946	0.941	0.937
Number of occurrences (h/y)	-	-	-	1	7	15
Line losses [% of load demand]	-	0.101	0.133	0.193	0.233	0.268
Maximum %VUF	2.000	1.974	1.569	1.831	2.043	2.858
Number of occurrences (h/y)	-	-	-	-	3	4
Maximum line loading (% on ampacity)	100	43.54	50.84	52.00	51.80	59.61
Maximum transformer loading (% on rated power)	100	58.83	58.84	61.65	64.58	71.13

From the data of Table 4.7, it can be seen how the factors that limit the EV integration in the network are the voltage magnitude and the voltage phase unbalance. The 5% undervoltage constraint is violated for the cases above the 50% EV share, and the voltage phase unbalance violates the 2% constraint for 70% and 100% EV shares.

A close look at the EV charging profile can explain this phenomena. As it can be seen from the cumulative plot of Fig. 4.1, most of the EVs start to charge simultaneously, as soon as the price of electricity moves to the off-peak value. The EV peak overlaps with the evening domestic load peak, resulting in high loading of the radial feeder and consequent

undervoltages at the end of it. The unequal distribution of the EV load during some hours of the year results into voltage phase unbalance, a phenomena more evident with higher EV shares in the network.

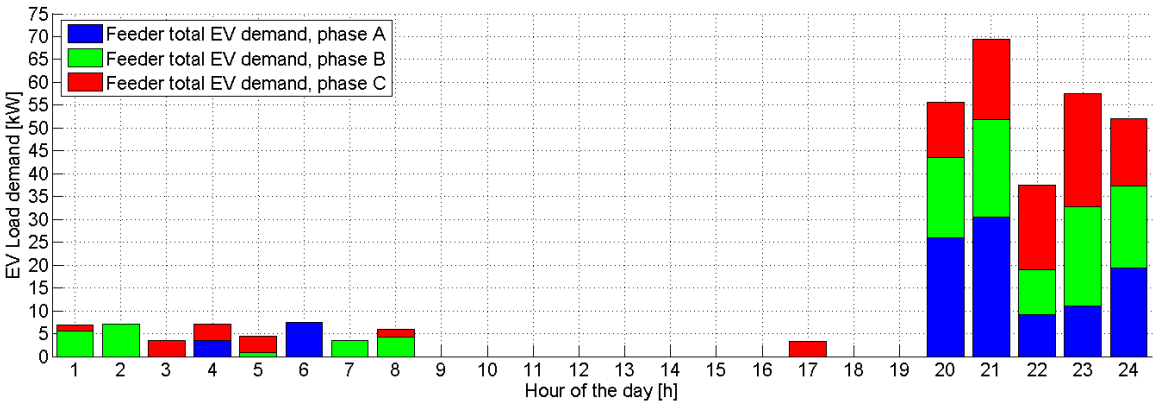

Figure 4.1: Cumulative load demand of 30 EVs during an example of one day of simulations, divided by the phase connection of the EV charger, TOD scenario, no VDC implemented.

The number of occurrences of the violation is for both the parameters limited to few hours of the year.

Since an increased number of EVs plugged into the network result in an additional load in the feeder, the line losses are affected by the EV share and their increase is proportional to the number of EVs in the feeder.

Regarding the impact of the EVs in the increase of the PV hosting capacity, it can be seen from Table 4.8 how the increase is limited to +4% for each share taken into account.

The PV hosting capacity does not increase with an increasing share of EVs, because the contribution of EVs is limited to the self-consumption of part of the generated energy by one EV close to the end of the feeder. The load profile of the EV and the PV power output can be seen in Fig. 4.2.

The reasons for the limited increase of the PV hosting capacity are to be found in the limitations of the TOD tariff structure. Since TOD tariffs encourage the consumption during off-peak hours, and those include daylight hours only during the weekend, as seen Table 4.4, the EV load is more likely to overlap with the evening peak consumption rather than the PV peak production.

Table 4.8: Increase of the PV hosting capacity for different EV shares, TOD scenario, no droop control activated.

	EV share (%)				
	(0)	20	50	70	100
Individual hosting capacity (kW)	2.775	2.886	2.886	2.886	2.886
Feeder hosting capacity (kW)	83.25	86.58	86.58	86.58	86.58
Variation of the hosting capacity (% compared to present scenario)	-	+4.0%	+4.0%	+4.0%	+4.0%

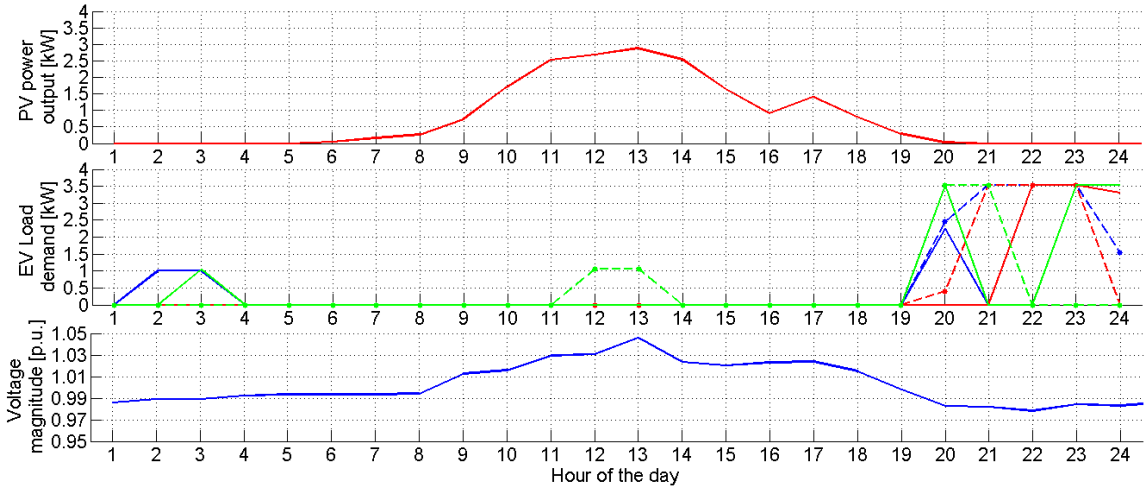

Figure 4.2: PV generation output, EV load profiles and voltage magnitude in the condition of maximum voltage magnitude in the feeder. It can be noticed how one EV consumes locally part of the PV generated energy during the hours of peak production. The contribution is however limited, and does not result in a significant increase of the feeder PV hosting capacity.

In the following paragraphs the same analysis will be performed for the case with voltage droop control applied.

TOD Tariff with Voltage Droop Control

The optimization process for the case with voltage droop control implemented results in an average cost function value $f(p)$ of 888.80 €. As in the previous case, the value is obtained as an average between the 30 EVs' cost functions, in order for the measurement not to be influenced by the single driver's habit. The average consumption is in this case 3754 kWh/y, resulting in an average cost of electricity of 23.68 c€/kWh. This value is almost identical to the cost per kWh of the case with no voltage droop control implemented. A comparison between the costs of electricity is available in the end of the chapter, in Table 4.16.

A first conclusion that can be drawn is that, with the restrictions of voltage droop control, the EV can still complete most of its charging during low peak hours; voltage droop control do not affect the customer's cost for the EV home-charging in the TOD scenario.

From the data of Table 4.9, it can be seen how the implementation of the voltage droop control is effective to allow a higher EV integration in the LV network. The restriction of the EV load demand during undervoltage conditions allows, in this case, EV shares in the grid up to 50%. For higher EV shares the voltage magnitude constraint is violated for 2 hours of the year only, where the EV load demand at the buses close to the distribution transformer (where the voltage magnitude is over 0.95 p.u.) overlaps with a high residential load demand, and results into voltage violations at the end of the feeder. It can be seen from the cumulative plot of Fig. 4.3 how the peak values of the total EV load demand are lower than in the case with no VDC implemented, available in Fig. 4.1. The lower peak demand results in lower voltage variations at the end of the feeder.

A comparison between the two TOD cases, with and without droop control, of the voltage profile during week 10 at BUS8 can be found in Fig. 4.4. From the plot it can be seen how

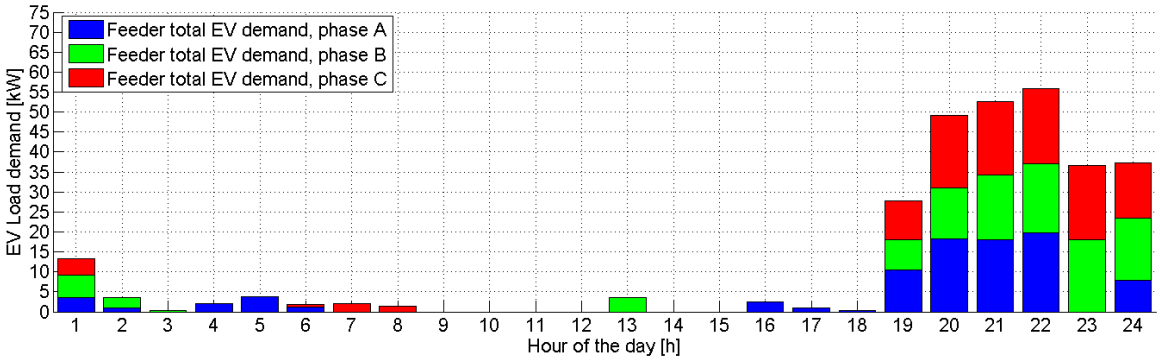

Figure 4.3: Cumulative load demand of 30 EVs during an example of one day of simulations, divided by the phase connection of the EV charger, TOD scenario, with VDC implemented.

the voltage droop control is effective in reducing the voltage violations in the network, by reducing the EV power demand when the bus voltage is lower than 1 p.u.

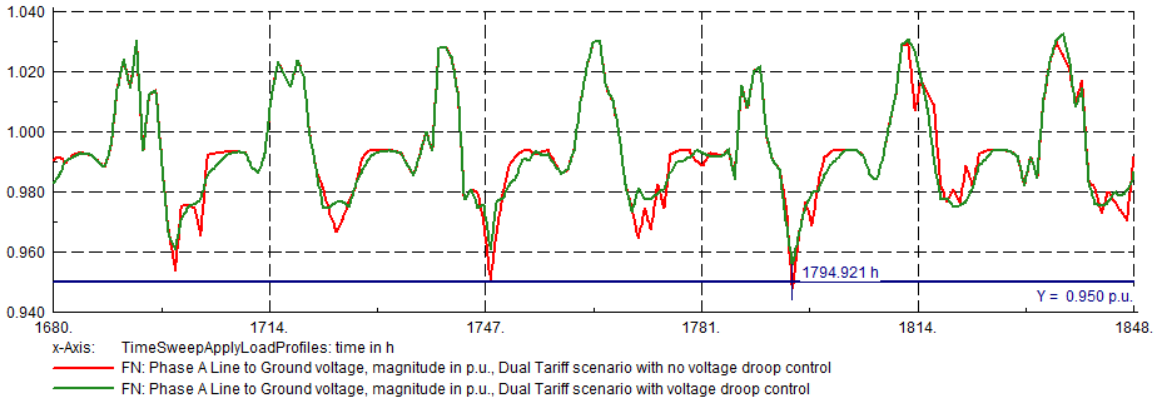

Figure 4.4: Comparison between the Phase A voltage at BUS8, the furthest bus of the feeder from the distribution transformer, during one week of simulation, with droop control implementation (in green) and without (in red).

Regarding other power quality indicators considered, the voltage phase unbalance never violates the 2% constraint in this case. The increase of the EV load demand results in an increase of the feeder line losses and maximum loading of the network components; this increase is proportional to the number of EVs plugged into the network, but it is less steep than in the TOD scenario without voltage droop control. A graphical comparison of the feeder line losses between the two cases of the TOD scenario is displayed in Fig. 4.5.

The increase of the PV hosting capacity compared to the case without voltage droop control is limited, as it can be seen from the data of Table 4.10. Only few EVs charge during daylight hours, reducing the possibility of self-consumption of the PV generated energy, and so the reduction of the reverse power flow in the feeder, main cause of the violation of the grid constraints.

Voltage droop control functionality is useful to increase the EV share in the network, while maintaining the power quality standards. However, its application does not have a significant

Table 4.9: Power quality indicators for different EV shares, TOD scenario, voltage droop control activated. Values in red indicated the violation of the limits considered (presented in the first column).

Indicator	Limit	EV share (%) (0)	20	50	70	100
Minimum bus voltage at BUS8 (p.u.)	0.950	0.955	0.952	0.951	0.947	0.944
Number of occurrences (h/y)	-	-	-	-	2	2
Line losses (% of load demand)	-	0.101	0.131	0.183	0.214	0.244
Maximum %VUF	2.000	1.974	1.760	1.792	1.761	1.792
Maximum line loading (% on ampacity)	100	43.54	46.77	46.77	46.77	50.82
Maximum transformer loading (% on rated power)	100	58.83	58.83	61.79	64.49	67.03

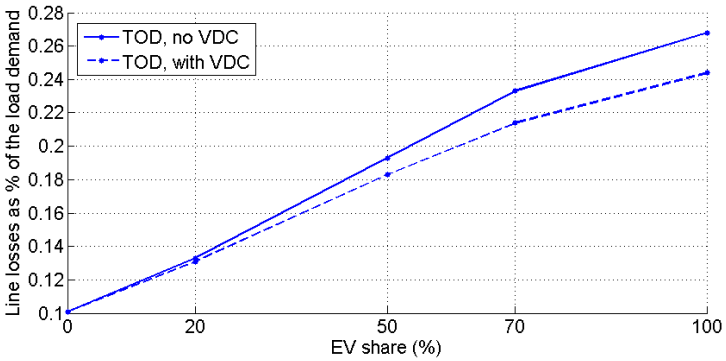

Figure 4.5: Comparison between the feeder line losses for the TOD scenario, in the case with no voltage droop control (VDC) implemented (solid line), and with this functionality implemented (dashed line). The implementation of VDC functionality reduces the line losses for every EV share considered.

Table 4.10: Increase of the PV hosting capacity for different EV shares, TOD scenario, voltage droop control activated.

	EV share (%) (0)	20	50	70	100
Hosting capacity (kW)	2.775	2.886	2.997	2.997	2.997
Feeder hosting capacity (kW)	83.25	86.58	89.91	89.91	89.91
Variation of the hosting capacity (% compared to present scenario)	-	+4.0%	+8.0%	+8.0%	+8.0%

impact on the PV hosting capacity. The next scenario proposed in this work, Net Metering, will approach the problem from a different angle, by modifying the cost function to optimize.

Instead of minimizing the cost of the EV home-charging only, the domestic load demand and the PV power output are included in the cost function as well. The proposed algorithm for generating the EV load profile will take into consideration the possibility of charging the EV with the PV power output that exceeds the domestic load demand. As it will be proved

in the next chapter, this possibility is economically more convenient for the EV owner than to charge during off-peak hour only, and it limits the reverse power flow in the feeder, resulting in a higher value of the PV hosting capacity in the residential network.

4.3 Net Metering Scenario

4.3.1 Net Metering Service in the Italian Scenario

As introduced in Section 2.5.2, Net Metering is a service available for electrical customers who own also a generating unit, such as SPV.

The payback for the Italian PV owner under net metering conditions is the sum of two components. The first is the value of the PV energy self-consumed that has not to be purchased from the grid. It can be calculated as the PV energy produced and self-consumed multiplied by the hourly TOD electricity tariffs.

The second component is the value of the excess PV generated energy injected into the network. This parameter, known as *contributo in conto scambio* (in Italian), or CS, is evaluated on a yearly base and is the sum of the smaller between two terms (O_E and C_{Ei}, explained in the following paragraph) and the product between the exchanged energy and a constant accounting for network charges. The CS component of the payback for the PV owner can be expressed as:

$$CS = min(O_E; C_{Ei}) + CU_{Sf} \cdot E_S \tag{4.6}$$

where:
O_E [€] is the product between the yearly energy consumption [kWh] and the Standard Price for Electricity (*Prezzo Unico Nazionale* or PUN. PUN values in 2015 were around 5c€/kWh on average [64]);
C_{Ei} [€] is the value of the energy fed into the grid, accounted as the product of the energy fed into the grid [kWh] and the day-before prices of electricity. Those prices are usually higher than the PUN [64];
CU_{Sf} [c€/kWh] is a term accounting for the network and general charges;
E_S [kWh] is the yearly energy exchange at the PCC, calculated as the minimum between the energy bought and the energy fed into the grid [65].

Net Metering has been planned with the purpose to reduce the reverse power flow in the feeder. For this reason the maximum economic benefit for the PV owner is realized when the PV generated energy is instantaneously self-consumed, rather than injected and consumed in a different time.

In order to have a numerical example, the same domestic load demand and PV production as used in the simulation model are considered, 2979 and 3441 kWh/y respectively. All the data used for this calculation are listed in Table 4.11.

The PV energy self-consumed is evaluated for each hour of the year, as the hourly difference between P_{dom} and P_{PV}, and accounts for 1176 kWh/y. The PV energy self-consumed results in savings for 280 € for the residential customer, or 23.81 c€/kWh of energy self-consumed. This value is close to the cost of electricity during peak hours, since the Italian TOD tariff peak values are during most of daylight hours.

Table 4.11: Data used to determine the value of the PV energy fed into the grid [65].

Parameter	Symbol	Value	Unit
Domestic yearly energy consumption	E_{dom}	2979	kWh
PV yearly energy production	E_{PV}	3441	kWh
PV energy self-consumption	E_{self}	1177	kWh
Energy withdrawn from the grid	E_{wit}	1862	kWh
Energy injected into the grid	E_{inj}	2324	kWh
PUN	PUN	5.207	c€/kWh
CUsf	$CUsf$	5.937	c€/kWh

Regarding the excess PV energy injected into the network, on a yearly base the residential unit injects into the grid $E_{inj} = 2324$ kWh and withdraws $E_{wit} = 1862$ kWh; the component CS is calculated using Eq. 4.6, and results into 207.5 €. The value of the electricity injected into the grid can be calculated as the ratio between the calculated CS and the amount of energy sold, resulting into an electricity price $c_{PV} = CS/E_{inj} = 8.93$ c€/kWh.

It can be noticed how the value of the PV generated energy in the network, 8.93 c€/kWh, is sensibly lower than the cost of purchasing energy from the grid during both peak and off-peak hours, 24.08 and 23.45 c€/kWh respectively. Those values are summarized in Table 4.12.

Table 4.12: Comparison between the present Italian TOD tariffs and the calculated value for the exceeding PV energy sold to the network in Net Metering functionality. Values in c€/kWh.

Base Price	Symbol	Rate (c€/kWh)
Energy consumption (peak hours)	$c_{TOD,F1}$	24.08
Energy consumption (off-peak hours)	$c_{TOD,F2}$	23.45
PV energy net production	c_{PV}	8.93

For this reason a solution for optimizing the economical benefit for the residential customer is to increase the self-consumption of the PV generated energy, by shifting the deferrable loads' consumption when the PV production is high.

Since the EV is a flexible load, a smart charging algorithm that maximize the PV energy self-consumption is proposed for this scenario. No modification of the domestic load profile is considered in this work, since there is no knowledge of the deferrable loads' share in the total domestic load demand obtained by measurements.

4.3.2 Optimization Process

The smart charging strategy is translated into an optimization problem, with the purpose to minimize the energy cost for the household and EV owner.

A similar procedure as the one described in Section 4.2.2 is used, with the addition of the domestic consumption P_{dom} and the PV production P_{PV} in the cost function. The energy price is the one derived from the TOD tariff (introduced in Section 4.2.1) if the

hourly consumption exceeds the production, or the previously calculated value c_{PV} if the PV production exceeds the domestic and EV consumption combined. The optimization problem for this scenario can be expressed as:

$$\text{Cost function } f(p) = \sum_{i=1}^{24} c_i \cdot (p_i + P_{dom} - P_{PV})$$

where

$$c_i = \begin{cases} c_{TOD} & \text{if } p_i + P_{dom} - P_{PV} \geq 0 \\ c_{PV} & \text{if } p_i + P_{dom} - P_{PV} < 0 \end{cases} \tag{4.7}$$

Subject to:

$$\left.\begin{array}{ll} p_i & \geq 0 \\ p_i & \leq P_{max,i} \\ \sum\limits_i p_i & = 0.9 - SOC_{arr} \end{array}\right\} i = 1, 2, \ldots, 24$$

4.3.3 Simulations and Results

This section presents the results of the introduction of EVs in the grid with the Net Metering charging scenario. The same approach as in Section 4.2.3 is followed.

The EV profiles for every vehicle are generated using the previously described optimization process with the MATLAB script *EVProfiles.m*, available in the CD attached.

As in the previous scenario, the simulations are performed for different EV shares and with and without voltage droop control.

Net Metering without Voltage Droop Control

The minimization of the yearly cost of electricity for the residential user results in an average cost function value $f(p)$ of 889.54 €. This value is comprehensive of the domestic load demand, the energy cost for the home-charging, the savings originated from the self-consumption of part of the PV generated energy and the payback CS, originated from the excess PV energy injected into the network. The yearly household consumption, sum of the domestic and the EV load demands, results to be 6699.71 kWh, for an average cost of the electricity of 13.28c€/kWh. This value is not directly comparable with the result of the TOD scenario, since the cost functions minimized are different.

Table 4.13 presents the power quality indicators for each of the EV shares considered. It can be seen how the grid bottleneck for EV integration is the voltage phase unbalance. The violation of the 2% constraint occurs in a range from 3 to 5 hour per year.

The voltage phase unbalance depends more on the phase where the EVs are charging, rather than the number of EVs simultaneously connected to the grid. In the Net Metering scenario, since the EV charging profile depends on a larger series of factors than in the TOD scenario, including the vehicle availability for home-charging during daytime, the PV power output and the domestic load demand, the EV load demand is spread during the 24h of the day. For this reasons it is more likely that few EVs are charging on the same phase, rather then to have an uniform distribution of the charging profile over the 3 phases, as it can be seen from the plot of Fig. 4.6. This unequal distribution results in a higher voltage unbalance in the system.

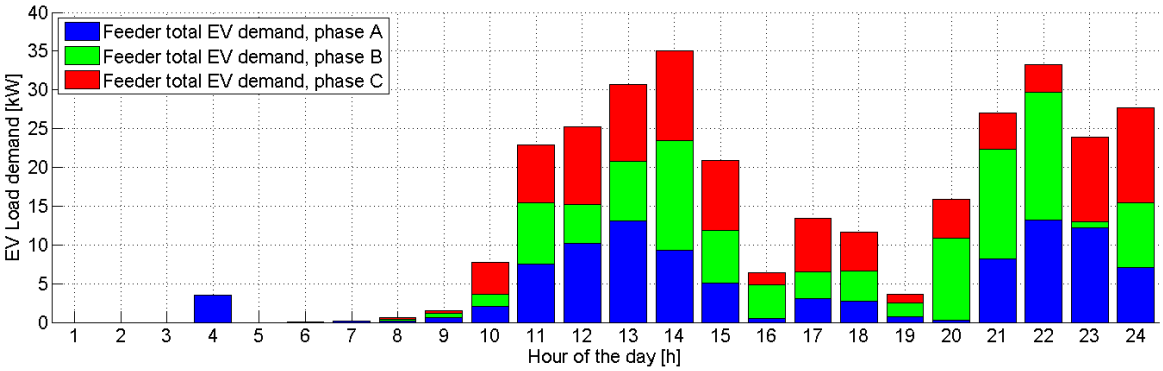

Figure 4.6: Cumulative load demand of 30 EVs during an example of one day of simulations, divided by the phase connection of the EV charger, Net Metering scenario, no VDC implemented.

The second limiting factor is the voltage magnitude at the furthest node of the feeder, BUS8, which violates the 5% undervoltage limit for EV shares over 70% in the feeder. Since no voltage droop control is implemented, the EV demand for high EV penetration in the network results into undervoltages at the end of the feeder.

All the other parameters taken into consideration (maximum loading of all network components, feeder line losses) present an increasing trend with the increase number of EVs plugged into the network, as in the TOD scenario previously described.

Table 4.13: Power quality indicators for different EV shares, Net metering scenario, no droop control. Values in red indicates the violation of the limits considered (listed in the first column).

		EV share (%)				
Indicator	Limit	(0)	20	50	70	100
Minimum bus voltage at BUS8 (p.u.)	0.950	0.955	0.952	0.950	0.949	0.945
Number of occurrences (h/y)	-	-	-	-	3	7
Line losses (% of load demand)	-	0.101	0.120	0.150	0.174	0.196
Maximum %VUF	2.000	1.954	2.209	2.279	2.398	2.007
Number of occurrences (h/y)	-	-	3	3	5	3
Maximum line loading (% on ampacity)	100	43.54	59.09	62.85	63.28	63.44
Maximum transformer loading (% on rated power)	100	58.83	59.81	63.61	64.38	68.40

In this scenario the increase of the PV hosting capacity is relevant, and proportional to the EV share in the network. The maximum hosting capacity for the all feeder is over 136 kW for a 100% EV share in the grid, more than 60% over the hosting capacity at the present state of the grid. Unlike the TOD scenario, with Net Metering functionality it is more convenient for the EV owner to self-consume the PV generated energy, by charging during daylight hours.

Table 4.14: Increase of the PV hosting capacity for different EV shares, Net Metering scenario, no voltage droop control implemented.

	EV share (%)				
	(0)	20	50	70	100
Individual hosting capacity (kW)	2.775	3.335	4.329	4.396	4.551
Feeder hosting capacity (kW)	83.25	100.57	129.87	131.87	136.53
Variation of the hosting capacity (% compared to present scenario)	-	+20.8%	+56.0%	+58.4%	+64.0%

Net Metering with Voltage Droop Control

Voltage droop control functionality is added on top of the Net Metering charging scenario, in order to prove its efficacy in integrating more EVs in the network.

The minimization of the yearly cost of electricity, inclusive of domestic and EV load demands and the paybacks originated from PV generation, results in an average cost function value $f(p)$ of 895.10 €. The yearly household consumption, sum of the domestic and the EV load demands, results to be 6674.71 kWh, for an average cost of the electricity of 13.41 c€/kWh.

From the analysis of the results listed in Table 4.15 it can be seen how the maximum voltage phase unbalance remains the limiting factor for the EV integration in the network.

The implementation of voltage droop control for the EV chargers is effective in reducing the impact of the EVs in the grid regarding the voltage magnitude and the loading of the network components. While there are still voltage magnitude violations for the 70% and 100% EV shares, the minimum bus voltage is closer to the 0.95 p.u. value assumed as a constraint. The number of occurrences of these violations is also reduced when compared to the case with no voltage droop control (see Table 4.13).

The line losses and the loading of the network elements are increasing with the number of EVs in the grid, but with a less steep curve than without voltage droop control. A graphical comparison between the two cases of the Net Metering scenario can be seen from the plot of Figure 4.7.

The feeder PV hosting capacity for this case presents identical values as the case without voltage droop control; for this reason the data of Table 4.14 apply also to this case. A possible reason is that the droop control reduces the EV power demand during load peak hours only, when the voltage is below the rated value, while the EV load demand is not affected when the residential load demand is low and the PV production is high, resulting in possible overvoltage in the feeder.

In the next section of a general conclusion of the application of the EV load in the network is drawn, and the scenarios proposed and analyzed in the next chapter are introduced.

Table 4.15: Power quality indicators for different EV shares, Net metering scenario, voltage droop control implemented. Values in red indicates the violation of the limits considered (listed in the first column).

Indicator	Limit	EV share (%) (0)	20	50	70	100
Minimum bus voltage at BUS8 (p.u.)	0.950	0.955	0.952	0.952	0.949	0.948
Number of occurrences (h/y)	-	-	-	-	2	3
Line losses (% of load demand)	-	0.101	0.117	0.142	0.161	0.176
Maximum %VUF	2.000	1.974	2.493	1.803	2.018	2.852
Number of occurrences (h/y)	-	-	2	-	1	1
Maximum line loading (% on ampacity)	100	43.54	46.58	46.59	46.60	51.69
Maximum transformer loading (% on rated power)	100	58.83	58.84	62.55	64.57	64.97

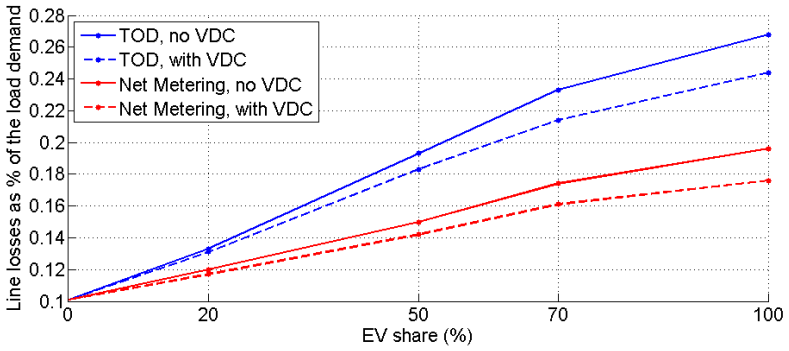

Figure 4.7: Comparison between the feeder line losses for the TOD and Net Metering scenarios, in both cases with no voltage droop control (VDC) implemented (solid line), and with this functionality (dashed line). The introduction of Net Metering reduces the feeder line losses, while the implementation of VDC functionality reduces the line losses for both scenarios.

4.4 Discussion

In this section a comparison between the results of the scenarios considered so far, TOD and Net Metering, with and without voltage droop control, is performed. First, the impact of the EV charging scenarios on the EV owner perspective, in terms of average cost of the purchased electricity, is presented. The EV integration in the network is then discussed, based on the analysis of the simulation results. In the end, the impact of the different EV charging strategies on the feeder PV hosting capacity is analyzed.

4.4.1 Cost for the EV owner

A comparison between the average cost of electricity for the Italian residential customer in the scenarios analyzed in this chapter is to be found in Table 4.16.

As previously introduced, the average costs of electricity between TOD and Net Metering scenarios are not directly comparable, since no PV generation and domestic load demand are included in the TOD scenario cost function.

It can be noticed how the implementation of voltage droop control does not affect significantly the cost of electricity for both scenarios. The EV can still complete most of the charging process during off-peak hours, even when the maximum allowed charging power is reduced due to undervoltages in the network.

Table 4.16: Comparison between the average cost of electricity between TOD and Net Metering scenarios, inclusive of the cases with and without VDC functionality for the EV charger.

Scenario	Case	Average cost of electricity (c€/kWh)
TOD	no VDC	23.67
	with VDC	23.68
Net Metering	no VDC	13.27
	with VDC	13.41

4.4.2 EV Integration in the Network

From the results of the simulations conducted and analyzed in this chapter, it can be seen how the grid bottlenecks for the integration of EVs, in residential LV networks, are the voltage magnitude at the end of the radial feeder and voltage phase unbalance. The loading of the network components does not represent an issue, even for the maximum EV share considered.

The implementation of voltage droop control for the EV charger is effective in reducing the impact of the EV load on the voltage magnitude, and allows higher shares of EV in the feeder for both the scenarios proposed. Voltage droop control is effective in reducing the line losses and the maximum loading of the network components.

On the other hand, voltage droop control is ineffective in reducing the maximum voltage phase unbalance in the system, which is still over the limit value for a limited number of hours of the year.

4.4.3 Impact on the PV hosting capacity

The PV hosting capacity is significantly increased in the Net Metering scenario, when the EV daytime charging is more convenient for the EV owner. TOD tariff structure, when not supported by Net Metering functionality, has been proven inefficient for the integration of EVs and PVs in the network, since the EV owner is encouraged to overlap the EV loading profile with the evening peak load demand rather than the PV peak production.

The results obtained in the increase of the PV hosting capacity are independent from the implementation of voltage droop control, since this functionality does not affect the grid bottlenecks that limit the PV hosting capacity in the feeder, such as overvoltages and voltage phase unbalance. Table 4.17 summarizes the results in term of PV hosting capacity for the scenarios considered so far.

Table 4.17: Comparison between the variation in the PV hosting capacity compared to the present scenario for the four scenario so far considered

		EV share (%)			
Scenario	Case	20	50	70	100
TOD	no VDC	+4.0%	+4.0%	+4.0%	+4.0%
	with VDC	+4.0%	+8.0%	+8.0%	+8.0%
Net Metering	no VDC	+20.8%	+56.0%	+58.4%	+64.0%
	with VDC	+20.8%	+56.0%	+58.4%	+64.0%

4.5 Conclusion

Two different EV charging scenarios, based on the present electricity tariffs for Italian residential customers, have been analyzed in this chapter: Time-of-Day (TOD) and Net Metering.

The main limitation of the TOD scenario is that the electricity prices during most of daylight hours are higher than during evening and nighttime. For this reason, a coordination between EV load demand and PV generation is rarely convenient for the EV owner. As a consequence of this, the introduction of EVs does not result into a significant increase in the feeder PV hosting capacity.

Net Metering service has been proven to be effective in allowing a higher PV integration in the network, by encouraging the PV self-consumption. However it does not differentiate the electricity tariffs according to the grid conditions. The PV generated energy injected back into the network is rewarded with the same tariff either if it helps improving the feeder power quality, e.g providing local generation during hours of high load demand, or if it creates grid bottlenecks, e.g. increasing the reverse power flow in the feeder during hours of low load demand, when overvoltage is registered. The same limitation applies to the EV load: the electricity tariff remains constant whether the EV locally consumes the excessive PV energy, or if it overlaps with conditions of already high consumption in the feeder. As a consequence of this, while Net Metering is effective in increasing the PV hosting capacity to more than 60% of the present scenario, a series of EV integration issues are registered, such as voltage phase unbalance and voltage variations below the minimum limit.

The implementation of voltage droop control has been proven to be effective for both the scenario analyzed in reducing the EV integration issues on the feeder voltage magnitude, without compromising the EV charging process or increasing significantly the costs for the EV owner.

5 | EVs in Future Distribution Grids

In the previous chapter of this work, the focus has been put on the impact of EV charging on distribution grid bottlenecks and on the PV hosting capacity at the *present state* of the network. Two scenarios, representing the available electricity tariffs at the present day for an Italian residential customer, were proposed: Time of Day (TOD) and Net Metering.

In this chapter the focus is on *future perspectives*. This chapter contains an analysis on future developments in the distribution network operation and in the EV technology, e.g. the introduction of day-ahead real time pricing (introduced in Section 2.5.3) in the distribution level and EV's Vehicle-to-Grid (V2G) functionality.

Two future scenarios are proposed in this chapter. The first considers the implementation of Distribution Locational Marginal Pricing (DLMP), an application of real-time pricing [57], [66]. The second scenario considers EV's V2G functionality, in the context of the above mentioned DLMP pricing structure.

The proposed future scenarios represent possible future operating conditions for EVs [2]. The modeling of these scenarios is considered relevant for the scope of this work, since the proliferation of EVs will reach considerable numbers only in the next future, as it can be seen from the plot of Fig. 1.1.

Since the implementation of voltage droop control for the EV chargers has been proven to be effective for reducing the EV integration issues, as described in the conclusions of the previous chapter, in the proposed future scenarios it has been assumed that all EV chargers will be equipped with this functionality.

Regarding V2G functionality, it is assumed that all EVs plugged into the network in the V2G scenario can discharge their batteries to supply the domestic consumption.

In the next section DLMP concept is analyzed, and an algorithm is presented to calculate the real-time electricity prices. The simulation results are then presented, using a similar structure as in the previous chapter. The last scenario analyzed in this work will be V2G, where EV's V2G functionality will be added on top of the above mentioned DLMP pricing structure.

In the end of the chapter, a comparison with TOD and Net Metering scenarios is conducted, in order to determine if, and how, the future developments of the electricity tariffs and the EV technology considered in this work can improve the EV and PV integration in LV distribution networks, and increase the PV hosting capacity in the model of the residential LV grid.

5.1 Locational Marginal Prices for Distribution Grids

Locational Marginal Pricing (LMP) is a pricing structure based on real time pricing. It reflects the marginal cost of electricity supply for an additional increment of power to a node in the network [66], [67]. Since the cost for the DSO to supply loads connected at different nodes of the system can be different, due to the different line losses, LMP structure results in different prices for different nodes, hence the name *Locational*.

While LMP have already been adapted in some countries for the transmission network [68], this pricing structure has still to be implemented on the distribution level [57]. Distribution Location Marginal Pricing (DLMP) has been proposed as a solution to increase the system efficiency when compared to the present flat electricity rate, by encouraging customers to modify their load profile according to price signals. These prices are set in order to decrease the feeder line losses, being the cost of purchasing electricity proportional to the losses introduced by the customer's load demand, and to appropriately reward PV owners for the energy injected to the grid during high load demand, by rewarding the energy produced during peak load consumption more than during periods of high PV generation [57].

A scenario based on Distribution Locational Marginal Pricing (DLMP) in proposed. The target is to obtain a higher synchronization between load demand and PV production than in the previously analyzed TOD and Net Metering scenarios. This target is achieved by proposing a new price structure, where the cost of electricity is dependent on the marginal feeder line losses introduced by each load and generating unit in the system. The price calculation is based on loss sensitivity analysis, and it will be explained more in detail in Section 5.1.1.

DLMP consists of three components: *cost of energy*, *cost of losses* and *cost of congestion* [58], [69], [67].

The *cost of energy* depends on the energy price at the transmission level, and does not variate along the buses of a LV feeder [57]. In this work it is assumed that the cost of energy is the cost of electricity determined by the present TOD tariffs, described in Section 4.2. The electricity rates used in this work are listed in Table 4.6, and the time application of the Italian TOD tariff is described by Table 4.4.

The *cost of congestion* is a parameter used to quantify the marginal congestion of the network components, introduced by a variation in the load demand. In the radial residential network modeled in this work, no overloading is ever registered, even when the maximum EV share is considered, as it can be seen from the simulation results of the previous chapter. For this reason the cost of congestion is not considered in the modeling of the DLMP structure proposed in this work.

The *cost of losses* represents the cost associated to the marginal line losses, introduced by a variation in the load demand. This parameter in evaluated with an analysis based on loss sensitivity, presented in the next section. To summarize, in this work DLMP will be based on the present TOD tariffs, for the cost of energy, and the marginal line losses.

5.1.1 Price Calculation

The DLMP structure proposed in this work is based on the work of [57], [68], and can be expressed by Eq. 5.1.

$$c_{t,k} = c_{t,TOD} \cdot \left(1 + \frac{dLoss_t}{dS_t}\right) \tag{5.1}$$

where $c_{t,k}$ is the electricity price at the hour t for the bus k, $c_{t,TOD}$ is the reference price at the time t, originated from the present Italian TOD tariff, and $dLoss_t$ are the marginal losses due to the apparent power demand S_t at time t for the bus k.

Referring to [70], for unbalanced distribution systems loss sensitivity $\lambda = dLoss/dS$, for a node n and phase ϕ, can be approximated as:

$$\begin{aligned}\lambda_n, \phi = \frac{2}{|V_{n,\phi}|} \cdot \Bigg(\sum_l (I_{l,a} \cdot R_{l,a\phi} \cdot cos(\theta_{I,l,a} - \theta_{I,n,\phi}) + \\ I_{l,b} \cdot R_{l,b\phi} \cdot cos(\theta_{I,l,b} - \theta_{I,n,\phi}) + I_{l,c} \cdot R_{l,c\phi} \cdot cos(\theta_{I,l,c} - \theta_{I,n,\phi}))\Bigg)\end{aligned} \tag{5.2}$$

where:

$V_{n,\phi}$ is the voltage magnitude of phase ϕ at node n;
l is the number of lines in the radial network;
$I_{l,\phi}$ is the line current in line l and phase ϕ;
$R_{l,\phi_1\phi_2}$ is the real part of the line impedance $Z_{l,\phi_1\phi_2}$ for line l;
$\theta_{I,l,\phi}$ is the angle of phase current ϕ in line l;
$\theta_{I,n,\phi}$ is the angle of phase current ϕ at the node n where the loss sensitivity is evaluated;

Eq. 5.2 will be used in this work to calculate the loss sensitivity coefficient λ, used to determine the cost of electricity withdrawn and the value of the electricity injected to the network. Eq. 5.1 can be rewritten as:

$$c_{t,k} = c_{t,TOD} \cdot (1 + \lambda_{t,n}) \tag{5.3}$$

The coefficient $\lambda_{t,n}$, evaluated at hour t, increases proportionally to how much the power withdrawal at the node n increases the system line losses. In this work the base prices $c_{t,TOD}$ for the cost of the purchased energy have been assumed to be the present TOD rates. Regarding the value of PV energy sold to the network, the c_{PV} value calculated for the Net Metering scenario, described in Section 4.3, is used. These values are summarized in Table 4.12.

For the calculation of the values of $\lambda_{t,n}$, for every hour of the year t, any node of the network n and phase ϕ, an algorithm is implemented with a DPL script (available in the CD attached).

In order to avoid negative energy prices, which can occur when the marginal line losses are low enough to make $\lambda < -1$, so that Eq. 5.3 becomes negative, an additional condition is set for the variable λ: if $(1 + \lambda)$ is negative, the energy price is automatically limited to zero. This can be written as: $\lambda_{n,i} \geq 0$. The limitation to zero of the day-ahead price of electricity had already been registered in the Italian case, in conditions of high PV generation and minimum load demand [71].

The resulting price of electricity varies in a wide range along the year. As an example, the DLMP electricity prices for BUS8, the furthest of the network, are presented in the plot of Fig. 5.1. The most relevant values are listed in Table 5.1.

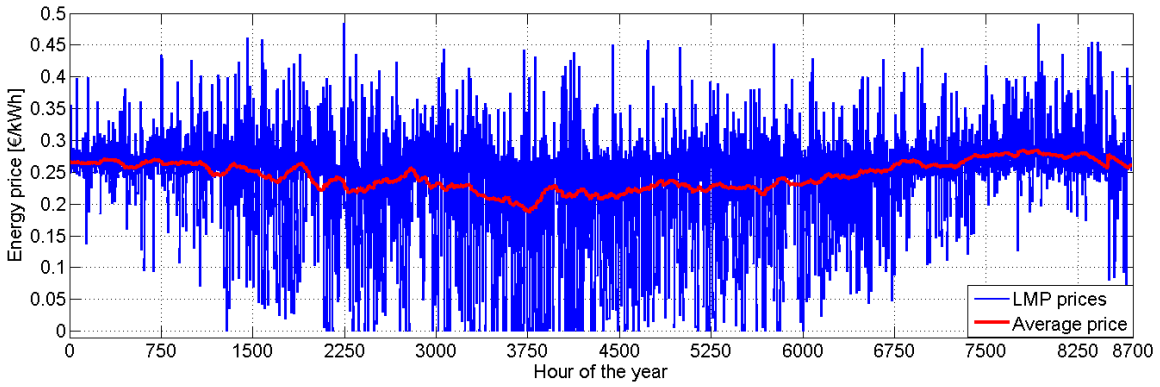

Figure 5.1: Plot of the DLMP electricity prices (in blue) and their average (in red) at BUS8, the furthest node of the feeder.

Table 5.1: Relevant data about the DLMP prices for the energy produced and consumed, DLMP and V2G scenarios. Values in c€/kWh.

	$c_{DLMP,c}$ (consumption)	$c_{DLMP,p}$ (production)
Average price (c€/kWh)	24.24	9.14
Minimum price (c€/kWh)	0.00	0.00
Maximum price (c€/kWh)	48.48	18.41

From the data of Table 5.1 that the resulting average price is similar to the cost of electricity with the present TOD tariffs, while the maximum price is approximately twice as much. The cost of the purchased electricity is on average lower during the central months of the year (see Fig. 5.1), due to the higher PV production and the lowering of the feeder kine losses introduced by the local load consumption.

5.1.2 Optimization Problem

A similar optimization process as for the Net Metering scenario, expressed by Eq. 4.7, is used in this DLMP scenario.

The modification introduced here regards the price of energy c_i, which will be dependent on the system losses according to Eq. 5.3.

The optimization problem proposed for the DLMP scenario can be expressed as:

$$\text{Cost function } f(p) = \sum_{i=1}^{24} c_i \cdot (p_i + P_{dom} - P_{PV})$$

where

$$c_i = \begin{cases} c_{DLMP,c} = c_{TOD} \cdot (1 + \lambda_{n\phi}) & \text{if } p_i + P_{dom} - P_{PV} \geq 0 \\ c_{DLMP,p} = c_{PV} \cdot (1 + \lambda_{n\phi}) & \text{if } p_i + P_{dom} - P_{PV} < 0 \end{cases} \tag{5.4}$$

Subject to:

$$\left.\begin{array}{ll} p_i & \geq 0 \\ p_i & \leq P_{max,i} \\ \sum\limits_i p_i & = 0.9 - SOC_{arr} \end{array}\right\} i = 1, 2, \ldots, 24$$

5.1.3 Simulations and Results

The minimization of the yearly cost of electricity for the residential user results in an average cost function value $f(p)$ of 1019.70 €. This value is comprehensive of the domestic load demand, the energy cost for the home-charging and the payback CS (explained in Section 4.3.1), this payback being generated by the PV energy injected into the network. The energy consumption, sum of the domestic and the EV load demand, results to be 6723.21 kWh, for an average cost of electricity of 15.16c€/kWh. This value is approximately 14% higher than the value of the cost function calculated in the Net Metering scenario, described in Section 4.3.3 and summarized in Table 4.16.

This increase in the yearly cost of electricity for the residential user can be explained by an analysis on how the total household load is composed. While the EV load demand is the result of the above mentioned optimization process, and it is shaped to minimize the cost for the EV owner to home-charge following the new pricing structure, the domestic load demand remains unchanged, despite the price structure is now different. Modeling and controlling the deferrable loads, which consist a portion of the total domestic load demand, could reduce this value. Since the domestic load demand is obtained from measurements data, without the knowledge of the share of deferrable loads, this idea has not been implemented in this work.

Table 5.2 illustrates the power quality indicators for the EV share considered.

Table 5.2: Power quality indicators for different EV shares, DLMP scenario. Values in red indicates the violation of the limits considered (listed in the first column).

		EV share (%)				
Power quality indicator	Limit	(0)	20	50	70	100
Minimum bus voltage at BUS8 (p.u.)	0.950	0.955	0.955	0.953	0.951	0.951
Line losses (% of load demand)	-	0.101	0.100	0.111	0.124	0.134
Maximum %VUF	2.000	1.974	2.747	2.394	2.398	2.730
Number of occurrences (h/y)	-	-	5	5	2	9
Maximum line loading (% on ampacity)	100	43.54	52.18	53.98	52.91	52.83
Maximum transformer loading (% on rated power)	100	58.83	62.26	64.27	66.49	71.65

The main improvement brought by the application of the DLMP scenario, compared to TOD and Net Metering, is that no undervoltage is registered in the network for any EV share, as anticipated from Table 5.2. The minimum yearly voltage is registered at BUS8 for the 100% EV share, and in this conditions the voltage magnitude does not violate the -5% limit assumed as constraint in this work. This can be visualized from the plot of the yearly voltage profile at BUS8, displayed in Fig. 5.2.

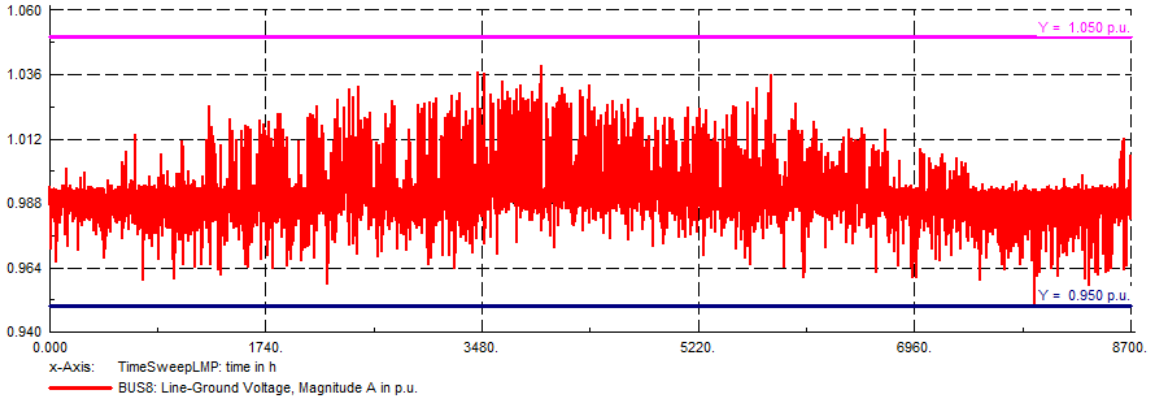

Figure 5.2: Yearly voltage profile of phase A at BUS8 with 100% EV share, DLMP scenario. The voltage magnitude is inside the ±5% range during all the hours of the year.

DLMP is a successful charging strategy for the integration of EVs in the residential feeder regarding the voltage magnitude bottleneck. The causes of this success are to be found in its pricing structure that penalizes the load demand during hours of high consumption, and in the implementation of Voltage Droop Control functionality for all EV chargers assumed, which limits the maximum allowed charging power according to the bus voltage where the EV is connected.

The line losses are proportional to the number of EVs in the network. As direct consequence of the structure of DLMP prices, described in Eq. 5.2, which penalizes the loads that introduce losses in the system with higher electricity prices, the line losses are much lower than in the previous scenarios. A graphical comparison between the simulation results about line losses, for all the scenarios considered so far in this work, is available in Fig. 5.3.

As in the scenarios representing the present state of the grid, the loading of the maximum loading of the network components does not represent an issue for the integration of EVs and PVs in the feeder, since the maximum values are still far from reaching the maximum limits assumed as constraints.

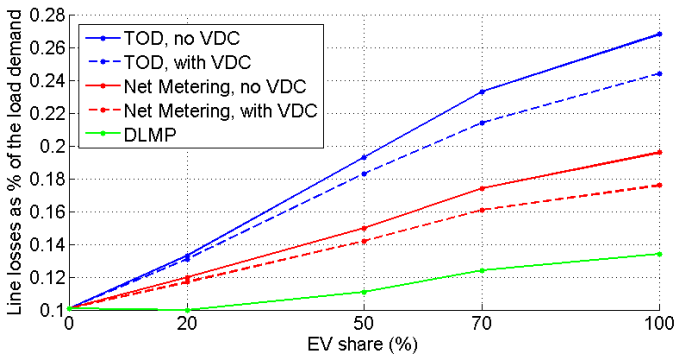

Figure 5.3: Comparison between the feeder line losses in each of the scenarios so far analyzed.

The grid bottleneck for the EV integration in this scenario is represented by the voltage phase unbalance, which presents maximum values over the 2% constraint for each EV share

considered. As in the Net Metering scenario described in Section 4.3, also in this DLMP scenario few EVs are charging simultaneously. If only a portion of the total share of EVs is charging at the same time, it is more likely to have more EV charging on one phase than to have an uniform distribution among the three phases of the system, which leads to an increase in the existing background unbalance. An example of the unequal distribution of the EV charging profile among the three phases, during an example of one day of simulation, can be found in the plot of Fig. 5.4.

The number of occurrences of the violation of the 2% %VUF constraint is limited to a maximum of 9 h/y, and the maximum %VUF value is limited to below 3%.

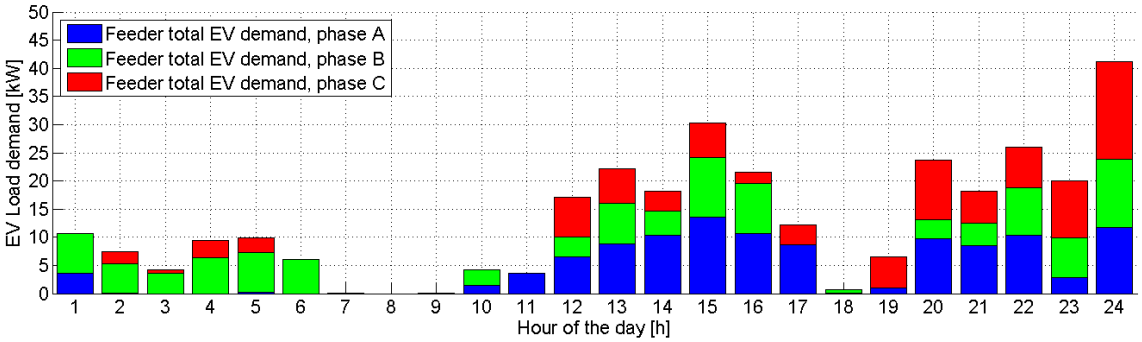

Figure 5.4: Cumulative load demand of 30 EVs during an example of one day of simulations, divided by the phase connection of the EV charger, DLMP scenario.

As it can be visualized from Table 5.3, the increase in the feeder PV hosting capacity is proportional to the number of EVs plugged into the feeder.

Table 5.3: Increase of the PV hosting capacity for different EV shares, DLMP scenario.

	EV share (%)				
	(0)	20	50	70	100
Individual hosting capacity (kW)	2.775	3.286	3.308	3.308	3.352
Feeder hosting capacity (kW)	83.25	98.57	99.23	99.23	100.57
Variation of the hosting capacity	-	+18.4%	+19.2%	+19.2%	+20.8%

5.2 Vehicle-to-Grid Scenario

Referring to the above mentioned DLMP structure, it can be seen how the electricity price varies on a wider range than with the present Italian TOD tariffs. For this reason, in a future perspective where RTP are implemented on the distribution level, the discharge of the EV battery might be convenient for the EV owner. On the DSO perspective, as introduced in Section 2.4.3, the EVs with V2G functionality represent a new opportunity, since they can operate as fast energy storages, and can reduce grid bottlenecks.

In the last scenario proposed in this work, the impact of EVs with V2G functionality in the case of the previously described DLMP price structure is analyzed. It is assumed, in the

context of future perspective, that all the EVs plugged into the feeder in this last scenario can perform V2G functionality. As in the previous DLMP scenario, it is assumed that all EV chargers are implemented with voltage droop control functionality.

The assumptions made in order to propose a method to evaluate the cost of the battery wear-out associated with V2G operation, introduced in Section 2.4.3, are presented in the next section. The simulation results are then presented and discussed, following the same structure as for the other scenarios analyzed in this work.

5.2.1 Vehicle to Grid Concept and Applications

As introduced in Section 2.4.3, the V2G operation has two major drawbacks: the low net efficiency and the battery wear-out, associated with a more frequent and aggressive cycling of the EV battery pack.

The charge-discharge cycle associated with V2G operation can theoretically take place at any hour of the day, involving any DOD in the operational limit of the battery; V2G operation can lead to an independent charge-discharge cycle, or simply an increased discharge of the battery after the EV gets home after the last trip of the day, followed by a longer charging process. Evaluating all these variable for each V2G operation cycle will require a deep analysis, which is outside the scope of this project.

A new approach to evaluate the cost associated to the battery wear-out in V2G operation is proposed in this work. Referring to [44], [40], the battery cycle life is exponentially affected by the Depth of Discharge (DOD) at which it is cycled. This exponential relation is expressed by Eq. 2.12. The energy En that can be cycled throughout the battery cycle life , however, variates in a limited range for different DOD, at it will be proved in the following example. En can be expressed by Eq. 5.5, where En is the cycled energy in the battery cycle life, L is the cycle life in terms of cycles, C_{rated} is the battery rated capacity and DOD is expressed as percentage of the battery capacity.

$$En = L \cdot DOD \cdot C_{rated} \tag{5.5}$$

As a numerical example, if the 24 kWh Li-ion battery considered in this work is always cycled at 20% DOD, the number of cycles the battery can perform in its cycle life L is:

$$L = 694 \cdot (0.2)^{-0.795} = 2495$$

The energy En that can be cycled in the battery cycle life can be calculated by using Eq. 5.5:

$$En_{20\%} = 2495 \cdot 0.2 \cdot 24 = 11.97 MWh$$

The battery wear-out per unit of energy cycled W_{out}, is defined in this work as the ratio between the battery lifetime (in p.u.), and the energy En that can be cycled in the lifetime (in kWh). This can be expressed by Eq. 5.6.

$$W_{out} = \frac{1}{En} \tag{5.6}$$

For the previously considered 20% DOD example, the deterioration per kWh of energy can be calculated using Eq. 5.6:

$$W_{out,20\%} = \frac{1}{11.97 \cdot 10^3} = 8.35 \cdot 10^{-5} kWh^{-1}$$

A series of DOD levels inside the operating battery range assumed in this work, listed in Table 2.5, has been selected, and can be found in the first column of Table 5.4. For each DOD level, the battery cycle life has been evaluated by using Eq. 2.12. The energy that can be cycled in the cycle life and the battery wear-out have been evaluated for each DOD level, by using Eq. 5.5 and 5.6 respectively. In the end of Table 5.4, an average of all the values is presented. It can be seen from Table 5.4 that En variates in a limited range, from a minimum of 10.39 MWh at 10% DOD to a maximum of 15.91 MWh at 80% DOD.

Table 5.4: Battery maximum number of cycles, cycled energy and battery wear out per unit of energy cycled in the battery cycle life, evaluated for different DOD.

DOD (% on C_{rated})	Battery cycle life L (from Eq. 2.12)	Energy En (MWh) (from Eq. 5.5)	Battery wear-out $W_{out}(kWh^{-1})$ (from Eq. 5.6)
10 %	4329	10.39	$9.63 \cdot 10^{-5}$
20 %	2495	11.97	$8.35 \cdot 10^{-5}$
30 %	1807	13.01	$7.68 \cdot 10^{-5}$
40 %	1438	13.80	$7.24 \cdot 10^{-5}$
50 %	1204	14.45	$6.92 \cdot 10^{-5}$
60 %	1048	15.00	$6.67 \cdot 10^{-5}$
70 %	922	15.48	$6.46 \cdot 10^{-5}$
80 %	829	15.91	$6.28 \cdot 10^{-5}$
Average	1759	13.75	$7.40 \cdot 10^{-5}$

In this work it has been considered a constant battery deterioration associated with V2G operation, directly proportional to the energy injected to the grid. Since the actual values and numbers of charge-discharge cycles are unknown, this value is set as the average between the values of Table 5.4, resulting in a wear-out of the battery of $7.40 \cdot 10^{-5}$ (0.0074 %) for each kWh injected into the grid.

The cost in terms of c€/kWh for the battery wear-out can be calculated once the cost of the battery replacement at the end of the cycle life is known. The battery replacement cost for the Nissan Leaf modeled in this work is estimated to be 5499 $ (approximately 5000€) [72], [73]. A value of 5000 € is assumed in this work. The wear-out cost per unit of energy cycled during V2G operation has been calculated in this work as:

$$c_{wearout} = 5000 \cdot 7.40 \cdot 10^{-5} = 37.02 \text{ c€/kWh}$$

5.2.2 Modeling of V2G cost

Based on the assumptions made in this work, illustrated in the previous section, the cost per kWh c_{V2G} associated with V2G operation is evaluated. This cost includes the cost of the additional battery wear-out associated with V2G operation $c_{wearout}$, and the cost for the energy c_{energy} that needs to be purchased, in order to recharge the battery to the previous SOC level. To take into consideration the charge-discharge overall efficiency the energy cost c_{energy} is divided by η_{net}, the net cycle efficiency calculated in Eq. 2.10.

The cost of 1 kWh injected by the EV into the network, using V2G operation as modeled in this work, can be expressed by Eq. 5.7.

$$c_{V2G} = c_{wearout} + \frac{c_{energy}}{\eta_{net}} \tag{5.7}$$

Some considerations can be done on the cost c_{V2G}. If the hourly DLMP price c_{DLMP}, evaluated using Eq. 5.3, is higher than the cost associated with V2G operation c_{V2G}, it will be economically convenient for the EV owner to discharge the vehicle to supply the domestic load demand. If the hourly price of the energy injected to the grid c_{PV} is higher than c_{V2G}, it will be more convenient to discharge the battery to supply the network. If none of those conditions is realized the V2G process is not convenient for the EV owner.

Since the cost of the battery wear out (37.02 c€/kWh) is always higher than the maximum value of the energy injected to the network (18.41 c€/kWh), it is never convenient for the EV owner to discharge the EV battery to sell energy to the power grid, neither if the energy is self produced from the PV unit nor if it is purchased at the yearly minimum price.

V2G operation to supply the domestic load demand is convenient only if the cost of the V2G process c_{V2G} is higher than the hourly electricity price c_{DLMP}. The maximum cost of electricity is higher than the cost of the wear out $c_{wearout}$ for some hours of the year. In the best case scenario the margin left is:

$$c_{DLMP,max} - c_{wearout} = 48.48 - 37.02 = 11.46 \text{ c€/kWh}$$

5.2.3 Optimization Problem

The main difference introduced by V2G operation is that the EVs can supply power back to the grid, and hence the EV charger power demand p_i can be negative. The limit to the discharge power is assumed to be equal in magnitude and opposed in sign to the maximum power demand P_{max}, the constraint set for when the battery is charging.

The optimization problem for the V2G proposed scenario can be expressed as:

$$\text{Cost function } f(p) = \sum_{i=1}^{24} \left(c_i \cdot (p_i + P_{dom} - P_{PV}) + W_{out,i}\right)$$

where

$$c_i = \begin{cases} c_{TOD} \cdot (1 + \lambda_{n\phi}) & \text{if } p_i + P_{dom} - P_{PV} \geq 0 \\ c_{PV} \cdot (1 + \lambda_{n\phi}) & \text{if } p_i + P_{dom} - P_{PV} < 0 \end{cases} \tag{5.8}$$

and

$$W_{out,i} = \begin{cases} -c_{wearout} \cdot p_i & \text{if } p_i < 0 \\ 0 & \text{if } p_i \geq 0 \end{cases} \tag{5.9}$$

Subject to:

$$\left.\begin{array}{ll} p_i & \geq -P_{max,i} \\ p_i & \leq P_{max,i} \\ \sum\limits_i p_i & = 0.9 - SOC_{arr} + (1 - \eta_{net}) \cdot \frac{W_{out}}{c_{wearout}} \end{array}\right\} i = 1, 2, \ldots, 24$$

5.2.4 Simulations and Results

Following the same procedure as in the previous scenarios, the EVs are now introduced in the network and their impact on the grid bottlenecks and the PV hosting capacity is evaluated.

The minimization of the yearly cost of electricity for the residential user, in the V2G scenario, results in an average cost function value $f(p)$ of 956.32 €. As in all the other scenarios analyzed, this value is obtained as the average between 30 EV charging profiles, in order for the measurements not to be affected by the single driver's behavior. The cost function value is comprehensive of the cost for supplying the domestic load demand, the cost for the EV home-charging (inclusive of the extra energy needed for V2G operation), the cost of the additional battery wear-out associated with V2G operation and the payback CS originated by the PV energy injected into the network (explained in Section 4.3).

The yearly energy consumption results to be 3900 kWh, inclusive of the domestic and the EV load demand. The average cost of electricity is 13.90 c€/kWh, lower than in the DLMP scenario. This result confirms the concept behind V2G scenario, since V2G operation will take place only when it is economically convenient for the EV owner to discharge the vehicle rather than to purchase electricity from the grid.

A large portion of the total cost regards the battery wear-out, on average 370 €/y, around 38% of the total. The energy cycled in V2G operation is on average 1000 kWh. Since the EV battery wear-out accounts for a large portion of the cost for the residential customer modeled in this work, a decrease in the battery cost, or better performances in terms of cycle life, or both, will result in increased savings for the EV owner.

Table 5.5 illustrates the power quality indicators for each of the EV share considered.

Table 5.5: Power quality indicators for different EV shares, V2G scenario. Values in red indicates the violation of the limits considered (listed in the first column).

		EV share (%)				
Power quality indicator	Limit	(0)	20	50	70	100
Minimum bus voltage at BUS8 (p.u.)	0.950	0.955	0.955	0.951	0.950	0.950
Line losses (% of load demand)	-	0.101	0.104	0.123	0.133	0.138
Maximum %VUF	2.000	1.974	2.434	2.655	2.355	2.421
Number of occurrences (h/y)	-	-	2	4	5	9
Maximum line loading (% on ampacity)	100	43.54	46.75	55.04	55.04	61.32
Maximum transformer loading (% on rated power)	100	58.83	59.92	62.13	63.62	68.88

In this V2G scenario no voltage magnitude violations are registered, for any of the EV shares considered. The DLMP pricing structure on which EVs with V2G functionality are expected to operate, together with the implementation of VDC functionality, is effective in the suppression of the voltage magnitude bottleneck for the EV integration in the network.

The bottleneck for this scenario, as in DLMP and Net Metering, is represented by voltage phase unbalance. The %VUF index exceeds the 2% constraint for all the EV shares considered. As in the DLMP scenario, the explanation of this phenomena is to be found in the unequal distribution of the EV load among the three phases of the system. A graphical representation of the cumulative distribution of the EV load demand on the three phases, for an example of one day of simulations, can be found in the plot of Fig. 5.5. The violation of the %VUF index is limited to a a maximum of 9 hours per year, and the peak values are always below 3%. All the other power quality indicators considered in this work are within the assumed limits, as in the previous DLMP scenario.

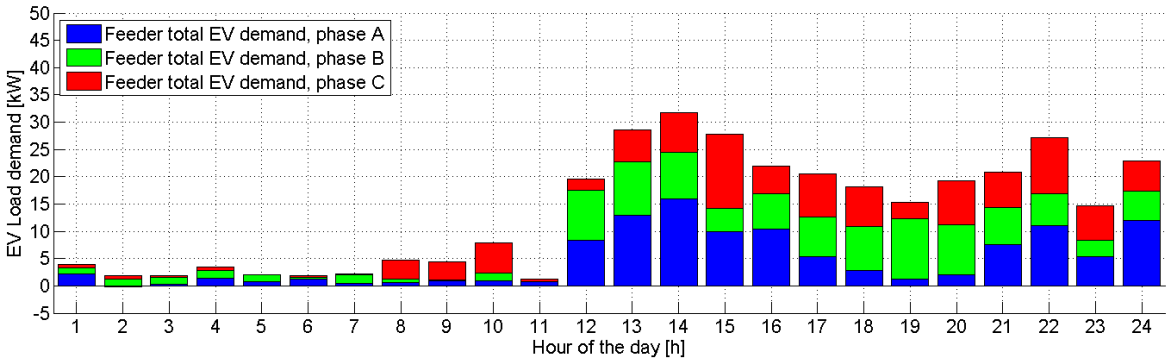

Figure 5.5: Cumulative load demand of 30 EVs during an example of one day of simulations, divided by the phase connection of the EV charger, V2G scenario.

As illustrated in Table 5.6, the increase of the PV hosting capacity is proportional to the number of EVs connected to the residential feeder. The PV hosting capacity results are improved, when compared to the DLMP scenario (shown in Table 5.3). The discharge of the EV battery results into a higher average energy demand from the EVs. This additional consumption is supplied by an increased charging during daytime hours, resulting into an incremental PV local consumption. As a consequence of this, the reverse power flow in the feeder is reduced, and the grid bottlenecks that limit the installation of more PV units in LV networks are diminished.

Table 5.6: Increase of the PV hosting capacity for different EV shares, V2G scenario.

	EV share (%)				
	(0)	20	50	70	100
Individual hosting capacity (kW)	2.775	3.308	3.552	3.552	3.685
Feeder hosting capacity (kW)	83.25	99.23	106.56	106.56	110.56
Variation of the hosting capacity (% compared to present scenario)	-	+19.2%	+28.0%	+28.0%	+32.8%

5.3 Discussion

In this last section of this chapter, a comparison between the results of the future scenarios proposed and analyzed in this work, DLMP and V2G, is performed. Following the same procedure as in Section 4.4, at first the cost of electricity for the EV owner is discussed. EV integration in the network is then considered, based on an analysis of the simulation results, followed by an investigation on the impact of the different EV charging strategies on the feeder PV hosting capacity.

5.3.1 Cost for the EV Owner

A comparison between the average cost of electricity for the Italian residential customer for the scenarios analyzed in this chapter, and the two cases of Net Metering analyzed in Chapter 4, is presented in Table 5.7.

As explained in Section 5.1.3, the domestic load demand does not variate according to the price signals, since no information is available about the share of deferrable loads in the measurements data. For this reason the average cost of electricity is higher in the future scenarios, based on real time pricing, than on the present Net Metering scenario. Further studies on the composition of the domestic load demand, and an optimization of the load profile of the deferrable loads can lead to a decrease in this cost.

Table 5.7: Comparison between the average cost of electricity between DLMP and V2G scenarios.

Scenario	Case	Average cost of electricity (c€/kWh)
Net Metering	no VDC	13.27
	with VDC	13.41
DLMP		15.16
V2G		13.90

From the above mentioned results it can be concluded that V2G functionality is effective in reducing the cost of electricity for the EV owner.

5.3.2 EV Integration in the Network

From the results of the simulations conducted and analyzed in this chapter, it can be seen how the grid bottleneck for the integration of EVs on a future perspective, in a model of an Italian LV residential network, is the voltage phase unbalance.

The violation of the voltage magnitude constraint, the major bottleneck in both the scenarios analyzed representing the present state of the grid, is not an issue for the future scenarios analyzed in this chapter.

5.3.3 Impact on the PV Hosting Capacity

The increase in the PV hosting capacity is proportional to the number of EVs plugged into the network for both the proposed future scenarios, DLMP and V2G. The addition of EV's V2G functionality is effective in allowing higher shares of PV in the feeder than with DLMP only.

A comparison between the results of all of the scenarios proposed, in terms of increase in the feeder PV hosting capacity, is presented in Table 5.8.

It can be seen how the highest values are reached with the Net Metering scenario. However, it has to be highlighted that this scenario present the most critical EV integration issues, involving both the voltage magnitude and the voltage phase unbalance.

Table 5.8: Comparison between the results of the introduction of different EV charging scenarios in terms of increase of the feeder PV hosting capacity.

Scenario	Case	EV share (%)			
		20	50	70	100
TOD	no VDC	+4.0%	+4.0%	+4.0%	+4.0%
	with VDC	+4.0%	+8.0%	+8.0%	+8.0%
Net Metering	no VDC	+20.8%	+56.0%	+58.4%	+64.0%
	with VDC	+20.8%	+56.0%	+58.4%	+64.0%
DLMP		+18.4%	+19.2%	+19.2%	+20.8%
V2G		+19.2%	+28.0%	+28.0%	+32.8%

5.4 Conclusion

The proposed future developments of the electricity market, with the introduction of real time pricing, and the integration of EVs with V2G functionality will lead to an improved integration of EVs and PVs in the distribution network.

Voltage phase unbalance will represent a possible issue for future developments, as it is for the present scenario. The proposed future scenario mitigate this phenomena, without solving it completely. It has to be highlighted that the %VUF index presents values over the 2% limit, assumed as a constraint in this work, for a limited number of the year only. In the worst case scenario, the violation is registered for only 9h/y, less than 0.02% of the total. In addition to this consideration, it can be noticed from the results listed in Table 5.2 and 5.5, how the maximum %VUF is less than 3% for each scenario considered. Further, this violation could be the result of a particular combination which happened to be applied in this study.

There is a correlation between EV share in the network and increase in the PV hosting capacity, proving the efficacy of the use of distributed storages, such as EV, to solve the grid bottlenecks that limit a further integration of distributed generation in the network.

6 | Conclusion and Future Works

In this work a series of studies has been conducted. In the beginning, the theoretical background regarding the integration of PV units in Italian LV networks has been analyzed. The rapid increase of the PV installed power in recent years, with the connection of more than 18 GW of distributed generation in networks planned for a one-way operation only, resulted in the raise of integration issues. The most relevant are found to be overvoltages, overloading of the network components and voltage phase unbalance.

The use of EVs as distributed storage systems, in order to reduce the reverse power flow in the residential feeder, has been found to be a possible solution for these problems. Since EVs present some integration issues as well, because their charging process can overlap with the domestic load demand, a study on the EV charging profiles has been conducted.

In this project, a series of EV charging scenarios has been proposed, and their impact on the grid bottlenecks for a large integration of PV units in LV networks has been analyzed.

A simulation model based on the CIGRÉ LV benchmark has been created and tested, in order to represent an example set of a radial residential grid in the Italian case. Steady-state analysis has been carried out to determine the PV feeder hosting capacity, concluding that the main grid bottlenecks are the voltage variation at the end of the feeder and voltage phase unbalance.

The EV interaction with SPV and the residential load demand has been then analyzed. Different EV charging strategies, based on the present electricity tariffs for Italian residential customers (TOD and Net Metering) and future technical and economical developments (voltage droop control, DLMP, V2G) has been identified.

From the simulation results obtained, it has been concluded that with the present Italian TOD electricity tariffs, the introduction of the EV load in the network cannot increase significantly the PV penetration. The present TOD structure sets lower prices during nighttime and the weekend, and for this reason it encourages the EV owner to overlap the charging process of its vehicle with the evening domestic load peak, rather than with the PV peak production. As a consequence of this, the number of EVs that can be plugged into the network is also limited. With high shares of EVs in the feeder, the voltage magnitude for the furthest customers from the distribution transformer can violate the lower boundaries, resulting in a deterioration of the power quality.

For the other scenarios proposed and analyzed in this work, Net Metering, DLMP and V2G, a positive correlation between the number of EVs introduced in the network and the increase of the PV capacity is proven.

From the DSO perspective, EVs were proven to help the increase of the PV installations in LV grids under the existing Net Metering structure, and the future possible developments such as the introduction of real time pricing applied to the distribution level. The additional

PV hosting capacity generated by the EV introduction in the grid can lead to postponements or reduction of the need for grid upgrades and reinforcements, such as ring connections and replacement of the network components.

V2G functionality, applied in this work in a future scenario with the hypothesis of a real time pricing structure based on marginal line losses, has been proven to be effective in the increase of the PV hosting capacity and the reduction of the total cost of electricity for the EV owner.

A series of integrations issues for the EVs, however, persist. While the introduction of Voltage Droop Control for the EV charger and DLMP are effective in solving the voltage magnitude issue, voltage phase unbalance remains a problem. The violation of the %VUF index considered has been registered for every EV share introduced, even if the number of occurrences is limited and the peak values are close to the 2% value that defines the constraint.

To conclude, the present Net Metering tariff and the considered future developments, such as the introduction of real time pricing, VDC functionality for the EV charger and V2G operation, has been confirmed to be effective for the increase of the PV penetration in residential LV networks. Regarding the impact of EVs in the grid power quality, further research is needed.

This study is applicable to other grid topologies and to other cases than the Italian one. The original CIGRÉ benchmark model, on which the adapted model proposed in this work is based, has the advantages of generality, and it represent a benchmark for all European LV grids. The simulations results might vary, but the principles on which this project is based are unchanged.

6.1 Future Works

As EVs are proven to potentially increase the PV hosting capacity in residential LV grids, a series of possible future works based on this project might be worth considering. Some of the most important future perspectives are summarized in the following list:

- More EVs types can be included in the simulation network, e.g. hybrid vehicles and BEVs with different battery range. A study based on different options for the EV charging, such as charging at the workplace, battery swapping and fast charging stations, can be carried out. Driving patterns based on EV measurements data, when those will be available, will represent a step forward for the EV load modeling.

- The participation of the EVs in other energy markets is a future step for this work. EVs can participate the regulating market, providing both upward regulation, by reducing the load demand or proving V2G functionality (if available) and downward regulation, by increasing the battery charging power. EVs can also provide ancillary services, to support system power imbalance. In the context of the participation on other than day-ahead market, the figure of the EV aggregator can be investigated;

- Other deferrable loads in residential networks can be modeled. Heat pumps, air conditioning and other domestic appliances can modify their power demand according to price signals, without compromising their functionalities, and can contribute to the increase in the local self-consumption of the PV generated energy;

- An analysis of power quality indicators not considered in this work, such as current harmonics, frequency fluctuations and reliability of distribution grids with SPV and EVs can be investigated. Voltage and frequency control strategies, and an analysis of the dynamic behavior of the case study network, can be included in an extension of this work;
- In the end, network reinforcements and variations in the grid topology can be considered, as complementary to EVs for the increase of the PV penetration in LV grids.

Bibliography

[1] Stoker, "Summary for policymakers," *Climate Change 2013: The Physical Science Basis.*, 2013.

[2] R. Garcia-Valle and J. A. P. Lopes, *Electric vehicle integration into modern power networks.* Springer, 2013.

[3] T. Trigg, P. Telleen, R. Boyd, F. Cuenot, D. D'Ambrosio, R. Gaghen, J. Gagné, A. Hardcastle, D. Houssin, A. Jones, *et al.*, "Global EV Outlook: Understanding the Electric Vehicle Landscape to 2020," April 2013.

[4] M. Brenna, A. Dolara, F. Foiadelli, S. Leva, and M. Longo, "Urban scale photovoltaic charging stations for electric vehicles," 2014.

[5] P. Mock and Z. Yang, "Driving Electrification - A global comparison of fiscal incentive policy for electric vehicles," *The International Council of Clean Transportation (ICCT)*, pp. 22–23, 2014.

[6] B. Geier. http://fortune.com/2015/01/08/electric-vehicle-sales-2014/, 2015.

[7] EPIA, "Global Market Outlook for Photovoltaics 2014-2018," 2014.

[8] TERNA, "Dati statistici sull'energia elettrica in Italia - 2013." http://www.terna.it/default/Home/SISTEMA_ELETTRICO/statistiche/dati_statistici.aspx, 2014. (in Italian).

[9] E. Demirok, D. Sera, R. Teodorescu, P. Rodriguez, and U. Borup, "Clustered PV inverters in LV networks: An overview of impacts and comparison of voltage control strategies," in *Electrical Power & Energy Conference (EPEC), 2009 IEEE*, pp. 1–6, IEEE, 2009.

[10] GSE, "Rapporto Statistico 2012 Solare Fotovoltaico," 2013. (in Italian).

[11] A. Bracale, P. Caramia, G. Carpinelli, A. Russo, and P. Verde, "Site and system indices for power-quality characterization of distribution networks with distributed generation," *Power Delivery, IEEE Transactions on*, vol. 26, no. 3, pp. 1304–1316, 2011.

[12] E. Demirok, D. Sera, and R. Teodorescu, "Estimation of maximum allowable PV power connection to low voltage residential networks: A case study of Braedstrup," in *1st Int. Workshop Integr. Solar Power Power Syst., Aarhus, Denmark, Oct*, vol. 24, 2011.

[13] W. H. Kersting, *Distribution system modeling and analysis.* CRC press, 2002.

[14] M. Yue and X. Wang, "Assessing cloud transient impacts on grid with solar and battery energy systems," in *Photovoltaic Specialists Conference (PVSC), 2013 IEEE 39th*, pp. 2348–2353, June 2013.

[15] E. Demirok, D. Sera, R. Teodorescu, P. Rodriguez, and U. Borup, "Evaluation of the voltage support strategies for the low voltage grid connected PV generators," in *Energy Conversion Congress and Exposition (ECCE), 2010 IEEE*, pp. 710–717, IEEE, 2010.

[16] F. Marra, Y. Fawzy, T. Bulo, and B. Blazic, "Energy storage options for voltage support in low-voltage grids with high penetration of photovoltaic," in *Innovative Smart Grid Technologies (ISGT Europe), 2012 3rd IEEE PES International Conference and Exhibition on*, pp. 1–7, Oct 2012.

[17] E. Lakervi and E. J. Holmes, *Electricity distribution network design*. No. 21, IET, 1995.

[18] A. L'Abbate, G. Fulli, F. Starr, and S. D. Peteves, "Distributed power generation in europe: technical issues for further integration," *Joint Research Center Institute for Energy*, 2007.

[19] J. Dickert, M. Domagk, and P. Schegner, "Benchmark low voltage distribution networks based on cluster analysis of actual grid properties," in *PowerTech (POWERTECH), 2013 IEEE Grenoble*, pp. 1–6, IEEE, 2013.

[20] R. Benato and L. Fellin, *Impianti elettrici*. UTET scienze tecniche, 2011. (in Italian).

[21] D. Parmar and L. Yao, "Impact of unbalanced penetration of single phase grid connected photovoltaic generators on distribution network," in *Universities' Power Engineering Conference (UPEC), Proceedings of 2011 46th International*, pp. 1–8, Sept 2011.

[22] C. Bogdan-Ionut, A. M. Elena, M. Vlad, S. Dezso, K. Tamas, and T. Remus, "Improved Voltage Regulation Strategies by PV Inverters in LV Rural Networks," *3rd IEEE International Symposium on Power Electronics for Distributed Generation Systems (PEDG), 2012*, pp. 1–7, 2012.

[23] A. Keyhani, *Design of smart power grid renewable energy systems*. John Wiley & Sons, 2011.

[24] S. Chandra, P. Twomey, and D. Randles, "Impact of PV and load penetration on LV network voltages and unbalance and potential solutions," in *Electricity Distribution (CIRED 2013), 22nd International Conference and Exhibition on*, pp. 1–4, IET, 2013.

[25] I. Knight, N. Kreutzer, M. Manning, M. Swinton, and H. Ribberink, "Residential cogeneration systems: European and Canadian residential non-HVAC electric and DHW load profiles," *IEA/ECBCS Annex*, vol. 42, 2007.

[26] ISTAT, "Consumo di energia per i comuni capoluogo di provincia," 2014. (in Italian).

[27] EurObserv'ER, "Photovoltaic barometer," 2011. (in French).

[28] EurObserv'ER, "Photovoltaic barometer," 2014.

[29] E. Distribuzione, "Piano di Sviluppo annuale e pluriennale delle Infrastrutture di Enel Distribuzione S.p.A. 2014-2016," 2014. (in Italian).

[30] J. Van Roy, N. Leemput, F. Geth, R. Salenbien, J. Buscher, and J. Driesen, "Apartment building electricity system impact of operational electric vehicle charging strategies," 2013.

[31] C. EPRI, Palo Alto, "Effects of Temporary Overvoltage on Residential Products: System Compatibility Research Project," 2005.

[32] Y. Ueda, K. Kurokawa, T. Tanabe, K. Kitamura, and H. Sugihara, "Analysis results of output power loss due to the grid voltage rise in grid-connected photovoltaic power generation systems," *Industrial Electronics, IEEE Transactions on*, vol. 55, no. 7, pp. 2744–2751, 2008.

[33] M. Kleinberg, J. Harrison, and N. Mirhosseini, "Using energy storage to mitigate PV impacts on distribution feeders," in *Innovative Smart Grid Technologies Conference (ISGT), 2014 IEEE PES*, pp. 1–5, Feb 2014.

[34] J. Traube, F. Lu, D. Maksimovic, J. Mossoba, M. Kromer, P. Faill, S. Katz, B. Borowy, S. Nichols, and L. Casey, "Mitigation of solar irradiance intermittency in photovoltaic power systems with integrated electric-vehicle charging functionality," *Power Electronics, IEEE Transactions on*, vol. 28, no. 6, pp. 3058–3067, 2013.

[35] N. Etherden and M. H. Bollen, "Increasing the hosting capacity of distribution networks by curtailment of renewable energy resources," in *PowerTech, 2011 IEEE Trondheim*, pp. 1–7, IEEE, 2011.

[36] H. Markiewicz and A. Klajn, "Voltage Disturbances–Standard EN 50160," *Copper Development Association, lEE Endorsed Provider, Wroclaw University of Technology*, 2004.

[37] P. Pillay and M. Manyage, "Definitions of voltage unbalance," *IEEE Power Engineering Review*, vol. 21, no. 5, pp. 50–51, 2001.

[38] Bahra Cables Company, "Low voltage power cables." http://www.bahra-cables.com/downloads/Low_Voltage.pdf.

[39] PlanetSolar S.A. http://www.planetsolar.org/boat/sections/the_boat, 2014.

[40] C. Zhou, K. Qian, M. Allan, and W. Zhou, "Modeling of the cost of EV battery wear due to V2G application in power systems," *Energy Conversion, IEEE Transactions on*, vol. 26, no. 4, pp. 1041–1050, 2011.

[41] K. Qian, C. Zhou, M. Allan, and Y. Yuan, "Modeling of load demand due to EV battery charging in distribution systems," *Power Systems, IEEE Transactions on*, vol. 26, no. 2, pp. 802–810, 2011.

[42] T. Horiba, "Lithium-ion battery systems," *Proceedings of the IEEE*, vol. 102, no. 6, pp. 939–950, 2014.

[43] J. G. Hayes, "Simplified electric vehicle models for use in undergraduate teaching and research," in *Energy Conversion Congress and Exposition (ECCE), 2014 IEEE*, pp. 1271–1277, Sept 2014.

[44] USABC, "Electrochemical energy storage technical team technology development." http://www1.eere.energy.gov/vehiclesandfuels/pdfs/program/electrochemical_energy_storage_roadmap.pdf, 2006.

[45] E. Energy, "Cost and performance of EV batteries," *Final report for The Committee on Climate Change*, vol. 21, no. 03, 2012.

[46] L. Zhao, S. Prousch, M. Hubner, and A. Moser, "Simulation methods for assessing electric vehicle impact on distribution grids," in *Transmission and Distribution Conference and Exposition, 2010 IEEE PES*, pp. 1–7, IEEE, 2010.

[47] P. Papadopoulos, S. Skarvelis-Kazakos, I. Grau, L. Cipcigan, and N. Jenkins, "Electric vehicles' impact on british distribution networks," *Electrical Systems in Transportation, IET*, vol. 2, pp. 91–102, September 2012.

[48] M. Cresta et al., "Prospective Installation of EV Charging Points in a Real LV Network: Two Case Studies," *2nd IEEE ENERGYCON Conference & Exibition, 2012*, pp. 1–6, 2012.

[49] L. Kutt, E. Saarijarvi, M. Lehtonen, H. Molder, and J. Niitsoo, "A review of the harmonic and unbalance effects in electrical distribution networks due to EV charging," in *Environment and Electrical Engineering (EEEIC), 2013 12th International Conference on*, pp. 556–561, IEEE, 2013.

[50] Q. Wu, A. H. Nielsen, J. Østergaard, S. T. Cha, F. Marra, Y. Chen, and C. Træholt, "Driving pattern analysis for electric vehicle (EV) grid integration study," in *Innovative Smart Grid Technologies Conference Europe (ISGT Europe), 2010 IEEE PES*, IEEE, 2010.

[51] G. Pasaoglu, D. Fiorello, A. Martino, G. Scarcella, A. Alemanno, C. Zubaryeva, and C. Thiel, *Driving and Parking Patterns of European Car Drivers: A Mobility Survey.* Publications Office, 2012.

[52] S. Huang, J. Pillai, B. Bak-Jensen, and P. Thogersen, "Voltage support from electric vehicles in distribution grid," in *Power Electronics and Applications (EPE), 2013 15th European Conference on*, pp. 1–8, Sept 2013.

[53] G. Coppez, S. Chowdhury, and S. Chowdhury, "Review of battery storage optimisation in distributed generation," in *Power Electronics, Drives and Energy Systems (PEDES) 2010 Power India, 2010 Joint International Conference on*, pp. 1–6, Dec 2010.

[54] M. Aachiq, T. Oozeki, Y. Iwafune, and J. G. Fonseca Jr, "Reduction of PV Reverse Power Flow through the Usage of EV's Battery with Consideration of the Demand and Solar Radiation Forecast," in *Electric Vehicle Conference (IEVC), 2013 IEEE International*, pp. 1–3, IEEE, 2013.

[55] F. Marra, G. Yang, Y. Fawzy, C. Traeholt, E. Larsen, R. Garcia-Valle, and M. Moeller Jensen, "Improvement of Local Voltage in Feeders With Photovoltaic Using Electric Vehicles," *IEEE Transaction on Power Systems, Vol 28, no. 3 August 2013*, 2013.

[56] Autorità per l'energia elettrica, il gas ed il sistema idrico. http://www.autorita.energia.it, 2015.

[57] M. J. Reno, K. Coogan, J. Peppanen, and S. Grijalva, "Using distribution LMP and time-of-delivery pricing to promote optimal placement and increased profitability of residential PV systems," in *North American Power Symposium (NAPS), 2014*, pp. 1–6, IEEE, 2014.

[58] F. Sahriatzadeh, P. Nirbhavane, and A. K. Srivastava, "Locational marginal price for distribution system considering demand response," in *North American Power Symposium (NAPS), 2012*, pp. 1–5, IEEE, 2012.

[59] S. Papathanassiou, N. Hatziargyriou, K. Strunz, *et al.*, "A benchmark low voltage microgrid network," in *Proceedings of the CIGRE Symposium: Power Systems with Dispersed Generation*, pp. 1–8, 2005.

[60] K. Strunz *et al.*, "Benchmark systems for network integration of renewable and distributed energy resources," *Cigre Task Force C6.04.02*, vol. 6, 2011.

[61] F. Marra, G. Yang, and C. Træholt, "A decentralized storage strategy for residential feeders with photovoltaics," *Smart Grid, IEEE transaction on*, pp. 1–8, Sep 2013.

[62] J. Pillai, P. Thogersen, J. Moller, and B. Bak-Jensen, "Integration of Electric Vehicles in low voltage Danish distribution grids," in *Power and Energy Society General Meeting, 2012 IEEE*, pp. 1–8, July 2012.

[63] ENEL. https://www.enelservizioelettrico.it/it-IT/tariffe/uso-domestico/biorarie/d3, 2015.

[64] Gestore Mercati Elettrici. http://www.mercatoelettrico.org/, 2015. (in Italian.

[65] AA.VV., "Relazione tecnica modalità e condizioni tecnico economiche per l'erogazione del servizio di scambio sul posto," 2012. (in Italian).

[66] N. O'Connell, Q. Wu, J. Østergaard, A. H. Nielsen, S. T. Cha, and Y. Ding, "Day-ahead tariffs for the alleviation of distribution grid congestion from electric vehicles," *Electric Power Systems Research*, vol. 92, pp. 106–114, 2012.

[67] F. Sahriatzadeh, P. Nirbhavane, and A. K. Srivastava, "Locational marginal price for distribution system considering demand response," in *North American Power Symposium (NAPS), 2012*, pp. 1–5, IEEE, 2012.

[68] P. M. Sotkiewicz and J. M. Vignolo, "Nodal pricing for distribution networks: efficient pricing for efficiency enhancing dg," *Power Systems, IEEE Transactions on*, vol. 21, no. 2, pp. 1013–1014, 2006.

[69] F. Meng and B. H. Chowdhury, "Distribution LMP-based economic operation for future smart grid," in *Power and Energy Conference at Illinois (PECI), 2011 IEEE*, pp. 1–5, IEEE, 2011.

[70] M. Hong, "An approximate method for loss sensitivity calculation in unbalanced distribution systems," *Power Systems, IEEE Transactions on*, vol. 29, no. 3, pp. 1435–1436, 2014.

[71] Gestore Mercati Elettrici. http://www.mercatoelettrico.org/It/WebServerDataStore/MGP_ReportGiornaliero/20130412MGPReportGiornaliero.pdf, 2015. (in Italian).

[72] Auto Express. http://www.autoexpress.co.uk/nissan/89694/nissan-leaf-battery-replacement-to-cost-4920, 2015.

[73] B. Brockman. http://www.mynissanleaf.com/viewtopic.php?f=4&t=17168, 2015.

Appendix A

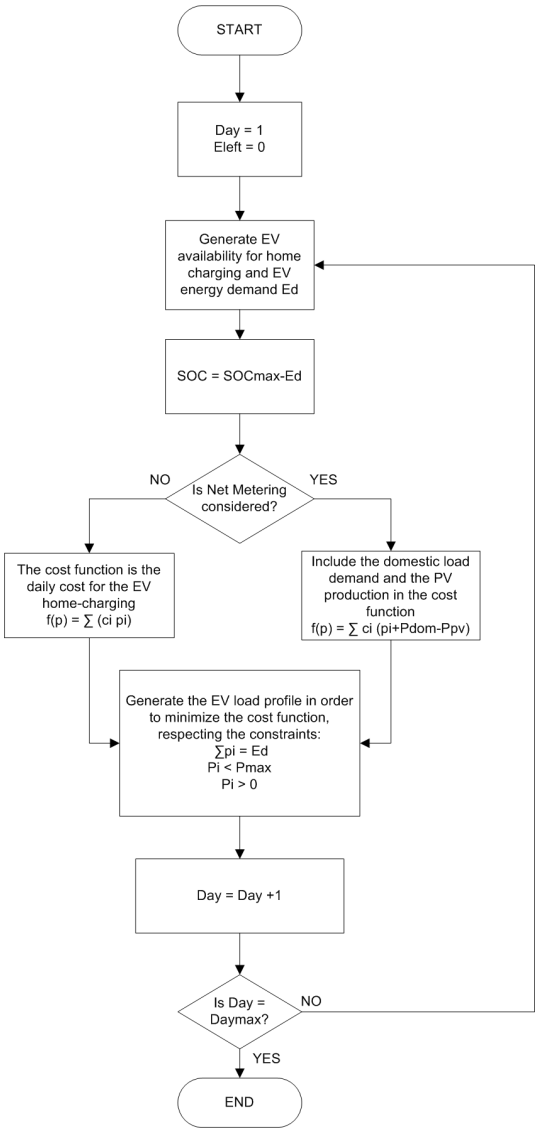

Figure 1: Flowchart of the algorithm used to generate the load profile of a single EV for both TOD tariff and Net Metering scenarios. The algorithm is repeated for each EV introduced in the network in order to have different load profiles for each EV.

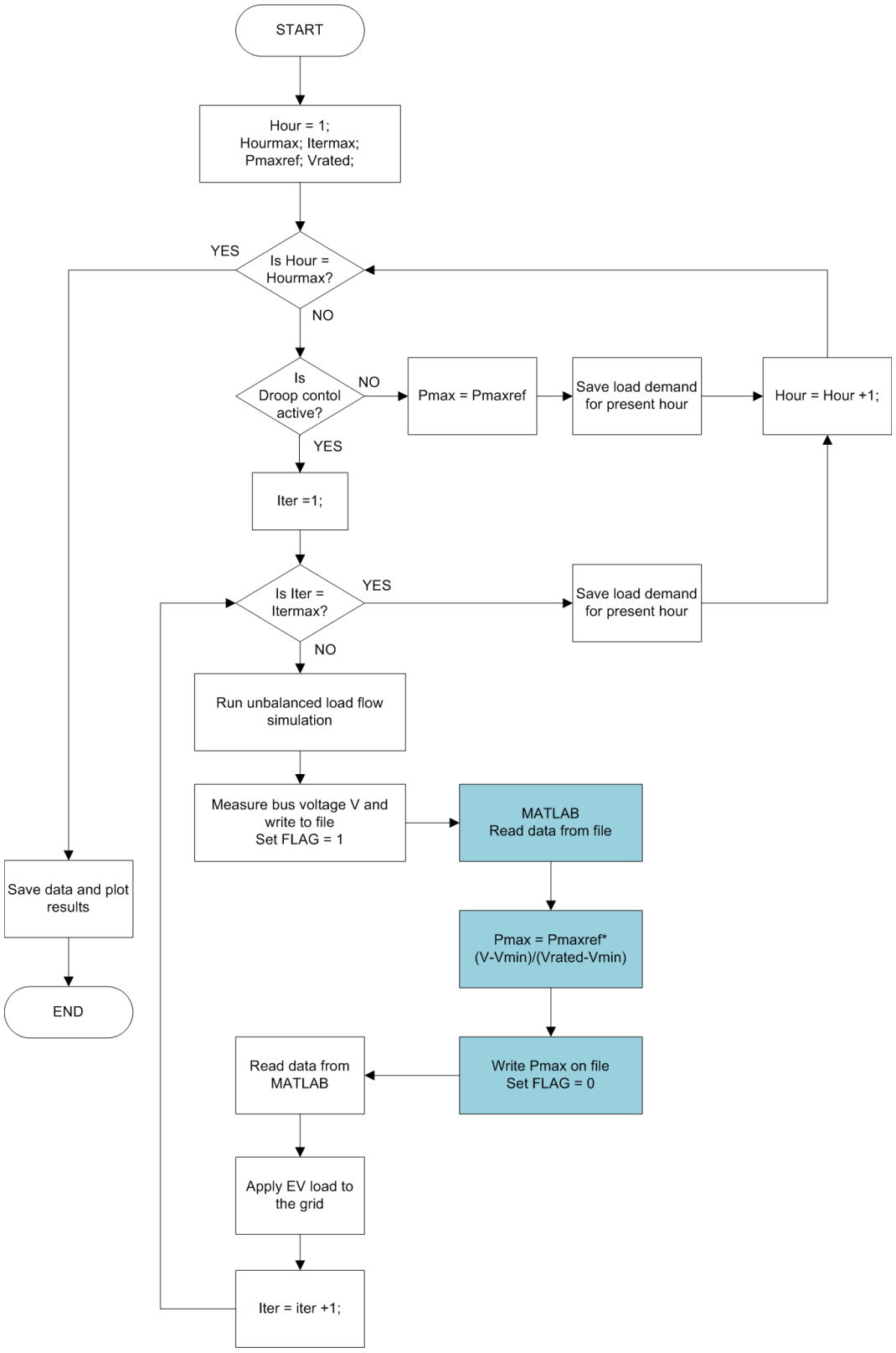

Figure 2: Flowchart of the co-simulation algorithm used to calculate the maximum power demand of the EV charger when voltage droop control is used. The boxes in white are the operations performed with PowerFactory, while the boxes in turquoise are those performed with MATLAB.